

Matter in 2+1 Dimensions at Finite Density with Chern-Simons Interactions



Swansea University
Prifysgol Abertawe

Stanislav Stratiev

Department of Physics

Swansea University

Submitted to Swansea University in fulfilment
of the requirements for the degree of

Doctor of Philosophy

2020

Declaration

This work has not previously been accepted in substance for any degree and is not being concurrently submitted for any degree.

Signed:(candidate)

Date:

Statement 1

This thesis is the result of my own investigations, except where otherwise stated. Where correction services have been used, the extent and nature of the correction is clearly marked in a footnote(s). Other sources are acknowledged by footnotes giving explicit references. A bibliography is appended.

Signed:(candidate)

Date:

Statement 2

I hereby give consent for my thesis, if accepted, to be available for photocopying and for inter-library loan, and for the title and summary to be made available to outside organisations.

Signed:(candidate)

Date:

Contents

List of Figures	ix
List of Tables	xiii
Introduction	1
1 Background	5
1.1 Chern-Simons Theory	6
1.1.1 Chern-Simons-Maxwell Theory	11
1.1.2 Chern-Simons Matter Theory	12
1.2 Statistical Physics	15
1.2.1 Functional Integral Representation of the Partition Function	15
1.2.2 Grand Canonical Ensemble	18
1.2.2.1 Chemical Potential for a Local Symmetry	20
1.3 Fractional Quantum Hall Effect	22
1.3.1 Classical Hall Effect	22
1.3.2 Quantum Hall Effect	25
1.4 Vortices	26
1.4.1 Global U(1) Vortex	26
1.4.2 Local U(1) Vortex	27
1.4.3 Particle-Vortex Duality	31
1.5 Fermi-Bose Duality	34
1.6 Non-Commutative Fluids	36
1.6.1 Review of Non-Commutative Geometry	37

CONTENTS

1.6.2	Non-Commutative Field Theory	38
2	Abelian Chern-Simons vortices at finite chemical potential	41
2.1	Introduction	41
2.2	The Abelian theory at finite chemical potential	44
2.2.1	Perturbative spectrum	46
2.3	Vortex equations	47
2.3.1	Qualitative features	48
2.4	Vortex energy and BPS-like scaling	51
2.4.1	The quartic potential $s = 2$	54
2.4.2	General power law potential ($s \geq 2$)	55
2.4.3	Positive flux vortices	55
2.5	Numerical results	56
2.5.1	Quartic potential ($s = 2$)	56
2.5.2	Sextic potential ($s = 3$)	63
2.6	Discussion	65
3	Roton-phonon excitations in Chern-Simons matter theory at finite density	67
3.1	Introduction	67
3.2	The $SU(2)_k$ theory	70
3.2.1	Classical ground states with $\mu_B \neq 0$	71
3.2.2	Colour-flavour locked symmetry	76
3.3	Spectrum of fluctuations	77
3.3.1	The $k \rightarrow \infty$ theory	77
3.3.2	Finite, large k	78
3.3.2.1	Physical states	79
3.3.3	Roton minimum and complete spectrum	83
3.3.4	Landau critical velocity	86
3.3.5	The $U(2)_k$ theory	87
3.4	The $SU(N > 2)$ case	88
3.4.1	Vacuum configuration	89
3.4.2	Interpretation as quantum Hall droplet state	91
3.5	Summary and future directions	93

CONTENTS

4 Vortices in U(2) and SU(2) Chern-Simons scalar theories.	97
4.1 U(2) theory	98
4.2 SU(2) theory	103
Conclusions	104
A Determinant of fluctuation matrix for $SU(2)$	107
References	109

Acknowledgements

I'd like to thank Prem Kumar for his patient supervision over the past few years.

List of Figures

1.1	(a) is topologically distinct from the rest, yet they are all gauge equivalent configurations.	10
1.2	A collection of localized charge distributions, and with magnetic flux lines of strength $\frac{4\pi\hbar\rho(x,y)}{k}$ tied to the charges. The charge and flux are tied together throughout the motion of the particles as a result of the Chern-Simons equations (1.18) - (1.19).	14
1.3	Scalar and magnetic field profiles for $n=1$ and $\lambda = (10, 1, 0.1) * \lambda_c$	32
2.1	The dispersion relations of the two branches of perturbative fluctuations for the quartic potential ($s = 2$), with different values of the dimensionless coupling α	47
2.2	<i>Left:</i> The scalar field profile $\tilde{f}(\tilde{r})$ for $\alpha = 5$ and negative flux. <i>Right:</i> The dimensionless magnetic field $\tilde{B}(\tilde{r})$ for the same values of α and magnetic flux.	57
2.3	The electric field has support only at the edge of the vortex implying a ring-like profile. The width of the transition region remains fixed as $ n $ is cranked up.	57
2.4	The radii of large- n vortex solutions follow very closely the curve $\mu R_n = \sqrt{2\mu n }$. We define the radius of the vortex as the position at which the dimensionless energy density falls below a threshold $\sim 10^{-4}$	58
2.5	<i>Left:</i> This shows that $\alpha < 2$ vortices are type I (attractive), separated from type II (repulsive) solutions for $\alpha > 2$ by the $\alpha = 2$ line where the solutions have vanishing interaction energy. <i>Right:</i> The α -dependence of the n -vortex mass formula agrees with analytical arguments at large $ n $	59

LIST OF FIGURES

2.6	The figure shows the three quantities: rf'/f (red), $(A_\theta + n)$ (green), and $(- B(0) r^2/2 + n)$ (purple) evaluated on the exact numerical solutions for $\alpha = 1$ and $\alpha = 2$	60
2.7	<i>Left:</i> $(\tilde{f}' - a\tilde{f})$ plotted for 3 values of α including critical case. $\alpha = 2$. <i>Right:</i> The value of \tilde{A}_0 at the origin for different α as a function of $ n $	61
2.8	Magnetic and electric fields for positive flux vortices have support near the edge of the vortex and their peak values grow without bound as n is increased.	62
2.9	Positive flux vortices have higher energy than their negative flux counterparts.	63
2.10	Vortex profiles with negative winding number for quartic(solid) and sextic(dashed) potentials.	64
2.11	The scaling of the energy of the n -vortex with $ n $ and α , with sextic potential.	64
2.12	Value of \tilde{A}_0 at the origin for different values of α , as a function of $ n $, with the sextic potential.	65
3.1	The effective potential (free energy density) as a function of the VEV v for $\mu_B = 1$, $m = 0.5$ and $g_4 = 0$	76
3.2	The solid blue curve shows the slope of the phonon dispersion relation at $\mathbf{p} = 0$ as a function of $\tilde{\mu} = \pi \mu_B/g_4 k $ for the massless theory, It interpolates between $c_s = 1/\sqrt{3}$ at small $\tilde{\mu}$ and the conformal value of $c_s = 1/\sqrt{2}$ when g_4 is taken to zero.	81
3.3	Left: The $k = \infty$ theory displays two gapless excitations with linear and quadratic dispersion relation. Right: At finite large k , the two modes potentially cross, and also mix. The diagonalized modes display a splitting and “repulsion” resulting in a local maximum in the phonon branch.	83
3.4	Left: The spectrum for $m = 0$ with $\tilde{\mu} = \pi\mu_B/g_4 k = \pi/20$. Right: The two lightest states, including the phonon-roton branch (blue) with $\tilde{\mu} = \pi/500$. The dotted lines indicate the large- k limiting values of the roton maximum and minimum.	84

LIST OF FIGURES

3.5	Left: The physical spectrum for the massive case. Right: In the scale invariant situation, the dispersion relations have a universal form, independent of k and μ . The dotted blue line with slope $1/\sqrt{2}$ matches the phonon velocity at low momentum.	85
3.6	The Landau critical velocity as a function of the dimensionless parameter $\pi\mu_B/g_4k$ in the theory with $m = 0$	87
3.7	The semiclassical spectrum of the $U(2) \simeq SU(2) \times U(1)$ theory. All states are gapped. Nevertheless, the lightest state displays a roton-like minimum. The dotted blue line passing through the origin with slope $1/\sqrt{2}$ is shown to emphasize the absence of phonon-like linear dispersion.	88

LIST OF FIGURES

List of Tables

1.1 This table shows the matching of the phases of the XY model and the Abelian Higgs model	33
----------------------------------------------------------------------------------------------------------	----

LIST OF TABLES

Introduction

On the second day of my graduate studies, The Nobel prize in Physics was awarded to D. Thouless, M. Kosterlitz and D. Haldane for the discovery of topological phase transitions. At the time I thought topology was a subject about open neighbourhoods, hausdorff spaces and counting holes on mugs and doughnuts. I could not fathom how these ideas could have anything to do with the description of the real world. I had to understand how these concepts were connected. This thesis follows my path of exploring the mystery of topological physics from the perspective of high energy physics and quantum field theory (QFT).

Today, topology has become ubiquitous in the study of physics. It provides us with new models to gain insight into nature. In addition, it provides the stability for new kinds of excitations in models whose initial purpose had more to do with the study of particles (*e.g.* Glashow-Salam model). Even very deep questions such as the understanding of confinement and the attempts to study strongly correlated gauge theories seem to be intimately related to the study of continuous deformations. There are hints that confinement might be related to instanton condensation [1]. And most relevant to this work, it seems that the promising path of relating strongly and weakly coupled theories through dualities, relate the conserved current of a theory to the topological current of its dual. It was our hope that we can shed some more light on the details of these dualities at finite matter density and for this reason, this thesis has been centered around the study of the grand canonical ensemble of Chern-Simons matter theories, specifically scalar field theories.

The first novelty that we stumbled upon was a ground state that had been overlooked since it only manifests itself in the finite chemical potential regime.

LIST OF TABLES

It is a ground state with non-zero expectation value for the gauge fields, seemingly breaking rotational symmetry. In reality, color-flavor locking remedies this and the rotational symmetry is preserved. In order to confirm this, we also computed the quadratic spectrum of the theory, which showed no signs of rotational asymmetry. We discovered further, owing to Goldstone's theorem and the broken $U(1)_B$ global symmetry, that the long wave-length dynamics of the $SU(2)$ theory behaved as a superfluid and predicts the existence of a roton excitation. What was even more surprising is that this non-trivial ground state exists in the zero coupling free scalar theory coupled to Chern-Simons. This is peculiar since we generally expect there to be a potential that drives the symmetry breaking.

Correlation functions for the scalar Chern-Simons theory at $\mu = 0$ have been computed exactly in the large N limit [56]. Since the $\mu = 0$ results cannot be extrapolated to finite μ , we would need to take the ground state discussed in the previous paragraph into account. A natural question that arises is what do the correlation functions look like in the presence of this new condensate at large N ? This was the ultimate aim that we in commencing this work, *i.e.* solving this theory in the large N limit. In order to pursue this direction, we set ourselves the more conservative goal of computing the quadratic spectrum in the general N $SU(N)$ theory. The ground state in the $SU(N)$ theory has the same algebraic structure as the non-commutative Chern-Simons theory used as a model for the FQHE. The approach to diagonalizing the large N spectrum of fluctuations that we outlined involves translating the problem to a non-commutative Chern-Simons theory and using the solutions of that model to arrive at an exact result.

Aside from studying the ground state and the fundamental excitations of finite density Chern-Simons models, we have also explored the existence and properties of solitons (vortices) in these models. Our main results in this line are the discovery and study of an approximate numerical BPS state in the abelian theory. Additionally, we find a self consistent vortex ansatz for the $SU(2)$ and $U(2)$ theories. We have left the numerical study of the resulting equations for future work.

This thesis is structured in the following way:

LIST OF TABLES

In Chapter 1, we cover the necessary background required to understand the rest of the thesis and how it fits in the wider field of research. We present a condensed introduction to the topics of Chern-Simons field theory, the Quantum Hall effect, vortices, particle-vortex duality, Fermi-Bose duality, the statistical grand canonical ensemble in quantum field theory and non-commutative field theory.

Chapter 2 presents the analytical and numerical study of abelian vortex solutions interpolating between a symmetric and asymmetric phase, where the symmetry breaking is chemical potential driven.

Chapter 3 showcases the derivation of the peculiar ground state mentioned earlier, the spectrum of fluctuations is analyzed in the SU(2) theory. The chapter concludes with the SU(N) ground state and the observation that it resembles non-commutative Chern-Simons theory.

In Chapter 4 we switch gears back to vortices, except this time we consider the possibility of topological solutions in the non-abelian theory. We show that there is a self-consistent circularly symmetric ansatz for a global vortex in the SU(2) theory and a local vortex in the U(2) theory.

LIST OF TABLES

Chapter 1

Background

This chapter provides the necessary background technical knowledge required to understand the main results of this thesis and their implications to related fields of physics. These include both the theoretical framework we will use and the real world phenomena to which it relates to. As should already be clear by now, in this text, we will concern ourselves with the study of planar systems at finite density. We will approach the study of these two dimensional systems through the framework of Quantum Field Theory (QFT).

There are two important aspects of QFT that will play a major role for us. One of them is the relation between the grand canonical statistical partition function and QFT. The other aspect is the distinct way in which the gauge principle manifests itself in 2+1 dimensional theories. The latter is addressed in 1.1, where we review the basics of *Chern-Simons theory*. The former is discussed in 1.2.2, where we will spend time reminding ourselves some basic statistical mechanics.

After we have covered these, , we will spend some time looking at the problems of the *fractional and integer quantum hall effects* (FQHE/IQHE) in 1.3 and emphasize its relation to Chern-Simons matter theories. This will help us understand the applications and motivate the study of the models we are concerned with in this text.

Then, we shall continue by reviewing the properties of *vortices* in section 1.4. Specifically, we look at vortices in the abelian Higgs model, Pure abelian Chern-Simons theory with scalar matter and the mixed case where both S_{Maxwell}

1. BACKGROUND

and S_{CS} play a role. We emphasize the importance of a *BPS* bound for these systems. Finally, we discuss some subtleties relating to non-abelian vortices.

We continue by addressing *Fermi-Bose and particle-vortex dualities* in 1.5, which were the primary motivation for this work. We provide the relevant information about CFTs and RG flows in order to keep the presentation self-contained. We outline important aspects of the dualities in order to highlight where our work fits in that context.

Finally, we include a section concerning the physics of *non-commutative* field theory, its relation to the theory of fluids, in particular, the description of the Quantum Hall fluid in terms of a '*fuzzy*' underlying space, in which the coordinates do not commute. We shall see that this description is a Chern-Simons theory and it seems to arise naturally out of the ground state in the finite density non-abelian model that we have studied.

1.1 Chern-Simons Theory

Chern-Simons (CS) theory is a very unusual type of QFT both in its origin and its applications. It is a testament to the power and universality of mathematics, first conceived of as an abstract tool in the theory of differential operators and their connections to topology, it has grown to encompass many facets of modern physics and mathematics. From the computation of knot invariants to the prediction of non-abelian anyons, which are the ingredients necessary for performing a topological quantum computation – currently one of the most promising approaches to fault tolerant quantum computation, due to the topological stability of the qubits. It is an example of a topological field theory (TQFT), which means that it is independent of the metric and so any observable is related to a topological invariant. It is the basis for three dimensional gravity [2], provides a field theoretic explanation for the Quantum Hall Effect and anyonic physics [3, 4], has been instrumental in the classification of rational 2D CFTs [5], creates a bridge between theoretical physics and knot theory [6] and, recently, it has uncovered an equivalence between two types of matter, previously thought to have been fundamentally different – namely Fermi-Bose duality [7]. These are among the most noteworthy applications of CS theory.

1.1 Chern-Simons Theory

Therefore, in this section we justly take the time to review essential aspects of CS theory. Most of the results seen in this section, can also be found in the excellent review by Dunne [8].

In the study of fundamental physics, we should assume that any term in the Lagrangian that is not forbidden by a basic principle (*e.g.* a symmetry or gauge-invariance) should be included in order to account for all aspects of the system at hand. From gauge theory we are familiar with the idea of introducing a gauge field to render a Lagrangian gauge invariant and then include a gauge-invariant Yang-Mills term that is responsible for the dynamics of the gauge potential. Modulo subtleties, this is true in any number of dimensions. Taking these subtleties into account, it turns out that in 2+1 dimensions, the Yang-Mills term is not the only gauge invariant term one can include. One can write down a term in the action, which is the integral of a three-form, depending solely on the gauge field A_μ . This term, whilst not manifestly gauge invariant, leaves the partition function unchanged under gauge transformations. This three-form is the Chern-Simons Lagrangian, which we write down here.

$$\mathcal{L}_{CS} = \kappa \epsilon^{\mu\nu\rho} \operatorname{Tr} \left[A_\mu \partial_\nu A_\rho + \frac{2}{3} A_\mu A_\nu A_\rho \right]. \quad (1.1)$$

The gauge field A_μ takes values in a finite dimensional representation of the (semi-simple) gauge Lie algebra \mathfrak{G} . In an abelian theory, the gauge fields A_μ commute, and so the trilinear term in (1.1) vanishes due to the antisymmetry of the $\epsilon^{\mu\nu\rho}$ symbol. In the nonabelian case (just as in Yang-Mills theory) we write

$$A_\mu = A_\mu^a T^a, \quad (1.2)$$

where the T^a are the generators of \mathfrak{G} (for $a = 1, \dots, \dim(\mathfrak{G})$), satisfying the commutation relations

$$[T^a, T^b] = f^{abc} T^c, \quad (1.3)$$

1. BACKGROUND

and the normalization

$$tr(T^a T^b) = -\frac{1}{2} \delta^{ab}. \quad (1.4)$$

We can define the field strength tensor in the usual way for a non-abelian gauge theory

$$F_{\mu\nu} = \partial_\mu A_\nu - \partial_\nu A_\mu + [A_\mu, A_\nu]. \quad (1.5)$$

$F_{\mu\nu}$ transforms in such a way that any expression that is the trace of a string of F 's is gauge invariant. Since this Lagrangian is written in terms of A_μ as opposed to F , gauge invariance is no manifest.

Before we delve into the details of the gauge invariance, it is helpful to venture into a quick digression about *topology*. Topological invariants are such properties of spaces (and hence of field configurations defined on those spaces) that do not change under continuous transformations. And since most phenomena in the real world are continuous, we should expect that these invariants are important tools that we can use to better understand the physical world. Indeed, we shall see that these expectations are justified.

One way topologists use to classify spaces is through *homotopy groups*. An example is the first homotopy group π_1 or the *fundamental group*. This group is an indicator of the “connectivity” of a manifold. Its definition has to do with whether a given loop can be contracted to a point. More precisely, one can define a group at each point on a manifold, whose elements are equivalency classes of loops that start and end at that point *and* are continuously deformable into each other. For example, if all loops on a given space can be contracted to a point, then the fundamental group π_1 is trivial, since all elements of the group are the identity. The group operation on these loops is such that we create a new loop from g_1 and g_2 by going around g_1 first, then followed by going around g_2 . It turns out that loops that encircle a singular point (or hole in the space) n times are **not** continuously deformable into loops that encircle said point n' times, if $n \neq n'$. This is an intuitive way of understanding the fact that for each hole in the space-time manifold, the fundamental group

1.1 Chern-Simons Theory

acquires a cartesian factor of \mathbb{Z} . Meaning that loops can wind around singular points arbitrarily many integer number of times and the number of loops around one singular point is independent of the number around another.

Such a classification is not restricted to loops but can also be applied to higher dimensional spheres. For example, the classes of mappings from the 3-sphere to 3-dimensional Euclidean space-time are classified by π_3 . If π_3 is non-trivial, this tells us that not all gauge transformations are connected to the identity. Importantly for the purposes of theoretical physics, it is known that $\pi_3(SU(N))$, $N \geq 2$ is non-trivial. We shall now see how this fact plays a role in the gauge invariance of Chern-Simons.

To convince ourselves of the gauge invariance, let us perform a gauge transformation

$$A_\mu \rightarrow A'_\mu \equiv g^{-1}A_\mu g + g^{-1}\partial_\mu g \quad (1.6)$$

Under this transformation, the Lagrangian changes in the following way

$$\mathcal{L}_{\text{CS}} \rightarrow \mathcal{L}_{\text{CS}} - \kappa \epsilon^{\mu\nu\rho} \partial_\mu \text{Tr} \left[\partial_\nu g g^{-1} A_\rho \right] - \frac{\kappa}{3} \epsilon^{\mu\nu\rho} \text{Tr} \left[g^{-1} \partial_\mu g g^{-1} \partial_\nu g g^{-1} \partial_\rho g \right] \quad (1.7)$$

The first term is just a boundary term which vanishes. The second term turns out to be proportional to the *winding density* of the gauge transformation, whose integral is an integer N homotopy invariant.

$$w(g) = \frac{1}{24\pi^2} \epsilon^{\mu\nu\rho} \text{Tr} \left[g^{-1} \partial_\mu g g^{-1} \partial_\nu g g^{-1} \partial_\rho g \right], \quad \int d^3x w(g(x)) = N \in \mathbb{Z} \quad (1.8)$$

Showing that the integral of this quantity is indeed a topological invariant is beyond the scope of this presentation. We refer the skeptical reader to the proof of Theorem 10.7 in Nakahara [9], which should at least provide some intuition.

Gauge transformations with a non-zero winding number are called *large gauge transformations*. Another way of saying this, is that they are mappings that are *not* continuously connected to the identity transformation. Here we give an example to illustrate how these gauge transformations are different.

1. BACKGROUND

Suppose we have a complex scalar field φ defined on S^1

$$\varphi : S^1 \rightarrow \mathbb{C}, \quad (1.9)$$

such that $\varphi = f(\theta)e^{i\alpha(\theta)}$, where $f \in \mathbb{R}$ and θ describes the position on the S^1 . Here the $e^{i\alpha(\theta)}$ can be absorbed into a $U(1)$ gauge transformation. Below (Fig 1.1) we have represented pictorially the phase of the scalar at a point on the manifold (in this case S^1) as a red arrow pointing in a direction on the plane. In (a) we have $\alpha(\theta) = \frac{\pi}{2}$. It is not hard to convince ourselves that we can transform this configuration to $\alpha(\theta) = 0$ by making the same infinitesimal changes at every point on S^1 . Thus $\alpha(\theta) = \frac{\pi}{2}$ is an example of the familiar kind of “small gauge transformation”. One can go from (a) to (b) by setting $\alpha = \theta - \pi$. However, in this case we see that there is no way to make small transformations that are continuous. Configurations (b) and (c) are said to be in different homotopy classes, but they are in the same gauge equivalency class as (a).

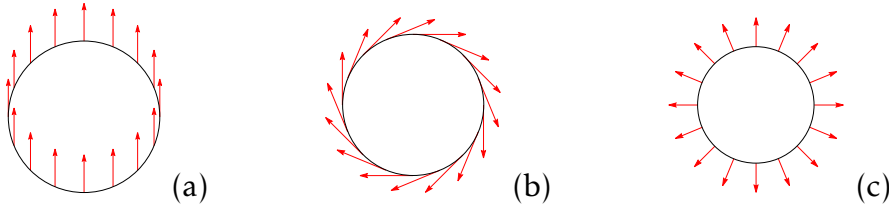


Figure 1.1: (a) is topologically distinct from the rest, yet they are all gauge equivalent configurations.

As a final remark to counter the point that “We don’t live on a circle”, I shall say that when studying a non-singular circularly symmetric planar setup, we would require boundary conditions which identify the point at infinity with the same gauge-field configuration. It turns out that the point at infinity is an S^1 , so inevitably abelian gauge transformations *would be* separated into distinct homotopy classes.

This above passage illustrates the essence of large gauge transformations in the simplest possible case, where we have a non-trivial homotopy group. The situation is precisely the same with more complicated homotopy groups but they just happen to be more difficult to visualize.

1.1 Chern-Simons Theory

Going back to the Lagrangian transformation law, we pick g , s.t. $w(g) = N$. Therefore

$$S_{\text{CS}} \rightarrow S_{\text{CS}} + 8\pi^2\kappa N. \quad (1.10)$$

Here we see that the action is *not* gauge invariant! However, keep in mind that what plays a role in the path integral is e^{iS} , which transforms as

$$e^{iS_{\text{CS}}} \rightarrow e^{i8\pi^2\kappa N} e^{iS_{\text{CS}}}. \quad (1.11)$$

This implies that if we set $\kappa = \frac{k}{4\pi}$, where $k \in \mathbb{Z}$, we have restored gauge invariance, which means that we ought to include this term in the study of planar physics.

Let us look at some physical properties that the action functional $S_{\text{CS}} = \int d^3x \mathcal{L}_{\text{CS}}$ possesses. Performing the functional variation, we get the equation of motion $F_{\mu\nu} = 0$, implying only pure gauge solutions exist. This might make one wonder, what could possibly be so interesting about CS theory if the classical equations of motion are trivial!? The reason that this theory is in fact interesting and non-trivial, despite the fact that $F = 0$, is two-fold. Firstly, CS is a topological field theory. It has trivial local properties. All of the physics is encoded in the topology of the manifold and in the non-local observables such as Wilson loops that require us to study the full quantum theory.

The second way in which CS is interesting teaches us the old lesson that sometimes the whole is greater than the sum of its parts. In this case, adding matter or a Maxwell term to the Lagrangian alters the pure Maxwell/matter theories immensely. Let us see how these alterations play out.

1.1.1 Chern-Simons-Maxwell Theory

Here we consider the familiar Maxwell theory deformed by a Chern-Simons term.

$$\mathcal{L}_{\text{MCS}} = \int d^3x \left[\frac{-1}{4g^2} F_{\mu\nu} F^{\mu\nu} + \frac{k}{4\pi} \epsilon^{\mu\nu\rho} A_\mu \partial_\nu A_\rho \right] \quad (1.12)$$

1. BACKGROUND

This leads to the equations of motion

$$\partial_\mu F^{\mu\nu} + \frac{k}{4\pi} g^2 \epsilon^{\nu\alpha\beta} F_{\alpha\beta} = 0 \quad (1.13)$$

If we rewrite this equation in terms of the dual field strength $\tilde{F}_\mu = \frac{1}{2}\epsilon_{\mu\nu\rho}F^{\nu\rho}$ by contracting with an ϵ tensor, followed by a ∂ contraction, using the equations of motion again and noting that $\partial_\mu \tilde{F}^\mu = 0$ (3D Bianchi identity), we arrive at

$$\left[\partial_\mu \partial^\mu + \left(\frac{k}{2\pi} g^2 \right)^2 \right] \tilde{F}^\nu = 0. \quad (1.14)$$

Observing that \tilde{F}^μ is gauge-invariant, we deduce that these equations describe a propagating wave with mass $(\frac{k}{2\pi}g^2)$. Even though in this work we shall promptly be ignoring the Maxwell contribution to the planar physics, it is important to note that despite the fact that the gauge bosons are heavy, we still observe global effects. This provides us with a more general lesson about CS. Namely, that we can have significant long-range global effects, such as the anyonic phase change interaction, even in the case of a gapped phase (such as the Quantum Hall droplet). Next, we turn to the matter sector.

1.1.2 Chern-Simons Matter Theory

We begin by coupling the Chern-Simons gauge field to a general conserved matter current.

$$S = \int d^3x \frac{k}{4\pi} \epsilon^{\mu\nu\rho} Tr \left[A_\mu \partial_\nu A_\rho + \frac{2}{3} A_\mu A_\nu A_\rho \right] + J^\mu A_\mu. \quad (1.15)$$

This action leads to a modified equation of motion.

$$\frac{k}{4\pi} \epsilon^{\mu\nu\rho} F_{\nu\rho}^a = J^{\mu a}, \quad (1.16)$$

1.1 Chern-Simons Theory

where $a = 1, \dots, \dim(\mathfrak{G})$ and $F_{\mu\nu}^a = \partial_\mu A_\nu^a - \partial_\nu A_\mu^a + [A_\mu, A_\nu]^a$. Note that covariant current conservation is equivalent to the non-abelian Bianchi identity

$$D_\mu J^{\mu a} = \frac{k}{4\pi} \epsilon^{\mu\nu\rho} D_\mu F^{\nu\rho a} = 0, \quad (1.17)$$

where $D_\mu F_{\nu\rho} = \partial_\mu F_{\nu\rho} + [A_\mu, F_{\nu\rho}]$.

Restricting ourselves to the abelian case, we examine the equations of motion component by component. If $J_\mu = (\rho, J^i)$ then

$$\rho = \frac{k}{4\pi} B, \quad (1.18)$$

$$J^i = \frac{k}{4\pi} \epsilon^{ij} E_j, \quad (1.19)$$

where B is the magnetic field perpendicular to the plane and E_j is the electric field. The first equation (1.18) relates the charge density to the magnetic field. So for a non-zero value of k , we find that anywhere there is charge, there is also magnetic flux penetrating through it perpendicular to the plane. This is something quite unlike Maxwell theory, where charge *movement* generates a magnetic field, as opposed to charge *presence*. This is illustrated in Figure 1.2 for a collection of localized charge distributions. The second equation (1.19) ensures that this charge-flux relation is preserved under time evolution. If we act with ∂ on (1.19) then we arrive at

$$\begin{aligned} \partial_i J^i &= \frac{k}{4\pi} \epsilon^{ij} \partial_i E_j \\ &= \frac{k}{4\pi} \epsilon^{ij} \partial_i (\partial_j A_0 - \partial_0 A_j) \\ &= -\frac{k}{4\pi} \dot{B} = -\dot{\rho}, \end{aligned} \quad (1.20)$$

which is just the continuity equation $\dot{\rho} + \partial_i J^i = 0$.

The final aspect of Chern-Simons theory that we will use is the fact that it is a *topological* field theory (TQFT). This means that the theory is independent of the metric. This consequently implies that the CS term does not contribute

1. BACKGROUND

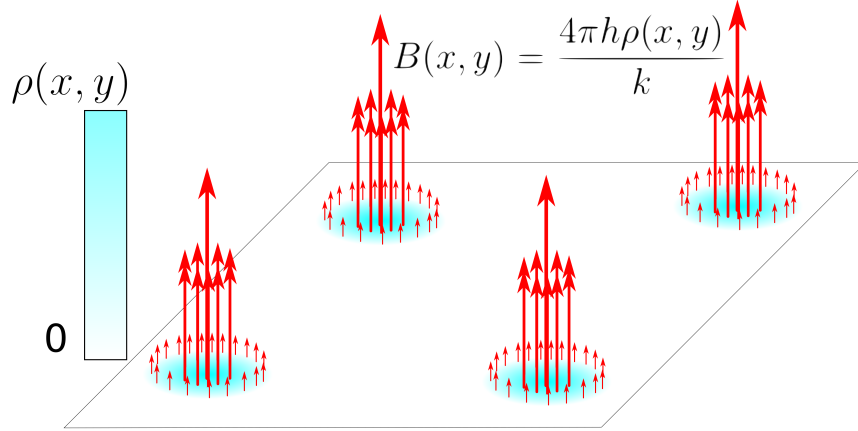


Figure 1.2: A collection of localized charge distributions, and with magnetic flux lines of strength $\frac{4\pi h\rho(x,y)}{k}$ tied to the charges. The charge and flux are tied together throughout the motion of the particles as a result of the Chern-Simons equations (1.18) - (1.19).

to the energy-momentum tensor, since

$$T^{\mu\nu} = \frac{-2}{\sqrt{-g}} \frac{\delta S_{\text{CS}}}{\delta g_{\mu\nu}} = 0. \quad (1.21)$$

One way to see that CS is a topological field theory is by writing it as an integral of a differential form.

$$S_{\text{CS}} = \frac{k}{4\pi} \int (A \wedge d \wedge A + A \wedge A \wedge A). \quad (1.22)$$

This construction does not require the metric to be defined, unlike the Yang-Mills term, which involves the hodge star (a metric dependent construct) in order to be defined through differential forms.

This concludes our review of CS theory. We now move on to a refresher of statistical physics.

1.2 Statistical Physics

Here we motivate the study of QFT as a gateway into understanding phenomena in many body physics. Physical phenomena at macro scale require micro scale explanations. The transition between a microscopic theory and its observable large scale properties is facilitated by the use of techniques in statistical mechanics. Here we review the connection between microscopic Lagrangian formulation and the statistical partition function through the formalism of the path integral. We follow through by accentuating the treatment of a chemical potential and the subtleties related to it. Before we go on, I note that this is the only part of this section that will be relevant to the calculations performed in this work. However, the rest of this section is meant to shine a light on why it is that we are interested in such an abstract problem.

Upon completing this summary, we go through a short review of statistical mechanical paradigms, their successes and shortcomings. In particular, we will highlight how the Landau-Fermi liquid theory manages to do away with the complications arising from interactions and how successful the Landau-Ginzburg symmetry breaking ideas have been in explaining large swathes of interesting phases of matter.

Finally, the failures of these extremely successful ideas will lead us to strongly correlated and topological systems. Notably, we discuss one system that seems to reject treatment from both of the above approaches – a system of strongly interacting electrons confined to 2 dimensions, namely, the physical setup in which we observe the quantum hall effect. As the reader might suspect, the planar confinement is what forces us into considering CS theory as a natural candidate to explain the exotic properties of this structure.

1.2.1 Functional Integral Representation of the Partition Function

In this section we derive the functional integral representation of the partition function for interacting relativistic non-gauge field theories. Let $\hat{\phi}(\mathbf{x}, 0)$ be a Schrödinger picture field operator at time $t = 0$. We define its conjugate

1. BACKGROUND

momentum operator to be $\hat{\pi}(\mathbf{x}, 0)$. The eigenstates of the field operator are labeled $|\phi\rangle$ and satisfy

$$\hat{\phi}(\mathbf{x}, 0)|\phi\rangle = \phi(\mathbf{x})|\phi\rangle, \quad (1.23)$$

where $\phi(\mathbf{x})$ is the eigenvalue of $|\phi\rangle$. This is complemented with the completeness and orthogonality relation

$$\int d\phi(\mathbf{x})|\phi\rangle\langle\phi| = 1, \quad (1.24)$$

$$\langle\phi_a|\phi_b\rangle = \prod_x \delta(\phi_a(\mathbf{x}) - \phi_b(\mathbf{x})) \quad (1.25)$$

And similarly for the conjugate momentum

$$\hat{\pi}(\mathbf{x}, 0)|\pi\rangle = \pi(\mathbf{x})|\pi\rangle, \quad (1.26)$$

$$\int d\pi(\mathbf{x})|\pi\rangle\langle\pi| = 1, \quad (1.27)$$

$$\langle\pi_a|\pi_b\rangle = \prod_x \delta(\pi_a(\mathbf{x}) - \pi_b(\mathbf{x})) \quad (1.28)$$

Suppose we have a Hamiltonian with no explicit time dependence

$$H = \int d^2x \mathcal{H}(\hat{\phi}, \hat{\pi}). \quad (1.29)$$

Assume that a system is in a state $|\phi_a\rangle$ at time $t = 0$. After a time t_f it evolves to $e^{-iHt_f}|\phi_a\rangle$, assuming that the Hamiltonian has no explicit time dependence. The transition amplitude for going from state $|\phi_a\rangle$ to state $|\phi_b\rangle$ after a time t_f is $\langle\phi_b|e^{-iHt_f}|\phi_a\rangle$. In order to study a system at thermodynamic equilibrium, we will be interested in the amplitude for the system returning to the same state after a time t_f . To be able to compute this amplitude, we divide the time interval $(0, t_f)$ into N equal time steps $\Delta t = \frac{t_f}{N}$. Then at each time interval, we insert a complete set of states, alternating between field operators and their conjugate momenta

$$\begin{aligned}
 \langle \phi_a | e^{-iHt_f} | \phi_a \rangle &= \lim_{N \rightarrow \infty} \int \left(\prod_{i=1}^N \frac{d\pi_i d\phi_i}{2\pi} \right) \\
 &\quad \times \langle \phi_a | \pi_N \rangle \langle \pi_N | e^{-iH\Delta t} | \phi_N \rangle \langle \phi_N | \pi_{N-1} \rangle \\
 &\quad \times \langle \pi_{N-1} | e^{-iH\Delta t} | \phi_{N-1} \rangle \dots \\
 &\quad \times \langle \phi_2 | \pi_1 \rangle \langle \pi_1 | e^{-iH\Delta t} | \phi_1 \rangle \langle \phi_1 | \phi_a \rangle. \tag{1.30}
 \end{aligned}$$

In order to evaluate this expression, we need to do several things. First of all, from single particle QM, we know that

$$\langle x | p \rangle = e^{ip \cdot x}. \tag{1.31}$$

So an appropriate generalization for this inner product to field operators is

$$\langle \phi_{i+1} | \pi_i \rangle = \exp \left(i \int d^2x \pi_i(\mathbf{x}) \phi_{i+1}(\mathbf{x}) \right) \tag{1.32}$$

Since $\Delta t \rightarrow 0$, we can expand as follows, keeping terms up to first order:

$$\begin{aligned}
 \langle \pi_i | e^{-iH_i \Delta t} | \phi_i \rangle &\sim \langle \pi_i | (1 - iH_i \Delta t) | \phi_i \rangle \\
 &= \langle \pi_i | \phi_i \rangle (1 - iH_i \Delta t) \\
 &= (1 - iH_i \Delta t) \exp \left(-i \int d^2x \pi_i(\mathbf{x}) \phi_i(\mathbf{x}) \right), \tag{1.33}
 \end{aligned}$$

where

$$H_i = \int d^2x \mathcal{H}(\pi_i(\mathbf{x}) \phi_i(\mathbf{x})) \tag{1.34}$$

1. BACKGROUND

In the end we arrive at

$$\begin{aligned} \langle \phi_a | e^{-iHt_f} | \phi_a \rangle &= \lim_{N \rightarrow \infty} \int \left(\prod_{i=1}^N \frac{d\pi_i d\phi_i}{2\pi} \right) \delta(\phi_1 - \phi_a) \\ &\quad \times \exp \left(i\Delta t \sum_{j=1}^N \int d^2x \left[\frac{\pi_j(\phi_{j+1} - \phi_j)}{\Delta t} - \mathcal{H}(\pi_j, \phi_j) \right] \right). \end{aligned} \quad (1.35)$$

And taking the continuum limit we arrive at the path integral representation of the partition function

$$\begin{aligned} \langle \phi_a | e^{-iHt_f} | \phi_a \rangle &= \int \mathcal{D}\pi \int_{\phi(x,0)=\phi_a(x)}^{\phi(x,t_f)=\phi_a(x)} \mathcal{D}\phi \\ &\quad \times \exp \left[i \int_0^{t_f} dt \int d^2x \left(\pi(x, t) \frac{\partial \phi(x, t)}{\partial t} - \mathcal{H}(\phi(x, t), \pi(x, t)) \right) \right]. \end{aligned} \quad (1.36)$$

For a Hamiltonian that is quadratic in the canonical momenta, we can just complete the square, integrate out the momenta and arrive at the usual expression for a transition amplitude in terms of a path integral over e^{iS} . Since our purpose here is to illuminate the connection between the statistical partition function and the path integral, we shall perform a few more manipulations.

1.2.2 Grand Canonical Ensemble

First, we note that the grand canonical partition function is defined as follows

$$Z = \text{tr} \left[e^{-\beta(H-\mu N)} \right], \quad (1.37)$$

where $\beta = \frac{1}{k_b T}$ and is the inverse temperature and μ is the *chemical potential*, and N is a particle number. In a QFT this particle number will be associated with a conserved charge that is discretized, which is the reason why it is associated to particle number. We can express the trace in the ϕ basis

$$Z = \int d\phi_a \langle \phi_a | e^{-\beta(H-\mu N)} | \phi_a \rangle. \quad (1.38)$$

We see that this expression is very similar to 1.36. In order to match the two expressions, we need to do three things. First, we set $t \rightarrow -i\tau$, such that $t_f \rightarrow -i\beta$. Then we shift the Hamiltonian density in order to account for the inclusion of a chemical potential

$$\mathcal{H}(\phi(\mathbf{x}, t), \pi(\mathbf{x}, t)) \rightarrow \mathcal{H}(\phi(\mathbf{x}, t), \pi(\mathbf{x}, t)) - \mu \mathcal{N}(\phi(\mathbf{x}, t), \pi(\mathbf{x}, t)), \quad (1.39)$$

where \mathcal{N} is a number density. Finally, we include the trace operation, which integrates over all possible boundary conditions. In the end we are left with

$$Z = \int \mathcal{D}\pi \int_{\text{periodic}} \mathcal{D}\phi \exp \left[\int_0^\beta \int d^2x \left(\pi \frac{\partial \phi}{\partial t} - \mathcal{H}(\pi, \phi) + \mu \mathcal{N}(\pi, \phi) \right) \right]. \quad (1.40)$$

This is the path integral representation of the partition function of the grand canonical ensemble of a single real scalar field. This expression is readily generalizable to more fields by integrating over the extra fields and their respective conjugate momenta.

Here we shall make a few observations that will come in use frequently for the rest of this work. For the purposes of presentation, we will elaborate on these points in the context of a somewhat simpler model. This should not alarm the reader, because the properties we are discussing are more general and model independent. With this in mind, we consider the Lagrangian description of a complex relativistic scalar in $2+1d$ with a potential $U(\phi)$.

$$\mathcal{L} = \left(\partial_\mu \phi^* \partial^\mu \phi - U(|\phi|) \right). \quad (1.41)$$

This system possesses a global symmetry

$$\phi \rightarrow e^{i\alpha} \phi, \quad \phi^* \rightarrow e^{-i\alpha} \phi^*. \quad (1.42)$$

This leads to a conserved Noether current and consequently a conserved charge

$$J_0 = -i \int d^2x (\pi \phi - \pi^\dagger \phi^\dagger), \quad (1.43)$$

where $\pi = \frac{\delta \mathcal{L}}{\delta(\partial_0 \phi)}$ is the canonical momentum. Based on the assumption of

1. BACKGROUND

identical particles with discrete charges, we postulate that $J_0 = \mathcal{N}$. Next, we perform the momentum integrals in (1.40). Since now we have a complex field, we have to integrate over all of ϕ , ϕ^\dagger , π and π^\dagger .

$$\begin{aligned} Z &= \int \mathcal{D}\pi \mathcal{D}\pi^\dagger \int_{\text{periodic}} \mathcal{D}\phi \mathcal{D}\phi^\dagger \\ &\times \exp \left[\int_0^\beta \int d^2x \left(\pi \frac{\partial \phi}{\partial t} + \pi^\dagger \frac{\partial \phi^\dagger}{\partial t} - \mathcal{H}(\pi, \pi^\dagger, \phi, \phi^\dagger) - i\mu(\pi\phi - \pi^\dagger\phi^\dagger) \right) \right] \\ &= \int \mathcal{D}\pi \mathcal{D}\pi^\dagger \int_{\text{periodic}} \mathcal{D}\phi \mathcal{D}\phi^\dagger \\ &\times \exp \left[\int_0^\beta \int d^2x \left(\pi \left(\frac{\partial \phi}{\partial t} - i\mu\phi \right) + \pi^\dagger \left(\frac{\partial \phi^\dagger}{\partial t} + i\mu\phi^\dagger \right) - \mathcal{H}(\pi, \pi^\dagger, \phi, \phi^\dagger) \right) \right] \quad (1.44) \end{aligned}$$

Performing the path integral leaves us with

$$Z = \int_{\text{periodic}} \mathcal{D}\phi \mathcal{D}\phi^\dagger \exp \left[\int_0^\tau d\tau \int d^2x \mathcal{L}' \right], \quad (1.45)$$

where \mathcal{L}' is the same as \mathcal{L} except for the time derivatives acting on ϕ now act as covariant derivatives in the presence of a constant background gauge field $A_0 = \mu$, i.e.

$$\partial_0 \rightarrow \partial_0 - i\mu. \quad (1.46)$$

This is a general result that we will be making use of numerous times.

1.2.2.1 Chemical Potential for a Local Symmetry

Now, let us see how this situation changes when we try to introduce a chemical potential for a gauged symmetry. First, we modify the Lagrangian \mathcal{L} by gauging the $U(1)$ and adding a Maxwell term $-\frac{1}{4g^2}F_{\mu\nu}F^{\mu\nu}$. For simplicity, let us assume that the potential has the monomial super-renormalizable form

$$U(|\phi|) = \lambda|\phi|^4. \quad (1.47)$$

Therefore

$$\mathcal{L} = (D_\mu \phi)^* D^\mu \phi - \lambda |\phi|^4 - \frac{1}{4g^2} F_{\mu\nu} F^{\mu\nu}, \quad (1.48)$$

where $D_\mu = \partial_\mu - iA_\mu$. According to the rule 1.46 that we established above ,

$$\mathcal{L} \rightarrow \mathcal{L}' = \mathcal{L}(\phi, D'_\mu \phi, A_\mu), \quad (1.49)$$

where $D'_\mu = D_\mu - i\mu \delta_{\mu 0}$. Let us also express ϕ in terms of a modulus and a phase

$$\phi(x) = \sigma(x) e^{i\alpha(x)}. \quad (1.50)$$

If we assume a homogenous, constant configuration, the equations of motion tell us that

$$\sigma = \sqrt{\frac{\mu^2}{2\lambda}} \quad (1.51)$$

$$\frac{1}{g^2} \partial_\mu F^{\mu 0} = \mu \sigma^2. \quad (1.52)$$

The first equation tells us that the scalars have condensed to the ground state. The second equation states that we have a non-zero charge density in this ground state. On the one hand, this makes sense, since the charged scalars have condensed. On the other hand, this is contradictory, since we are studying a system at equilibrium. And a charged system cannot be in equilibrium by definition. In order to fix this problem, we introduce a background charge density, which guarantees that the system is neutral.

$$\mathcal{L}' \rightarrow \mathcal{L}' - A_0 J_0, \quad (1.53)$$

where $J_0 = \frac{\mu^3}{2\lambda}$.

The statistical description of weakly interacting particles, for example, in a fluid can be thought of as the same as that of a free gas of non-interacting quasiparticles that are in one to one correspondence with the original interacting excitations of the material. We find that in order to explain some of the surprising feature of the charge carriers in a QH system, we need to go beyond

1. BACKGROUND

the weakly interacting description of a Landau-Fermi liquid.

1.3 Fractional Quantum Hall Effect

Here we discuss what is perhaps the most applied aspect of TQFT in the real world. But before we get to the point of discussing the highly non-trivial physics of the various types of Quantum Hall Effects, we take a moment to review the classical picture.

1.3.1 Classical Hall Effect

In the year 1879, Edwin Hall set up an experiment consisting of a conductor plate with two electrodes attached at either end of it, generating a current, and a magnetic field penetrating the surface of the conductor perpendicularly. He found that he could measure a non-zero potential across the conductor, orthogonal to the plane defined by the driving current and the magnetic field. The generation of this potential difference has since been known as the *Hall effect*. Despite this being an exciting discovery at the time, from our modern perspective this is all accounted by basic knowledge of conductors and classical electrodynamics. In the presence of a magnetic field, the charge carriers, which are responsible for the current in the conductor, get deflected in a direction orthogonal to their motion due to the Lorentz force

$$F = q(E + \mathbf{v} \times \mathbf{B}), \quad (1.54)$$

where q is the charge of the electrons, E is the electric field due to the potential difference in the electrodes, \mathbf{v} is the velocity of the charge carriers and \mathbf{B} is the magnetic field in the material. If we were to account for the possible collisions that may occur within a sample of the conductor, which will cause the charge carriers (in this case electrons) to slow down, we shall arrive at a slightly modified equation to the Lorentz law from above

$$m\dot{\mathbf{v}} = qE + q\mathbf{v} \times \mathbf{B} - \frac{1}{\tau}m\mathbf{v}, \quad (1.55)$$

where τ is the *scattering time* – it accounts for how frequently the electrons scatter, hence a large scattering time makes the term disappear completely. This description of the charge carriers in a material, subject to both electric and magnetic field, in the presence of impurities, is called the *Drude model*, named after the German physicist Paul Drude, who first proposed it. Before we look at the general solution of this model, we make several remarks about certain limiting cases.

First, assume that there are no collisions (*i.e.* the collision time diverges $\tau \rightarrow \infty$) and that there is no electric field. Then the system simplifies to

$$m\dot{\mathbf{v}} = q\mathbf{v} \times \mathbf{B}. \quad (1.56)$$

For a particle confined to the plane the velocity vector is $\mathbf{v} = (\dot{x}, \dot{y})$, which leads to the system of two coupled linear ODEs

$$m\ddot{x} = qB\dot{y}, \quad m\ddot{y} = -qB\dot{x}. \quad (1.57)$$

The general solution to this system is

$$x(t) = x_0 + R \sin(\omega_B t + \varphi) \quad (1.58)$$

$$y(t) = y_0 + R \cos(\omega_B t + \varphi), \quad (1.59)$$

where x_0, y_0, R, φ are all integration constants and

$$\omega_B = \frac{qB}{m} \quad (1.60)$$

is the *cyclotron frequency*. We see that the solution in the absence of collisions and an electric potential is circular motion with a fixed magnetic field dependent frequency.

Let us go back to the full Drude model. We would like to find out what the equilibrium of the system looks like. This implies that $\dot{v} = 0$. The equation of

1. BACKGROUND

motion becomes

$$\mathbf{v} - \frac{q\tau}{m}\mathbf{v} \times \mathbf{B} = \frac{\tau q}{m}\mathbf{E} \quad (1.61)$$

$$\begin{bmatrix} 1 & -\frac{q\tau B}{m} \\ \frac{q\tau B}{m} & 1 \end{bmatrix} \mathbf{v} = \frac{\tau q}{m} \mathbf{E}. \quad (1.62)$$

Subsituting $\mathbf{J} = q\mathbf{v}$ and $\omega_B = \frac{qB}{m}$

$$\begin{bmatrix} 1 & -\omega_B \tau \\ \omega_B \tau & 1 \end{bmatrix} \mathbf{J} = \frac{\tau q^2}{m} \mathbf{E}. \quad (1.63)$$

After inverting we arrive at *Ohm's law*

$$\mathbf{J} = \sigma \mathbf{E}, \quad (1.64)$$

where

$$\sigma = \frac{q^2 \tau}{m(\tau^2 \omega_B^2 + 1)} \begin{bmatrix} 1 & \tau \omega_B \\ -\tau \omega_B & 1 \end{bmatrix} \quad (1.65)$$

is the *conductivity tensor*. It is related to the *resistivity tensor* by

$$\rho = \sigma^{-1} = \frac{m}{q^2 \tau} \begin{bmatrix} 1 & -\tau \omega_B \\ \tau \omega_B & 1 \end{bmatrix} = \begin{bmatrix} \rho_{xx} & \rho_{xy} \\ \rho_{yx} & \rho_{yy} \end{bmatrix}, \quad (1.66)$$

where $\rho_{xx} = \rho_{yy}$ and $\rho_{xy} = -\rho_{yx}$.

This equation tells us that in the presence of a constant magnetic field, the charge carriers experience two types of resistivity. One is the usual type of resistivity that you can expect from a conductor $\rho_{xx} = \frac{m}{q^2 \tau}$ – It is independent of the magnetic field and as the scattering time increases, *i.e.* the number of scattering events decreases, the resistivity decreases. The other type of resistivity is different. The off-diagonal component of the resistivity $\rho_{yx} = \frac{m \omega_B}{q^2} = \frac{B}{q}$ is independent of τ . So somehow the resistivity in the direction orthogonal to that of the driving current does not depend on the impurities in the material. Another way in which ρ_{yx} is different is that it depends on the magnetic field. Surprisingly, as $B \rightarrow 0$ so does $\rho_{yx} \rightarrow 0$. It would be incorrect to assume that

the vanishing of ρ_{xy} implies that we achieve superconductivity, since σ_{xy} also vanishes so there is no current being generated perpendicular to the generating electric field.

The Drude model is successful when compared to the classical experimental results obtained by Hall since it predicts correctly that the resistivity ρ_{xy} would grow linearly with the magnetic field B .

1.3.2 Quantum Hall Effect

Now that we have an understanding of the classical Hall effect we are ready to delve into the physics of the quantum hall effect. It's important to distinguish two different types of quantum Hall effects, since they are qualitatively different, occur in different materials and seem to have fundamentally different physical explanations. The first type is the Integer Quantum Hall effect. In 1980, Klaus von Klitzing was performing the Hall experiment at ultralow temperatures with strong magnetic fields and found that the above relation between ρ_{yx} and B does not hold for large enough magnetic fields. He found that beyond a certain magnetic field strength, plateaux started appearing in the resistivity that could not be explained by the classical picture. Further, he found that in the plateaux, where ρ_{yx} was constant, ρ_{xx} was vanishing. The precise relation that he discovered was

$$\rho_{yx} = \frac{2\pi\hbar}{e^2} \frac{1}{\nu}, \quad \nu \in \mathbb{Z}. \quad (1.67)$$

Thus the quantity $\frac{2\pi\hbar}{e^2}$ is dubbed the quantum of resistivity. The explanation of the Integer Quantum Hall effect is based on the quantum mechanics of non-interacting particles confined to a plane. In the case of the fractional quantum hall effect (FQHE), where $\nu \in \mathbb{Q}$, we need to study a highly interacting system, which makes the FQHE a very interesting topic for theoretical physics.

Our exploration of the Quantum Hall Effect will stop here. What is important to take away from this section is that the understanding of the FQHE is underlied by the study of Chern-Simons theory. Thus studying the models, that are of interest in the present work, might lead to a better understanding of the fascinating problem that is the FQHE. A further connection to this

1. BACKGROUND

problem is provided by the non-commutative Chern-Simons theory that we explore at the end of this chapter and at the end of chapter 3. Next, we turn our attention to the study of vortices.

1.4 Vortices

This section takes up the task of summarizing basic aspects about vortices in general and specifically in Chern-Simons matter theories. Vortices are localized, exact solutions to the equations of motion. They may or may not be finite energy configurations. In 1957, Abrikosov showed that if the surface tension between two phases of matter (in his case those were superconducting and non-superconducting phases) is negative, then a phase transition would be accompanied by the creation of a lattice of regions, whose interiors reside in a phase different from their exteriors [22]. He also recognized the similarity between these regions of non-superconductivity have with the vortices formed in superfluid helium. This similarity is due to the winding of the phase of the order parameter wave function.

Later on, in 1973, Nielsen & Olesen [13] showed that a solution similar to that of Abrikosov can come about through the study of a microscopic Lagrangian, as opposed to in an effective Landau-Ginzburg description. This is the Lagrangian of the abelian Higgs model with a quartic interaction. Similar solutions have been found in the abelian Higgs model with a Chern-Simons interaction by Paul-Khare [14] and in the absence of a Maxwell term by Hong-Kim-Pac [15], Jackiw and Weinberg [16] and Jackiw, Lee and Weinberg [17].

1.4.1 Global U(1) Vortex

Now we look at the properties of these solutions more closely. Before we look at the gauge theory scenario, we focus on the simplest case of a complex massive scalar with a fourth order interaction, negative mass squared and a global $U(1)$ symmetry

$$\mathcal{L} = |\partial_\mu \phi|^2 + m^2|\phi|^2 - \lambda|\phi|^4. \quad (1.68)$$

This leads to the equations of motion

$$\partial_\mu \partial^\mu \phi = m^2 \phi - 2\lambda |\phi|^2 \phi \quad (1.69)$$

This system has an S^1 vacuum manifold, parametrized by $\phi = v e^{i\theta}$, where $\theta \in [0, 2\pi)$ is the planar polar angular coordinate and $v^2 = \frac{m^2}{2\lambda}$. We may consider a field configuration that is $\phi = 0$ at the origin but approaches a different point on the vacuum manifold at spatial infinity depending on θ . More precisely, we are looking at a field ϕ such that

$$\phi \xrightarrow{r \rightarrow \infty} v e^{in\theta}, \quad (1.70)$$

where $n \in \mathbb{Z}$ in order to guarantee that the physical configuration is single-valued. We would like to compute the energy of such a static circularly symmetric configuration

$$E = 2\pi \int_0^\infty r dr \left[\lambda |\phi|^4 - m^2 |\phi|^2 + |\phi'|^2 + \frac{n^2 v^2}{r^2} \right]. \quad (1.71)$$

Close to infinity, the potential term vanishes and so does ϕ' . In the end we are left with

$$E = 2\pi n^2 v^2 \int \frac{dr}{r} = 2\pi n^2 v^2 \log R, \quad (1.72)$$

where R is the sample size on which our theory is defined. We see that the global vortex, if it exists, would only have a finite energy for finite samples and is not well-defined in the most general case. It turns out that once the global symmetry is gauged, the divergence disappears and we have a vortex configurations that is well defined in the infinite volume limit.

1.4.2 Local U(1) Vortex

The gauged $U(1)$ vortex, also known as the Abrikosov-Nielsen-Olesen vortex is again a configuration that interpolates between two different vacua in a theory, but this time we introduce a gauge field, whose dynamics is governed by

1. BACKGROUND

a Maxwell term and is minimally coupled to a $U(1)$ scalar with a symmetry breaking potential. This is the familiar abelian Higgs model.

$$S_{\text{AH}} = \int d^3x \left[-\frac{1}{4}F_{\mu\nu}F^{\mu\nu} + |D_\mu\phi|^2 - U(\phi) \right], \quad (1.73)$$

where

$$U(\phi) = \frac{\lambda}{2}|\phi|^4 - m^2|\phi|^2. \quad (1.74)$$

Again, we have non-trivial manifold of ground states and we can repeat the construction from above. This time the energy of the static radially symmetric configuration ends up slightly different.

$$E = 2\pi \int_0^\infty r dr \left(\frac{1}{2}(B^2 + E^2) + |D_\mu\phi|^2 + U(\phi) \right) \quad (1.75)$$

This time we are aiming for eliminating the divergence that arose from the kinetic term $|\partial_\mu\phi|$ by requiring that A_μ asymptotes to a value that cancels it, in such a way that this value can be arrived at through a gauge transformation, ensuring that at $r \rightarrow \infty$, A_μ is pure gauge, thus yielding a finite contribution from the electromagnetic field. Such a choice for A_μ is

$$A_\mu = n\partial_\mu\alpha(x), \quad (1.76)$$

where $\alpha(x) = \theta$. Hence

$$A_0 = 0, \quad A_r = 0, \quad A_\theta = n. \quad (1.77)$$

This implies that

$$\int_0^\infty r dr |D_\mu\phi|^2 = v^2 \int_0^\infty r dr \frac{1}{r^2} |n - A_\theta|^2 = 0. \quad (1.78)$$

From here we see that the inclusion of a gauge field has cured the divergence and we are left with a sensible infinite volume limit.

Now that we know that these boundary conditions do not lead to a divergence in the energy, let us see whether a solution with such boundary condi-

tions exists. We write down the equations of motion.

$$\begin{aligned} \frac{1}{g^2} \partial_\rho (r F^{\mu\rho}) &= ir [\phi^* (D^\mu \phi) - (D^\mu \phi)^* \phi] \\ \partial_\mu (r D^\mu \phi) - i A_\mu D^\mu \phi + \frac{\delta U}{\delta \phi^*} &= 0 \end{aligned} \quad (1.79)$$

After substituting the ansatz

$$\phi = \sqrt{\frac{m^2}{\lambda}} v(r) e^{in\theta}, \quad A_\mu = n a(r) \delta_{\theta\mu}, \quad (1.80)$$

and rescaling $r \rightarrow \frac{\hat{r}}{m}$, we arrive at a system of equations for the dimensionless functions $v(r)$ and $a(r)$.

$$\frac{1}{\hat{r}} \frac{d}{d\hat{r}} \left(\hat{r} \frac{dv}{d\hat{r}} \right) - \frac{n^2(a-1)^2 v}{\hat{r}^2} - v^3 + v = 0 \quad (1.81)$$

$$\frac{d}{d\hat{r}} \left(\frac{1}{\hat{r}} \frac{d}{d\hat{r}} a \right) - \frac{2g^2}{\lambda r} (a-1)v^2 = 0. \quad (1.82)$$

In these variables, the boundary conditions become

$$v(0) = 0, \quad a(0) = 0, \quad (1.83)$$

$$v(\infty) = 1, \quad a(\infty) = 1. \quad (1.84)$$

For small r , the solutions to these equations look like

$$v(r) = J_n(r) \sim \frac{r^n}{2^n n!} \quad (1.85)$$

$$a(r) = Cr^2 \quad (1.86)$$

And asymptotically for large r we have

1. BACKGROUND

$$v(r) = K_0(\sqrt{2}r) \sim 2^{-\frac{3}{4}} \sqrt{\frac{\pi}{r}} e^{-\sqrt{2}r} \quad (1.87)$$

$$a(r) = rK_1\left(\frac{\sqrt{2}g}{\sqrt{\lambda}}r\right) \sim 2^{-\frac{3}{4}} \sqrt{\frac{\pi r \sqrt{\lambda}}{g}} e^{-\sqrt{2}\frac{g}{\sqrt{\lambda}}r} \quad (1.88)$$

From here we can recover the masses of the gauge field and Higgs field m_H and m_a , respectively, in the Higgsed phase of the theory.

$$m_H = \sqrt{2}m, \quad m_a = \sqrt{2}\frac{g^2}{\lambda}m \quad (1.89)$$

From the form of the propagator for scalar and vector theories, we know that scalar fields act attractively, whereas gauge fields act repulsively for like-charged configurations. This tells us that when $m_a > m_H$, the gauge field decays slower than the scalar field, so if we were to place two vortices on the plane, we will observe an attractive force between them. Likewise, if $m_a < m_H$, we expect the vortices to repel each other. This line of thought hints at us that there is a critical value of the couplings, where vortices are free (non-interacting). Here we present a more precise argument for this. In order to do this, we will Bogomol'nyi's identity.

$$|D_1\phi|^2 + |D_2\phi|^2 = |D_1\phi \pm D_2\phi|^2 \pm B|\phi|^2. \quad (1.90)$$

Further, we re-express the potential by completing the square.

$$U(\phi) = \frac{\lambda}{2} \left(|\phi|^2 - v^2 \right)^2 - \frac{m^2 v^2}{2}. \quad (1.91)$$

Here we can ignore the constant since the energy is defined up to a constant (albeit an infinite one). Utilizing (1.90) and (1.91) we reach the following expression for the energy of this configuration

$$\begin{aligned}
 E &= 2\pi \int r dr \left(\frac{1}{2g^2} B^2 \pm B(|\phi|^2 - v^2) + \frac{\lambda}{2} (|\phi|^2 - v^2)^2 \right. \\
 &\quad \left. + |D_1 \phi \pm i D_2 \phi|^2 \pm B v^2 \right) \\
 &= 2\pi \int r dr \left[|D_1 \phi \pm i D_2 \phi|^2 + \frac{1}{2} \left(\frac{B}{g} \pm \lambda (|\phi|^2 - v^2) \right)^2 \right]
 \end{aligned} \tag{1.92}$$

$$\pm \left(1 - \frac{\sqrt{\lambda}}{g} \right) B (|\phi|^2 - v^2) \left] \pm n v^2, \right. \tag{1.93}$$

where we have used Stokes' theorem.

$$\int r dr B = n. \tag{1.94}$$

In order to have no interaction between the vortices, we need the energy of the n vortex, the bound state of n vortices, to be the same as the energy of n separate vortices. This implies that there is no potential energy, hence no force between them. This condition is satisfied when

$$|D_1 \phi \pm i D_2 \phi|^2 = 0, \quad \frac{B}{g} \pm \lambda (|\phi|^2 - v^2) = 0, \tag{1.95}$$

$$\lambda = g^2. \tag{1.96}$$

The above equations ((1.95) and (1.96)) are known as the BPS equations of the vortex, named after the people who first discovered a non-interacting limit for solitonic solutions in field theory – Bogomol’nyi, Prasad and Sommerfield [18] [19].

1.4.3 Particle-Vortex Duality

The considerations of the previous section are more general and they apply for more than just systems in $2+1d$ even though the details differ. In a gen-

1. BACKGROUND

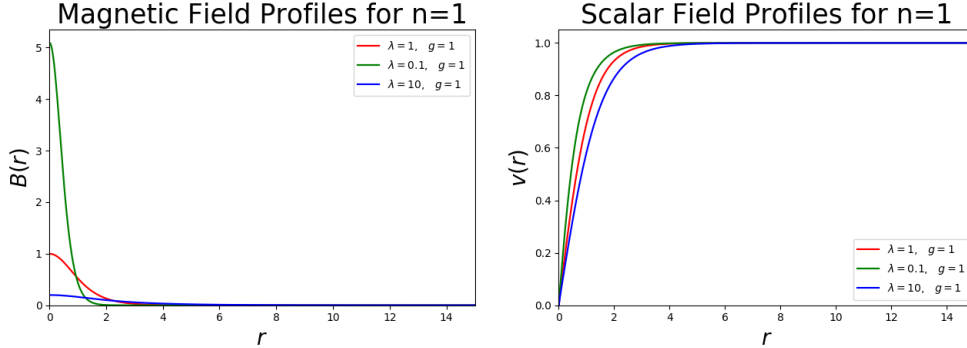


Figure 1.3: Scalar and magnetic field profiles for $n=1$ and $\lambda = (10, 1, 0.1) * \lambda_c$

eral QFT, we have roughly two different types of quantum excitations. One is the familiar type of elementary excitations that appear through the standard procedure of canonical quantization, where we introduce creation and annihilation operators that insert particles at a given position. The other type is, as we have just seen from the previous section, of a *solitonic nature* (such as vortices). In other words, a solution that we reach not through expanding around the free solution in a small coupling parameter, but is more generally associated with a stationary point parametrically far from the free theory. This makes these solutions grow in size and energy the smaller the coupling is so studying them in the quantum regime becomes tricky. Luckily, because their masses become large at small coupling, they decouple from the theory so one can study the quantum theory of the elementary excitations on its own without worrying about the solitons. Unfortunately, going in the other direction in terms of coupling strength, the solitons become light and their importance grows but so do quantum corrections for the elementary excitations and we reach a regime, where we do not understand the theory. So how do we learn more about these strongly coupled theories?

One approach that has become ever more popular in the past few decades is the idea of a *duality*. Duality suggests that instead of having one model or one Lagrangian that describes the physics of a system, we instead have two. For example, a way in which duality can manifest itself is the following. Theory *I* has elementary excitations that we can study at weak coupling and non-perturbative excitations which are inaccessible due their large mass. Whereas

m^2	< 0	$= 0$	> 0
S_{XY}	Coulomb phase $2d$ logarithmic potential	WF fixed point	SB phase local ANO vortices
S_{AH}	SB phase global vortices $E \xrightarrow{V \rightarrow \infty} \infty$	WF fixed point	Massive excitations in Coulomb phase

Table 1.1: This table shows the matching of the phases of the XY model and the Abelian Higgs model

theory II describes the solitons of theory I as its own elementary excitations at weak coupling (and a small mass) and the solitons present in theory II are in fact the elementary states of theory I . If the non-perturbative states in these systems are vortices in $2 + 1$ dimensions, then we have a type of Strong-Weak duality called a *Particle-Vortex duality*.

Since we now have a reasonable grasp of what vortices are, we are ready to introduce particle-vortex duality. And what better place to start than the Abelian Higgs model from the last section (1.73). Earlier we saw that non-perturbative solutions exist in this theory. It turns out that a model exists where the vortices of the Abelian Higgs model appear as elementary excitations. In other words, there is a duality between these two models

$$S_{\text{AH}} \longleftrightarrow S_{\text{XY}}, \quad (1.97)$$

where

$$S_{\text{XY}} = \int d^3x |\partial_\mu \tilde{\phi}|^2 - m^2 |\tilde{\phi}|^2 - \frac{\tilde{\lambda}}{2} |\tilde{\phi}|^4. \quad (1.98)$$

S_{XY} is the action for the so called *XY model* and S_{AH} is defined as in (1.73). The matching of the physics in the different phases is summarized in table (1.1).

In [20], the authors showed a link between this particle-vortex duality and bosonization. This naturally leads us to the next section, which focuses on Fermi-Bose duality.

1. BACKGROUND

1.5 Fermi-Bose Duality

We already met the idea of duality in the previous section. In general, they tend to be an equivalence of two theories. Two different ways in which we can state the same physics. Some of them are functional integral analogs of the Fourier transform (for functionals) – one phenomenon can be described either in coordinate or momentum space, by one action or another. This can be achieved by introducing a Lagrange multiplier field and integrating out the original fields. Others tend to arise in consequence of the idea of universality. Two models that flow to the same CFT in the IR will tend to be equivalent sufficiently close to the fixed point. Yet other types of duality are inspired by the study of black hole thermodynamics and the holographic principle, such as the AdS/CFT duality. Others still, seem to be a consequence of deep mathematical ideas, such as the level-rank duality.

Whatever the fundamental reasons for their existence is, dualities are interesting because they give us another point of view that allows us to explore and understand the world of fundamental physics in more depth. As Feynman once said, “Every theoretical physicist who is any good knows six or seven different theoretical representations for exactly the same physics”[24]. And in the spirit of his words, here duality is one more representation we wish to understand.

As pointed out above, dualities come in many flavours and the models we are considering here play a role in more than one type. $O(N)/U(N)$ (scalar or fermion) models are holographically dual to higher spin gravitational theories [25]. This duality seems to persist even after deforming the theories with a Chern-Simons term in the large N limit[26]. Fermions in 2+1d can be shown to be dual to vector fields via a Fourier transform-like functional integral transformation that we described above [27, 28]. And pure Chern-Simons theories are level-rank dual to each other [29–33]. In this section, we will concentrate on a duality that has all of the above ingredients in some form ($SU(N)/U(N)$ scalars/fermions and CS vector fields) that combine into what’s believed to be an IR duality. More precisely, we are talking about a set of dualities between 2 + 1d gauge theories that are collectively known as *Fermi-Bose duality*.

The duality between fermions and bosons was first conjectured in the su-

persymmetric context[34–37]. Evidence for the non-supersymmetric version of these dualities comes from large N computations on both sides both at finite temperature [38] and at $T = 0$ [39]. Furthermore, there is compelling evidence that the duality holds at finite N from supersymmetric theories flowing to their non-SUSY versions [40, 41].

Since $U(N) = (SU(N) \times U(1))/\mathbb{Z}_N$, we can in principle have different Chern-Simons levels for the $SU(N)$ and $U(1)$ symmetries. We will denote a $U(N)$ Chern-Simons theory with levels k_1 and k_2 corresponding to the $SU(N)$ and $U(1)$ symmetries, respectively, as a $U(N)_{k_1, k_2}$ theory. Prior to the inclusion of matter in our model, we state an important fact about these theories. Namely, that some choices of gauge groups and levels are dual to others. This is known as *level-rank duality*. Its generalization to include matter is the duality that we present below. In Yang-Mills regularization the Fermi-Bose dualities are as follows [7].

$$SU(N)_k + \text{scalars} \longleftrightarrow U(k)_{-N+\frac{N_f}{2}, -N+\frac{N_f}{2}} + \text{fermions}, \quad (1.99)$$

$$U(N)_{k,k} + \text{scalars} \longleftrightarrow SU(k)_{-N+\frac{N_f}{2}} + \text{fermions}, \quad (1.100)$$

$$U(N)_{k,k+N} + \text{scalars} \longleftrightarrow U(k)_{-N+\frac{N_f}{2}, -N+\frac{N_f}{2}-k} + \text{fermions}. \quad (1.101)$$

The scalars on the LHS of these equations are assumed to be tuned to a critical interacting point of the RG flow, known as the Wilson-Fisher fixed point. (Explain how the Wilson Fisher fixed point work). Similarly to PV duality, which maps elementary excitations to non-perturbative vortices, Fermi-Bose duality maps the fundamental perturbative states on one side to monopole or baryon operators on the other side.

Understanding the details of this duality subject to the inclusion of a chemical potential has been the formative motivation for this work. We believe that some of the results of this thesis have sown the seed for this understanding. More specifically, the role of the ground state discussed in chapter 3 in the duality still remains mysterious. The resolution of this mystery is left for future work. Thus we conclude our discussion of Fermi-Bose duality and move on to the physics of non-commutative fluids

1. BACKGROUND

1.6 Non-Commutative Fluids

In this section we will define important physical notions in a non-commutative geometry, show how it relates to the theory of fluids and demonstrate how the non-commutative version of the Landau problem leads directly to the non-commutative Chern-Simons action. Finally, we discuss the Fock space of this action to prepare the presentation of results that we have discovered. For a good summary of this topic, we refer the reader to this set of excellent reviews on physics on non-commutative geometry [44–46].

Non-commutative geometry can arise naturally from the quantization of a particle’s phase space coordinates. The simplest way to see this connection is through the Heisenberg algebra of the canonical commutation relations.

$$[\hat{x}, \hat{p}] = i\hbar. \quad (1.102)$$

As is well known, this quantization condition leads to a “smearing out” of the phase space structure of the theory. It makes it so that the notion of a point in phase space no longer makes sense, since one can no longer measure both position and momentum accurately.

However, there are more exotic cases, where the coordinate space becomes non-commutative or fuzzy, due to the specific form of the Poisson brackets in the problem. In such a problem, the notion of a point in space is no longer reasonable and one can no longer measure the position of a (quasi)particle to arbitrary accuracy on both axes at once. An example of a problem, where the different momenta exhibit such non-commutativity is the problem of particles in a magnetic field that we discussed earlier. Similarly, we all know that angular momentum also behaves in a non-commutative way so the idea of the spatial coordinates having non-zero commutator comes naturally. Finally, in the study of fluids, one can define a type of Poisson bracket that is restricted to the coordinate space, which leads to a non-commutative space following a canonical quantization [47]. These ideas of a non-commuting space-time were first explored by Snyder in 1947 [48, 49].

1.6.1 Review of Non-Commutative Geometry

Let us see how to define a *non-commutative space*. Here we will be concerned with a D dimensional space-time that has both a set of $D - 2p$ commuting $\{y_i, i = 2p + 1, \dots, D\}$ and $2p$ non-commuting coordinates $\{x_\alpha, \alpha = 1, \dots, 2p\}$. More precisely,

$$[y_i, y_j] = 0 \quad (1.103)$$

$$[x_\alpha, x_\beta] = i\theta_{\alpha\beta}, \quad (1.104)$$

where θ is an anti-symmetric constant one-form. One can perform linear transformations on the coordinates x_α so that the matrix θ is in canonical block form

$$\theta_{\alpha\beta} = \theta \begin{bmatrix} i\sigma_2 & & 0 \\ & \ddots & \\ 0 & & i\sigma_2 \end{bmatrix}, \quad (1.105)$$

where

$$i\sigma_2 = \begin{bmatrix} 0 & 1 \\ -1 & 0 \end{bmatrix}. \quad (1.106)$$

This leaves us with p pairs of the Heisenberg algebra

$$[x_{2\alpha-1}, x_{2\alpha}] = i\theta, \quad \alpha = 1, \dots, p. \quad (1.107)$$

This quantization of the spatial coordinates leads to the existence of a Hilbert space. Since we can now think of the coordinates as operators, then each operator has a set of eigenstates with associated quantum numbers. To make this

1. BACKGROUND

more explicit, let us define the *creation*, *annihilation* and *number* operators

$$\mathbf{a}_\alpha = \frac{x_{2\alpha-1} + ix_{2\alpha}}{\sqrt{2\theta}}, \quad \mathbf{a}_\alpha^\dagger = \frac{x_{2\alpha-1} - ix_{2\alpha}}{\sqrt{2\theta}} \quad (1.108)$$

$$\mathbf{n}_\alpha = \mathbf{a}_\alpha^\dagger \mathbf{a}_\alpha. \quad (1.109)$$

These operators allow us to build the familiar *Fock space* from QFT by acting on a vacuum state

$$|n_1, \dots, n_p\rangle = \mathbf{a}_1^{\dagger n_1} \dots \mathbf{a}_p^{\dagger n_p} |0\rangle \quad (1.110)$$

Further, we define the derivative operators through the relations

$$\partial_\mu \cdot x_\nu = [\partial_\mu, x_\nu] = \delta_{\mu\nu}, \quad \mu, \nu = 1, \dots, D. \quad (1.111)$$

Specifically for the non-commuting coordinates

$$\partial_\alpha = -i\omega_{\alpha\beta}x_\beta, \quad \alpha, \beta = 1, \dots, 2p. \quad (1.112)$$

where $\omega_{\alpha\beta} = (\theta^{-1})_{\alpha\beta}$. From here it follows that

$$[\partial_\alpha, \partial_\beta] = i\omega_{\alpha\beta}. \quad (1.113)$$

1.6.2 Non-Commutative Field Theory

Now that we understand some of the basic ideas of non-commutative geometry, we would like to define a field theory on this non-commutative space. The simplest possible gauge theory contains just a gauge field A_μ . Further, the easiest way to construct a gauge invariant theory is by forming an action that is composed of a trace of covariant derivatives

$$D_\mu = -i\partial_\mu + A_\mu, \quad (1.114)$$

since under a gauge transformation D_μ transforms as

$$D_\mu \rightarrow UD_\mu U^{-1}. \quad (1.115)$$

Restricting ourselves to the non-commuting submanifold, we have

$$D_\alpha = -i\partial_\alpha + A_\alpha = \omega_{\alpha\beta}x^\beta + A_\alpha = \omega_{\alpha\beta}(x^\beta + \theta^{\beta\gamma}A_\gamma) \equiv \omega_{\alpha\beta}X^\beta. \quad (1.116)$$

- Specifically, non-commutative Chern-Simons theory arises as the action of a massless particle confined to the plane in the presence of a magnetic field. [50] Let us take a look at the action of a particle of charge q and mass m moving in an electromagnetic field generated by the four-potential $A^\mu = (-V(\mathbf{x}, t), \mathbf{A}(\mathbf{x}, t))$

$$S = \int dt \left(\frac{1}{2}m^2v^2 - qV(\mathbf{x}, t) + q\mathbf{v} \cdot \mathbf{A}(\mathbf{x}, t) \right). \quad (1.117)$$

Now, let us assume that the particle is massless and in addition, it is in a constant magnetic field and the electric potential is 0. Since $\nabla \times \mathbf{A} = \mathbf{B}$, this implies that

$$A_i = \frac{B}{2}\epsilon_{ij}x_j, \quad (1.118)$$

where $B = |\mathbf{B}|$. Substituting this expression into (1.117)

$$S = \int dt \left(q\frac{B}{2}\epsilon_{ij}\dot{x}_i x_j \right). \quad (1.119)$$

From here we proceed by making the identification

$$x_i \leftrightarrow X_i. \quad (1.120)$$

And since the X_i 's transform under gauge transformations, we ought to make sure that the action remains invariant. To this end, we need to also gauge the time derivative $\partial_0 \rightarrow D_0 = \partial_0 + A_0$

$$S = \int dt \left[q\frac{B}{2}\epsilon_{ij}Tr(D_0X^iX^j) \right] = \int dt \left[q\frac{B}{2}\epsilon_{ij}Tr(\partial_0X^iX^j + [A_0, X^i]X^j) \right] \quad (1.121)$$

The introduction of the time component of the gauge field leads to a Gauss's

1. BACKGROUND

law constraint

$$[X^1, X^2] = 0. \quad (1.122)$$

It seems that this constraint has removed the non-commutativity that we tried to introduce into our model. In order to bring it back, we add an extra term to the action such that we get the Heisenberg algebra (1.104) that we explored earlier

$$S = \int dt \left[q \frac{B}{2} \epsilon_{ij} \text{Tr} \left(\partial_0 X^i X^j + [A_0, X^i] X^j + 2\theta A_0 \right) \right]. \quad (1.123)$$

Thus we have arrived at the non-commutative abelian Chern-Simons model by considering the movement of charged particles in a magnetic field confined to a two-dimensional plane.

Chapter 2

Abelian Chern-Simons vortices at finite chemical potential

2.1 Introduction

Chern-Simons theory and the dynamics of vortices are both intimately connected to the Quantum Hall Effect [12]. The Chern-Simons interaction has the effect of attaching a magnetic flux to a charged particle, and endowing magnetic flux carrying vortices with electric charge. Magnetic flux attachment changes the statistics of particles, so that fermions can be described as bosons with a Chern-Simons interaction. In particular, the effective theory of the fractional quantum hall state is a complex scalar interacting with an Abelian Chern-Simons gauge field [4, 12]. Vortex solitons in the relativistic Abelian-Higgs model in 2+1 dimensions in the presence of a Chern-Simons action (with or without a Maxwell term) have been extensively studied [8, 14–17, 51].

In this note we are interested in vortex solitons appearing in relativistic scalar field theory coupled to an Abelian Chern-Simons gauge field when a chemical potential for particle number is turned on. Our motivation is to investigate vortex configurations whose presence is triggered purely by finite density effects in Chern-Simons-matter theories. The Abelian Chern-Simons-scalar system offers the simplest such setting. Eventually, we would like to understand finite density vortex solutions in $SU(N)$ and $U(N)$ Chern-Simons-

2. ABELIAN CHERN-SIMONS VORTICES AT FINITE CHEMICAL POTENTIAL

scalar theories where finite chemical potential results in condensation of gauge fields, potentially breaking rotational invariance [52]¹. A broader aim for exploring different aspects of finite density physics in Chern-Simons-matter theories is to understand the implications of the associated web [20, 21, 55] of particle-vortex and Bose-Fermi dualities in 2+1 dimensions [7, 26, 38, 39, 56–60].

A chemical potential μ for a gauged $U(1)$ symmetry can only be turned on provided a source term representing a classical (frozen out) uniform background charge density is simultaneously introduced. In Chern-Simons theory, such a source can either be viewed as a distribution of heavy charges or as a uniform magnetic field. We focus on the massless scalar field with purely power law interaction potential

$$U = \frac{g_{2s}}{s} |\Phi|^{2s}, \quad s = 2, 3, \dots, \quad (2.1)$$

with no symmetry breaking minima in vacuum, and solve the equations of motion numerically with non-zero μ . Chern-Simons vortices with symmetry breaking potentials in vacuum have vanishing magnetic fields in the interior and on the outside, with the flux being supported at the edges. The finite μ vortex solutions are qualitatively different as the magnetic flux acquires support within the vortex interior, and depending on the sign of the quantized flux ($= 2\pi n$), there are two qualitatively distinct types of solutions: (i) Those with negative flux, given our choice of conventions ($\mu > 0$ and Chern-Simons level $k > 0$), where the majority of the flux resides in the vortex interior, and (ii) positive flux solutions wherein most of the flux sits at the edge of the vortex. The qualitatively different behaviour of configurations with winding numbers $n < 0$ and $n > 0$ is expected due to the breaking of charge conjugation symmetry when $\mu \neq 0$. Positive flux solutions are energetically disfavoured, or more precisely the grand potential for the n -vortex with $n > 0$ is parametrically larger, as a function of n , than that for the $n < 0$ vortex.

The negative flux solutions are the most interesting. We find these numeri-

¹An analogous situation in 3+1 dimensional Yang-Mills-Higgs system with $SU(2) \times U(1)$ gauge group was encountered in [53] where the finite density ground state breaks spatial isotropy due to condensation of vector fields. Vortex solutions in the condensed phase were subsequently found in [54].

cally for a wide range of winding numbers, $1 \leq |n| \lesssim 10^5$. Supported by simple analytical arguments, we confirm that for large $|n|$, negative flux vortices for power law potentials (2.1) with general s exhibit linear scaling of the grand potential with $|n|$:

$$\mathcal{E}(|n| \gg 1) = \frac{s-1}{2s} k \mu |n|. \quad (2.2)$$

For a specific value of the dimensionless coupling, the solutions are “BPS” or marginally bound:

$$\left. \frac{\mathcal{E}(|n|)}{|n|\mathcal{E}(1)} \right|_{\alpha=s/(s-1)} \rightarrow 1, \quad \alpha \equiv \frac{k}{4\pi} \left(\frac{g_{2s}}{\mu^{3-s}} \right)^{1/(s-1)}. \quad (2.3)$$

This critical value of α works surprisingly well even for low n vortices. Below this value individual vortices experience attractive interactions, and repulsive interactions above it. At the critical coupling, we find numerically that the vortex profiles closely (but not exactly) solve the first order Bogomolny'i type equation. Finally, the radius of the n -vortex in all cases is given by

$$R_n|_{|n| \gg 1} = \sqrt{2\alpha|n|} \mu^{-1}, \quad (2.4)$$

implying that the n -vortex behaves like a uniform incompressible droplet within which individual vortices are as closely packed as possible. The physical properties we have described closely resemble the non-relativistic supersymmetric Chern-Simons theory introduced in [61]. The scalings with n are in line with the “MIT bag” model for solitons with large winding number, advocated in [62–64].

The chapter is organised as follows: In Sections 2 and 3, we review the standard vortex equations of motion, but in the presence of chemical potential. We also point out some features of the finite density spectrum and qualitative aspects of vortex profiles. In Section 4, we discuss the energy functional or the grand potential, and argue its expected scaling for large winding numbers. In Section 5, we present several results of the numerical analysis of the vortex equations of motion for different choices of potentials and parameters.

2. ABELIAN CHERN-SIMONS VORTICES AT FINITE CHEMICAL POTENTIAL

2.2 The Abelian theory at finite chemical potential

Our starting point is the Abelian Chern-Simons theory at level k coupled to a relativistic scalar field in 2+1 dimensions. As is customary, we may regard this system as the infrared limit of the Abelian-Higgs model with a Maxwell-Chern-Simons gauge field, since the Maxwell action is irrelevant compared to the Chern-Simons term. We want to consider the theory in the grand canonical ensemble with a chemical potential for the $U(1)$ charge. Turning on a chemical potential for a local symmetry is a subtle issue since the Gauss constraint requires the total charge in the system to vanish. This putative obstacle can be overcome by introducing a uniform external classical charge density which can be viewed as a distribution of heavy charged species whose fluctuations are frozen out [65, 66]. In the presence of a Chern-Simons density this can also conveniently be viewed as a constant background magnetic field.

The $U(1)$ chemical potential is introduced as usual via a constant temporal background gauge field. Picking a $(- + +)$ metric signature, the Lagrangian density for the system is,

$$\mathcal{L} = \mathcal{L}_{matter} + \mathcal{L}_{CS} - J_0 A_0, \quad (2.5)$$

$$\mathcal{L}_{matter} = D_\nu \Phi^\dagger D^\nu \Phi + U(\Phi^\dagger \Phi)$$

$$\mathcal{L}_{CS} = \frac{k}{4\pi} \epsilon^{\nu\lambda\sigma} A_\nu \partial_\lambda A_\sigma.$$

The gauge-covariant derivatives on the complex scalar Φ include a background value μ for A_0 , which is identified as a chemical potential for the $U(1)$ charge:

$$D_\nu \equiv \partial_\nu - iA_\nu - i\mu \delta_{\nu,0}, \quad (2.6)$$

and J_0 is the background classical charge density. We assume a simple power law potential:

$$U(\Phi^\dagger \Phi) = \frac{g_{2s}}{s} |\Phi|^{2s}, \quad s \geq 2. \quad (2.7)$$

The cases of quartic ($s = 2$) and sextic ($s = 3$) potentials are special since they correspond to relevant and marginal interactions. Our main interest is in

2.2 The Abelian theory at finite chemical potential

monotonic potentials with a global minimum at $\Phi = 0$ (in the absence of a chemical potential), so that any stable vortex configurations only appear at finite density i.e. they are driven by scalar condensation in the presence of the chemical potential.

The quartic potential is of general interest because when μ vanishes, the theory flows to the 2+1 dimensional Wilson-Fisher fixed point coupled to a Chern-Simons gauge field. The critical scalar plays an important role in particle-vortex and the related web of Bose-Fermi dualities in 2+1 dimensions [7]. Semiclassical solutions are far removed from this critical point and only reliable when $\mu/g_4 \gg 1$.

The Lagrangian density expanded to show the μ -dependent terms is,

$$\begin{aligned} \mathcal{L} = & \partial_\nu \Phi^\dagger \partial^\nu \Phi + i A_\nu (\Phi^\dagger \partial^\nu \Phi - \partial^\nu \Phi^\dagger \Phi) + A_\nu A^\nu |\Phi|^2 + \frac{g_{2s}}{s} |\Phi|^{2s} - \mu^2 |\Phi|^2 \\ & + i \mu (\Phi^\dagger \partial^0 \Phi - \partial^0 \Phi^\dagger \Phi) - 2\mu A_0 |\Phi|^2 + \frac{k}{4\pi} \epsilon^{\nu\lambda\sigma} A_\nu \partial_\lambda A_\sigma - J_0 A_0. \end{aligned} \quad (2.8)$$

The background charge density J_0 is fixed by requiring that the expectation values of A_0 and the magnetic field vanish in the ground state:

$$\langle A_0 \rangle = 0 \implies J_0 = -2\mu \langle |\Phi| \rangle^2, \quad \langle |\Phi| \rangle = v = \left(\frac{\mu^2}{g_{2s}} \right)^{\frac{1}{2s-2}}. \quad (2.9)$$

The ground state conditions are also solved by a vanishing source $J_0 = 0$, and an A_0 expectation value set by the chemical potential. This latter solution is equivalent to absorbing the chemical potential via a shift in the gauge field leaving the partition function unchanged. This possibility is excluded by imposing a vanishing A_0 at infinity as a boundary condition.

The classical source J_0 can also be interpreted as a background magnetic field. Defining

$$B = \epsilon^{0ij} \partial_i A_j, \quad (2.10)$$

and assuming a static configuration, the equation of motion for A_0 yields,

$$J_0 - \frac{k}{2\pi} \langle B \rangle + 2(\mu + \langle A_0 \rangle) v^2 = 0. \quad (2.11)$$

Therefore, even if the source J_0 were not explicitly introduced, it is naturally

2. ABELIAN CHERN-SIMONS VORTICES AT FINITE CHEMICAL POTENTIAL

induced through a non-zero background value for B . We will treat this background value as distinct from the magnetic field carried by the vortex.

2.2.1 Perturbative spectrum

The vacuum expectation value for Φ Higgses the gauge group and since Chern-Simons gauge fields do not propagate, the physical perturbative spectrum consists of two gapped excitations. The dispersion relations can be found by expanding the gauge-fixed action¹ to quadratic order in fluctuations and identifying the gauge-invariant zeros of the fluctuation determinant. The dispersion relations for the two physical modes can be expressed in terms of dimensionless frequency and momentum and a single dimensionless coupling (assuming $k > 0, \mu > 0$)

$$\alpha \equiv \frac{k\mu}{4\pi\nu^2}, \quad \tilde{\omega} \equiv \omega/\mu, \quad \tilde{\mathbf{p}} \equiv \mathbf{p}/\mu. \quad (2.12)$$

We find,

$$\tilde{\omega}_{\pm} = \sqrt{\tilde{\mathbf{p}}^2 + (s+1) + \frac{1}{2\alpha^2}} \pm \sqrt{4\tilde{\mathbf{p}}^2 + \left(s+1 - \frac{1}{2\alpha^2}\right)^2}. \quad (2.13)$$

Both modes are gapped at $\tilde{\mathbf{p}} = 0$.

$$\begin{aligned} \tilde{\omega}_+^2 &\simeq 2(s+1) + \tilde{\mathbf{p}}^2 \frac{2\alpha^2(s+3)-1}{2\alpha^2(s+1)-1} \dots, \\ \tilde{\omega}_-^2 &\simeq \frac{1}{\alpha^2} + \tilde{\mathbf{p}}^2 \frac{2\alpha^2(s-1)-1}{2\alpha^2(s+1)-1} \dots, \quad |\tilde{\mathbf{p}}| \ll 1. \end{aligned} \quad (2.14)$$

When the Chern-Simons level is taken to be large the mode $\tilde{\omega}_-$ is the lighter of the two and becomes the phonon in the strict $k \rightarrow \infty$ limit. For the classically marginal sextic potential with $s = 3$, this limit yields $\tilde{\omega}_-^2 \simeq \tilde{\mathbf{p}}^2/2$ which implies a speed of sound $c_s = 1/\sqrt{2}$, expected from scale invariance in 2+1 dimensions. As the level k is lowered, the gaps of the two branches coincide when $\alpha = 1/\sqrt{2(s+1)}$, and below this value of α , the roots exchange roles.

¹We use an R_ξ gauge fixing term of the form $\mathcal{L}_{gf} = (\partial_\mu A^\mu - \xi \langle \Phi \rangle \delta \Phi^\dagger + \xi \delta \Phi \langle \Phi \rangle^\dagger)^2 / (2\xi)$

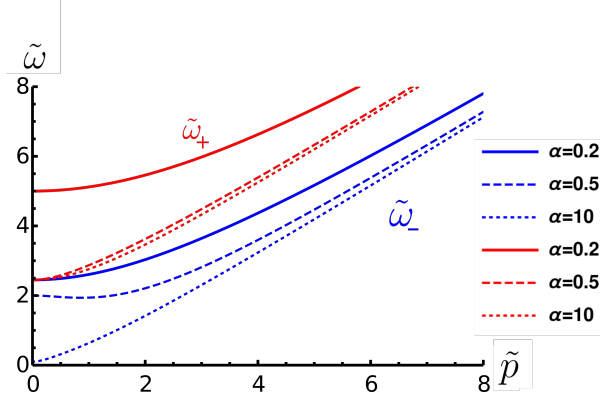


Figure 2.1: The dispersion relations of the two branches of perturbative fluctuations for the quartic potential ($s = 2$), with different values of the dimensionless coupling α .

Depending on the value of α , the sign of $\tilde{\omega}_{\pm}''(0)$ can be negative which implies a minimum in the dispersion relation away from $\tilde{p} = 0$, also called a magneto-roton minimum. One of the two branches will exhibit a magneto-roton minimum for values of α in the range:

$$\frac{1}{\sqrt{2(s+3)}} < \alpha < \frac{1}{\sqrt{2(s-1)}}. \quad (2.15)$$

2.3 Vortex equations

We want to solve the equations of motion in polar coordinates. Therefore, allowing for a non-trivial spatial metric h , the static field equations are:

$$\begin{aligned} \frac{1}{\sqrt{h}} \partial_j (\sqrt{h} \partial^j \Phi) - \frac{i}{\sqrt{h}} \partial_j (\sqrt{h} A^j \Phi) + (\mu + A_0)^2 \Phi - i A_j \partial^j \Phi - A_j A^j \Phi &= g_{2s} |\Phi|^{2s-2} \Phi \\ \frac{k}{2\pi} \epsilon^{\sigma\nu\rho} \partial_\nu A_\rho &= -\sqrt{h} [i(\partial^\sigma \Phi \Phi^\dagger - \Phi \partial^\sigma \Phi^\dagger) + 2A^\sigma |\Phi|^2 - \delta_{0\sigma} (2\mu |\Phi|^2 + J_0)]. \end{aligned} \quad (2.16)$$

As usual, a static vortex configuration carrying n units of magnetic flux is described by the rotationally symmetric ansatz in polar coordinates:

$$A_0 = A_0(r), \quad A_r = 0, \quad A_\theta = A_\theta(r), \quad \Phi = f(r) e^{in\theta}. \quad (2.17)$$

2. ABELIAN CHERN-SIMONS VORTICES AT FINITE CHEMICAL POTENTIAL

This ansatz leads to the following system of equations¹:

$$f'' + \frac{f'}{r} - \frac{1}{r^2} (A_\theta - n)^2 f + (A_0 + \mu)^2 f - g_{2s} f^{2s-1} = 0 \quad (2.18)$$

$$-\frac{f^2}{r} (A_\theta - n) + \frac{k}{4\pi} A'_0 = 0 \quad (2.19)$$

$$-f^2 A_0 - \mu f^2 + \frac{k}{4\pi} \left(\frac{A'_\theta}{r} \right) = \frac{J_0}{2}, \quad J_0 = -2\mu v^2. \quad (2.20)$$

We are looking for a configuration which asymptotes at infinity to the ground state with the fixed non-vanishing background value for J_0 , obeying the boundary conditions:

$$A_\theta(r) \xrightarrow{r \rightarrow \infty} n, \quad A_0(r) \xrightarrow{r \rightarrow \infty} 0, \quad f(r) \xrightarrow{r \rightarrow \infty} v, \quad f(0) = 0. \quad (2.21)$$

With the rotationally symmetric ansatz above, the magnetic field B only depends on r , and the configuration carries n units of flux:

$$B(r) = \frac{A'_\theta(r)}{r}, \quad \Phi_B = \lim_{r \rightarrow \infty} \int_0^{2\pi} A_\theta(r) d\theta = 2\pi n, \quad (2.22)$$

assuming A_θ vanishes at the origin.

2.3.1 Qualitative features

The equation of motion (2.20) for A_0 , which implements the Gauss constraint, fixes the value of the magnetic field at the core of the vortex where the scalar field vanishes. Thus,

$$B(0) = \frac{4\pi}{k} J_0 = -\frac{\mu^2}{\alpha}, \quad (2.23)$$

where α is the effective coupling defined in (2.12). For a given winding number n , the value of α completely characterizes the vortex solution when expressed in terms of rescaled dimensionless variables. The effect of the Gauss constraint is to induce a magnetic field B inside the vortex core to precisely cancel the

¹We omit the equation of motion for A_r , which is automatically satisfied.

background source J_0 which could also be viewed as a uniform background magnetic field. Outside the vortex B vanishes,

$$\lim_{r \rightarrow \infty} B(r) = 0. \quad (2.24)$$

The sign of $B(0)$ plays an important role in determining the properties of the vortex solutions. Without loss of generality, we assume that the chemical potential μ and the Chern-Simons level k are both positive:

$$\mu > 0 \quad k > 0. \quad (2.25)$$

With this choice $B(0)$ is negative definite, independently of the sign of the magnetic flux $2\pi n$. However, this means that solutions with positive and negative flux will be qualitatively different. This breaking of charge conjugation is precisely what we expect in the presence of the $U(1)$ chemical potential.

Negative flux $n < 0$: Assuming that the magnitude of the magnetic field $|B(r)|$ increases monotonically towards the vortex core, and given that the value of the core magnetic field is independent of $|n|$ (the number of units of flux) the vortex core size should increase with $|n|$ for negative n . Taking B to be uniform within the core for large enough $|n|$, we can estimate the radius R_n of a vortex solution with $|n| \gg 1$:

$$|B(0)|\pi R_n^2 \approx 2\pi|n| \implies R_n \approx \frac{\sqrt{2\alpha|n|}}{\mu}, \quad |n| \gg 1. \quad (2.26)$$

The assumption of uniformity of the vortex core region is self-consistently justified by first noting that for small r ,

$$f(r) = c_0 r^{|n|} + \dots, \quad c_0 > 0. \quad (2.27)$$

This is obtained by neglecting A_θ in comparison to n , and ignoring higher order terms for small r in eq.(2.18). Therefore, for large flux, the scalar profile is extremely flat near $r = 0$. With a uniform B field in the vortex interior, the

2. ABELIAN CHERN-SIMONS VORTICES AT FINITE CHEMICAL POTENTIAL

vector potential is determined as

$$A_\theta \approx -\frac{1}{2}|B(0)|r^2, \quad (2.28)$$

and this approximation breaks down precisely when $r \approx R_n$ (see eq.(2.26)). We see numerically that the scalar field profile, inside the vortex, closely follows the solution to the first order equation:

$$\begin{aligned} f'(r) &\approx \frac{1}{r} \left(|n| - \frac{1}{2}|B(0)|r^2 \right) f(r) \\ \implies f(r) &\approx c_0 r^{|n|} e^{-|B(0)|r^2/4}, \quad r < R_n. \end{aligned} \quad (2.29)$$

This feature of the solution is depicted in figure 2.6.

The equation of motion (2.19) for A_θ determines the radial electric field $E(r) = A'_0(r)$. The electrostatic potential A_0 remains constant inside the core region since $f(r)$ is vanishingly small and therefore the electric field is also vanishingly small. Outside the core region the electric and magnetic fields decay exponentially to zero. Linearizing about the asymptotic solution at large r we find,

$$\delta f \equiv f(r) - v, \quad \delta A_\theta = A_\theta - n, \quad (2.30)$$

$$\begin{aligned} \delta A_\theta &= \frac{\alpha}{\mu} r A'_0, \\ \delta f'' + \frac{\delta f'}{r} - (2s-2)\mu^2 \delta f &= -2A_0 \mu v, \\ A''_0 + \frac{A'_0}{r} - \frac{\mu^2}{\alpha^2} A_0 &= \frac{2\mu^3}{v\alpha^2} \delta f. \end{aligned}$$

The solutions to the homogeneous equations for the fluctuations δf and A_0 are the Bessel functions $K_0(\sqrt{2s-2}\mu r)$ and $K_0(\mu r/\alpha)$ respectively, and these control the exponential decay of fluctuations at large r ,

$$K_0(\sqrt{2s-2}\mu r) \Big|_{\mu r \rightarrow \infty} \sim \frac{e^{-\sqrt{2s-2}\mu r}}{\sqrt{\mu r}}, \quad K_0(\mu r/\alpha) \Big|_{\mu r \rightarrow \infty} \sim \frac{e^{-\mu r/\alpha}}{\sqrt{\mu r}}. \quad (2.31)$$

2.4 Vortex energy and BPS-like scaling

The two exponents are related to masses of the gapped perturbative excitations around the Higgsed ground state. Since $A_\theta(r) \simeq n$ outside the core region, according to eq. (2.19) the electric field is only significant in a strip along the edge of the vortex core. Numerically, we find that the width of this strip does not scale with $|n|$, so that in the limit of large $|n|$, the contribution from the transition region to the vortex energy is subleading in $|n|$.

We will see below that these qualitative aspects of the vortex solutions lead to linear dependence of the vortex energy on $|n|$ and BPS-like behaviour at a critical value of the effective coupling α .

Positive flux $n > 0$: Positive flux solutions are qualitatively distinct from the negative flux ones. This is because $B(0) < 0$ independent of n , so $B(r)$ must switch sign to yield a net positive flux. For large $n > 0$, most of this positive flux remains concentrated in a ring-like region at the edge of the vortex. In this case the total flux can be written as a sum of two contributions, one that scales with the area of the vortex and is negative, therefore must be subleading, and a positive dominant contribution which scales with the radius of the configuration,

$$2\pi n \sim -\pi R_n^2 \frac{\mu^2}{\alpha} + 2\pi R_n \Delta_{ring} B_{ring}. \quad (2.32)$$

Here Δ_{ring} is the width of the edge region which we take to be independent of n , whilst B_{ring} denotes the peak value of the magnetic field in the ring and R_n is the radius of the vortex for large enough n . The negative area-dependent contribution is a key difference from a similar situation discussed in [64]. We cannot exclude the possibility that both the area and perimeter contributions have faster than linear growth and a delicate cancellation yields the correct flux. It is possible to suppress the area contribution by making α arbitrarily large. The large α limit makes the magnetic field inside the vortex vanishingly small and the system then closely resembles an abelian Chern-Simons vortex in vacuum.

2.4 Vortex energy and BPS-like scaling

The “energy” functional appropriate for the grand canonical ensemble is the grand potential. The Chern-Simons term does not contribute to it for static

2. ABELIAN CHERN-SIMONS VORTICES AT FINITE CHEMICAL POTENTIAL

configurations. The grand potential is obtained by using the Lagrangian density (2.8) with $\mu \neq 0$ and passing to the Hamiltonian picture. Rewriting the Hamiltonian in terms of the fields and their derivatives, the desired energy functional is¹,

$$\mathcal{E} = \int d^2x \left(|D_i \Phi|^2 + A_0^2 |\Phi|^2 + \frac{g_{2s}}{s} |\Phi|^{2s} - \mu^2 |\Phi|^2 \right), \quad (2.34)$$

accompanied by the constraint which incorporates the effect of the Chern-Simons term,

$$\frac{k}{4\pi} B = A_0 |\Phi|^2 + \mu (|\Phi|^2 - v^2). \quad (2.35)$$

An interesting feature of the finite- μ vortices (with negative flux) is that they appear to be marginally bound (or BPS-like) for a specific value of the effective dimensionless parameter α . Recall that this parameter depends on the Chern-Simons level, the chemical potential and the interaction strength:

$$\alpha = \frac{k\mu}{4\pi v^2} = \frac{k}{4\pi} \left(\frac{g_{2s}}{\mu^{3-s}} \right)^{\frac{1}{s-1}}. \quad (2.36)$$

Let us perform a rescaling of variables and fields so that the equations of motion can be written explicitly in terms of dimensionless quantities:

$$\tilde{r} \equiv \mu r, \quad \tilde{f} \equiv \frac{f}{v}, \quad a \equiv \frac{1}{\tilde{r}} (A_\theta - n), \quad \tilde{A}_0 \equiv \frac{A_0}{\mu}. \quad (2.37)$$

The rescaled scalar profile vanishes at $\tilde{r} = 0$ and approaches unity for large \tilde{r} : $\tilde{f}(\tilde{r} \rightarrow \infty) = 1$. The asymptotic behaviours of $a(\tilde{r})$ and \tilde{A}_0 are,

$$\lim_{\tilde{r} \rightarrow 0} \tilde{r} a(\tilde{r}) = -n, \quad \lim_{\tilde{r} \rightarrow \infty} \tilde{r} a(\tilde{r}) = 0, \quad \lim_{\tilde{r} \rightarrow \infty} \tilde{A}_0(\tilde{r}) = 0. \quad (2.38)$$

The resulting dimensionless equations of motion (primes denote derivatives

¹For static configurations, the grand potential can be quickly derived by retaining only the spatial gradient and potential terms including the Chern-Simons density,

$$\mathcal{E} = \int d^2x \left(|D_i \Phi|^2 - (A_0 + \mu)^2 |\Phi|^2 + A_0 \left(\frac{k}{2\pi} B - J_0 \right) + \frac{g_{2s}}{s} |\Phi|^{2s} \right), \quad (2.33)$$

and then applying the constraint (2.35).

2.4 Vortex energy and BPS-like scaling

with respect to \tilde{r}) are,

$$\tilde{f}'' + \frac{\tilde{f}'}{\tilde{r}} - a^2 \tilde{f} + (\tilde{A}_0 + 1)^2 \tilde{f} - \tilde{f}^{2s-1} = 0 \quad (2.39)$$

$$\alpha \tilde{A}'_0 = a \tilde{f}^2 \quad (2.40)$$

$$\alpha \tilde{B} = (\tilde{f}^2 - 1) + \tilde{f}^2 \tilde{A}_0. \quad (2.41)$$

Therefore, for a fixed flux n , the solutions are only parametrised by the dimensionless effective coupling α . Note we have introduced the dimensionless magnetic field,

$$\tilde{B} = \frac{1}{\tilde{r}} (\tilde{r}a)' = \frac{A'_\theta}{\tilde{r}}. \quad (2.42)$$

We first rewrite the energy functional using the rescaled fields and variables,

$$\mathcal{E} = 2\pi v^2 \int_0^\infty \tilde{r} d\tilde{r} \left[(\tilde{f}' - a\tilde{f})^2 + a \frac{d}{d\tilde{r}} (\tilde{f}^2 - 1) + \tilde{A}_0^2 \tilde{f}^2 + \frac{\tilde{f}^{2s}}{s} - \tilde{f}^2 + \frac{s-1}{s} \right], \quad (2.43)$$

where we have included a constant zero-point shift so that the energy density is vanishing for the ground state at infinity. The second term in eq.(2.43) when integrated by parts yields a nonvanishing surface contribution,

$$\int_0^\infty d\tilde{r} (\tilde{r}a) \frac{d}{d\tilde{r}} (\tilde{f}^2 - 1) = |n| - \int_0^\infty \tilde{r} d\tilde{r} \tilde{B} (\tilde{f}^2 - 1). \quad (2.44)$$

Employing the Gauss constraint to eliminate \tilde{B} in favour of \tilde{A}_0 , we obtain an expression for the energy functional which is suitable for subsequent approximations and matching with numerical results,

$$\begin{aligned} \mathcal{E} = 2\pi v^2 |n| + 2\pi v^2 \int_0^\infty \tilde{r} d\tilde{r} & \left[(\tilde{f}' - a\tilde{f})^2 + \left(\frac{\tilde{f}^{2s}}{s} - \tilde{f}^2 + \frac{s-1}{s} \right) - \frac{1}{\alpha} (1 - \tilde{f}^2)^2 + \right. \\ & \left. \tilde{A}_0^2 \tilde{f}^2 + \frac{1}{\alpha} \tilde{A}_0 \tilde{f}^2 (1 - \tilde{f}^2) \right]. \end{aligned} \quad (2.45)$$

2. ABELIAN CHERN-SIMONS VORTICES AT FINITE CHEMICAL POTENTIAL

2.4.1 The quartic potential $s = 2$

Anticipating numerical results in the next section, we can make certain observations on the energetics of vortex solutions for large negative flux.

Our arguments rely on the fact that for n sufficiently large and negative, all fields are uniform inside and outside the vortex whose radius scales as $\sqrt{|n|}$, with a thin transition region whose width does not scale with n . In the case of the quartic potential the energy functional is,

$$\begin{aligned} \mathcal{E}(n, \alpha) \Big|_{s=2} = & 2\pi\nu^2|n| + 2\pi\nu^2 \int_0^\infty \tilde{r} d\tilde{r} \left[\left(\tilde{f}' - a\tilde{f} \right)^2 + \left(\frac{1}{2} - \frac{1}{\alpha} \right) \left(1 - \tilde{f}^2 \right)^2 + \right. \\ & \left. + \tilde{A}_0^2 \tilde{f}^2 + \frac{1}{\alpha} \tilde{A}_0 \tilde{f}^2 (1 - \tilde{f}^2) \right]. \end{aligned} \quad (2.46)$$

We know that \tilde{f} vanishes inside the vortex, whilst \tilde{A}_0 and $a(r)$ vanish outside it. Specifically when $\alpha = 2$, the scalar potential is precisely cancelled, and the integrand in the expression above has support only within the transition region at the edge of the vortex. If we assume that this contribution does not scale with n , we conclude that

$$\mathcal{E}(n, \alpha = 2) \Big|_{s=2, |n| \gg 1} = 2\pi\nu^2|n|. \quad (2.47)$$

Our numerical solutions confirm (figure 2.5) this conclusion which works remarkably well even for low values of n , including $|n| = 1, 2, \dots$. Another surprising feature of the solutions for $\alpha = 2$ is that they appear to solve the first order equation $\tilde{f}' = a\tilde{f}$ to very high numerical accuracy (figure 2.6)¹.

It is easy to extend the arguments to other values of α . When $\alpha \neq 2$, the second term in the integrand of (2.46) provides an approximately constant energy density inside the vortex where $\tilde{f} = 0$, while all other contributions remain vanishingly small. We therefore find,

$$\mathcal{E}(n, \alpha) \Big|_{s=2, |n| \gg 1} = 2\pi\nu^2 \left(|n| + \frac{1}{2} \mu^2 R_n^2 \left(\frac{1}{2} - \frac{1}{\alpha} \right) \right) = \alpha\pi\nu^2|n|. \quad (2.48)$$

¹In this context, it is worth noting that if the terms proportional to \tilde{A}_0 are omitted (or assumed to be negligible) in eqs. (2.39) and (2.41), then the resulting equations coincide, for a particular value of α , with equations of motion for a BPS vortex in $U(2) \times U(2)$ ABJM theory which solves an equivalent first order system [67].

2.4 Vortex energy and BPS-like scaling

This behaviour is also confirmed numerically in figure 2.5, albeit only for large $|n|$ as expected. Interestingly, although ν and α each depend on the quartic coupling constant g_4 , the large- $|n|$ vortex mass formula depends only the Chern-Simons level k and the chemical potential,

$$\mathcal{E}(n, \alpha) \Big|_{s=2, |n| \gg 1} = \alpha \pi \nu^2 |n| = \frac{k\mu}{4} |n|. \quad (2.49)$$

2.4.2 General power law potential ($s \geq 2$)

The energies of solutions for general power law potentials now work along similar lines. The integrand in the energy density (2.45) is negligible both inside and outside the vortex when $\alpha = \alpha_c$,

$$\alpha_c = \frac{s}{s-1}. \quad (2.50)$$

At this critical α we expect solutions with large flux to have energies $\mathcal{E}(n) \simeq 2\pi\nu^2|n|$. When α takes generic values away from α_c , adapting the $s = 2$ argument to general power law potentials $\sim g_{2s}|\Phi|^{2s}$ we obtain,

$$\mathcal{E}(n, \alpha; s) \Big|_{|n| \gg 1} = 2\alpha \pi \nu^2 |n| \frac{s-1}{s} = \frac{s-1}{2s} k\mu |n|. \quad (2.51)$$

This result is confirmed by our numerical solutions for the sextic potential below. As before the mass formula is independent of the interaction strength of the potential. We point out however that the radius of the vortex solution $R_n = \frac{1}{\mu} \sqrt{2\alpha|n|}$ depends nontrivially on all parameters. From the definition of α (2.36), increasing the interaction strength (for fixed μ and k) has the effect of increasing the vortex size.

2.4.3 Positive flux vortices

With our choice of conventions $\mu > 0$ and $k > 0$, positive flux solutions are energetically disfavoured. To see this, let us reconsider the energy functional (2.43). As in the case of the flux in eq.(2.32), there are different types of contributions to the energy, those that scale with the area of the vortex, those that scale with the perimeter, and finally (gauge-covariant) gradient terms which

2. ABELIAN CHERN-SIMONS VORTICES AT FINITE CHEMICAL POTENTIAL

become important at the edge of the vortex. If we pick α to be sufficiently large so that we can ignore the flux contribution from the vortex interior, then $B_{ring} \sim n/R_n$. Then the leading contributions to the energy take the schematic form,

$$\mathcal{E}(n) \sim (2\pi\nu^2) \left(\frac{n^2}{R_n} \Delta + c_0 \pi R_n^2 \right), \quad \alpha \gg 1 \quad (2.52)$$

Here the first term is a perimeter contribution from a covariant gradient while the second term is a potential energy contribution from the interior. Extremizing with respect to R_n , we obtain $R_n \sim n^{2/3}$ and $\mathcal{E}(n) \sim n^{4/3}$. However this argument will fail for finite α since $B(0) = -\mu^2/\alpha$ and the area scaling as $n^{4/3}$ would violate the flux condition (2.32). We have not found a satisfactory scaling argument for finite α and large n , but our numerical results indicate a faster than quadratic growth of the energy as a function of n in this situation.

2.5 Numerical results

The vortex equations of motion are not analytically solvable. We numerically solve the dimensionless equations of motion (2.39), (2.40) and (2.41) along with the accompanying boundary conditions. Below we outline the results for the quartic potential ($s = 2$) first, and subsequently summarize the results for the sextic ($s = 3$) case.

2.5.1 Quartic potential ($s = 2$)

Negative flux solutions: A well known feature of Chern-Simons-Higgs vortices in vacuum is the ring-like profile of electric and magnetic fields [51]. The finite density vortices we have studied are qualitatively distinct and retain this feature only partially. Figure 2.2 shows the (dimensionless) scalar field $\tilde{f}(\tilde{r})$ and magnetic field $\tilde{B}(\tilde{r})$ at $\alpha = 5$ and different negative values of the magnetic flux.

2.5 Numerical results

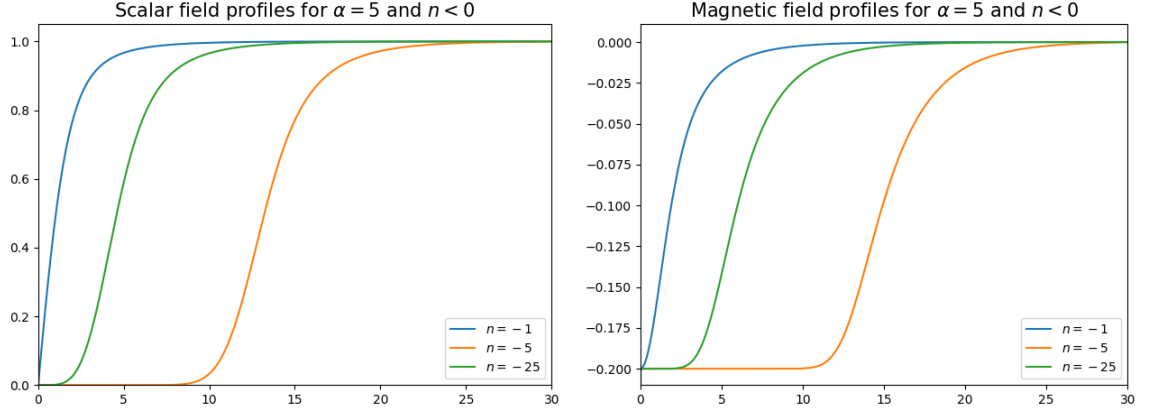


Figure 2.2: *Left:* The scalar field profile $\tilde{f}(\tilde{r})$ for $\alpha = 5$ and negative flux. *Right:* The dimensionless magnetic field $\tilde{B}(\tilde{r})$ for the same values of α and magnetic flux.

Unlike Chern-Simons vortices in vacuum [51, 64] the magnetic field is no longer expelled from the core of the vortex. Instead, the magnetic field and the scalar are both effectively constant separately inside and outside the vortex and we observe a kink-like transition in between. The value of the dimensionless magnetic field inside the vortex is $\tilde{B}(0) = -1/\alpha = -0.2$ for $\alpha = 5$.

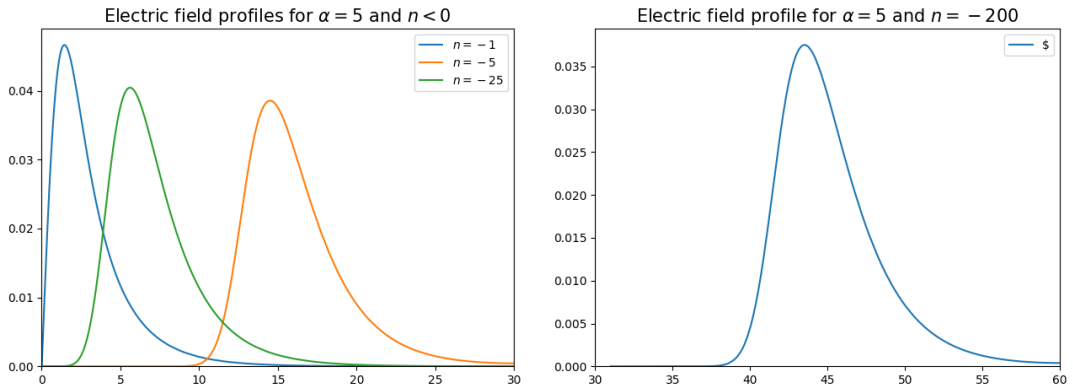


Figure 2.3: The electric field has support only at the edge of the vortex implying a ring-like profile. The width of the transition region remains fixed as $|n|$ is cranked up.

The electric field on the other hand has support only at the edge or the transition-region where the gradient of A_0 is significant. This is illustrated

2. ABELIAN CHERN-SIMONS VORTICES AT FINITE CHEMICAL POTENTIAL

in figure 2.3. Even for relatively low values of $|n|$, the location of the peak in the magnitude of the electric field begins to track the large $|n|$ estimate of the vortex radius (2.26):

$$\mu R_n = \sqrt{2|n|\alpha} = \begin{cases} 7.07 & n = -5, \alpha = 5 \\ 15.81 & n = -25, \alpha = 5 \\ 44.7 & n = -200, \alpha = 5. \end{cases} \quad (2.53)$$

The width of the ring-like transition region remains fixed as $|n|$ is increased. In particular, both the width of the ring and the peak magnitude of the electric field appear to be solely determined by α for large flux.

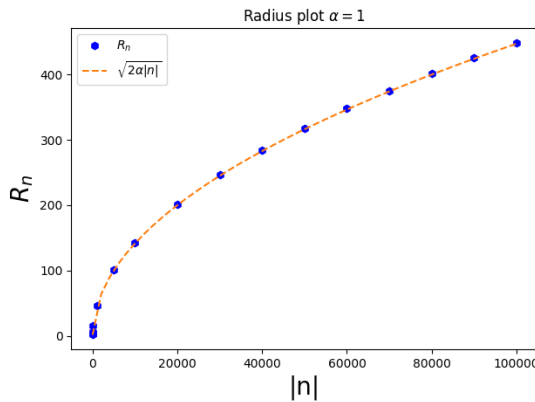


Figure 2.4: The radii of large- n vortex solutions follow very closely the curve $\mu R_n = \sqrt{2\mu|n|}$. We define the radius of the vortex as the position at which the dimensionless energy density falls below a threshold $\sim 10^{-4}$.

A precise agreement between the above scaling formula for the radius is obtained when the magnitude of the flux is significantly increased, as shown in the second plot in figure 2.4.

The most interesting aspect of the negative flux vortex solutions is the scaling of the energy with $|n|$. Using the energy functional (2.43), we compute the two dimensionless ratios,

$$\frac{\mathcal{E}(n, \alpha)}{|n|\mathcal{E}(1, \alpha)} \quad \text{and} \quad \frac{\mathcal{E}(n, \alpha)}{2\pi\nu^2|n|} \xrightarrow{|n|\gg 1} \frac{\alpha}{2}. \quad (2.54)$$

The first ratio measures the energy of the n -vortex relative to that of $|n|$ vortices each with unit (negative) flux. If this is less than unity, then the n -vortex has lower energy than $|n|$ separated -1 -vortices, and therefore the interactions between them must be attractive (type I). Conversely, if $\mathcal{E}(n, \alpha) > |n|\mathcal{E}(1, \alpha)$, the vortex interaction is repulsive (type II).

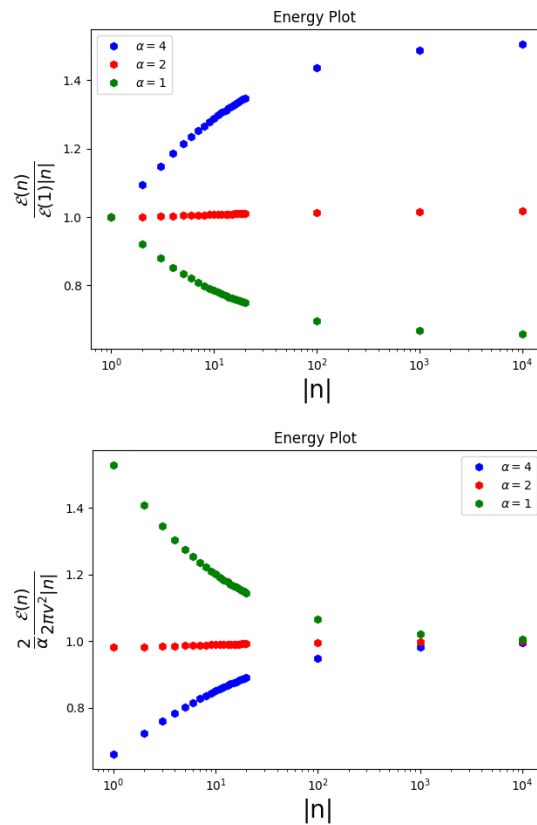


Figure 2.5: *Left:* This shows that $\alpha < 2$ vortices are type I (attractive), separated from type II (repulsive) solutions for $\alpha > 2$ by the $\alpha = 2$ line where the solutions have vanishing interaction energy. *Right:* The α -dependence of the n -vortex mass formula agrees with analytical arguments at large $|n|$.

The second ratio in (2.54) is the general formula for the α -dependence of the n -vortex energy which was deduced from arguments for large $|n|$. Figure 2.5 shows to significant numerical precision that negative flux solutions with $\alpha = 2$ are effectively “BPS” for any value of $|n|$, separating $\alpha > 2$ solutions which are type II (repulsive) from the solutions with $\alpha < 1$ which are type I or

2. ABELIAN CHERN-SIMONS VORTICES AT FINITE CHEMICAL POTENTIAL

attractive. Furthermore the α -dependence of the energies of type I and type II vortices for large flux matches the predicted behaviour in eq.(2.54).

A surprising feature of the numerical results is how closely the energies of the vortices with $\alpha = 2$ match the BPS result $2\pi|n|v^2$ even for low values of $|n|$. This matching is corroborated by figure 2.6, which shows that the vortex profile for $\alpha = 2$ almost solves the first order equation $\tilde{f}' = af$. This figure also demonstrates that the vector potential inside the vortex closely follows the result for a uniform magnetic field.

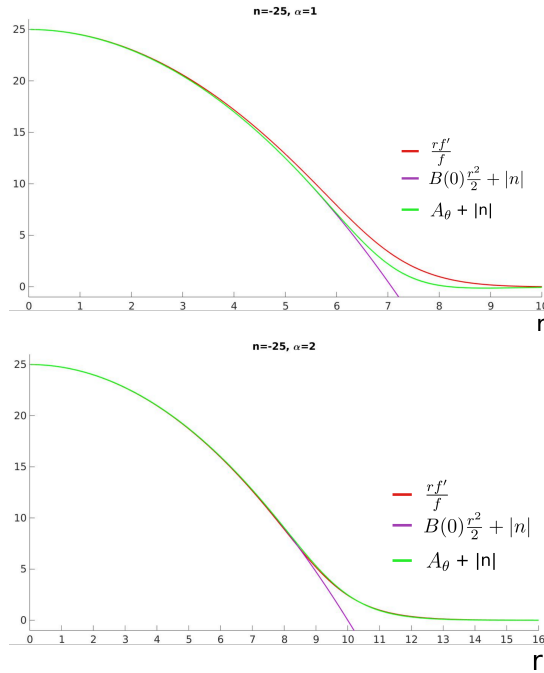


Figure 2.6: The figure shows the three quantities: rf'/f (red), $(A_\theta + |n|)$ (green), and $(-|B(0)|r^2/2 + |n|)$ (purple) evaluated on the exact numerical solutions for $\alpha = 1$ and $\alpha = 2$.

The extent of the departure of the vortex profile from an exact solution to the first order equation $\tilde{f}' = af$ is shown in figure 2.7. Evaluated on the $\alpha = 2$ solution, the quantity $(\tilde{f}' - af)$ deviates minimally from zero near the edge of the vortex.

2.5 Numerical results

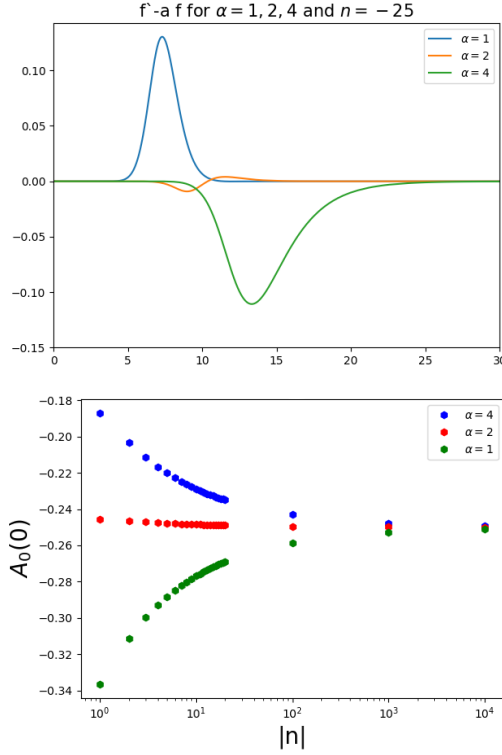


Figure 2.7: Left: $(\tilde{f}' - a\tilde{f})$ plotted for 3 values of α including critical case. $\alpha = 2$. Right: The value of \tilde{A}_0 at the origin for different α as a function of $|n|$.

Yet another measure of the relevance of the first order equation $\tilde{f}' = a\tilde{f}$ for the $\alpha = 2$ solutions is given by the value of $\tilde{A}_0(0)$. The value of the electrostatic potential at the origin is not fixed as a boundary condition, but an output of the solution. Let us use the equation of motion for the electric field (2.40) in conjunction with the first order equation at $\alpha = 2$,

$$\tilde{A}'_0 = \frac{1}{2}a\tilde{f}^2 \quad \xrightarrow{\tilde{f}'=a\tilde{f}} \quad \tilde{A}_0 = \frac{1}{4}(\tilde{f}^2 - 1), \quad (2.55)$$

where the integration constant on the right hand side is fixed by requiring that \tilde{A}_0 vanishes as $r \rightarrow \infty$. We therefore arrive at a prediction,

$$\tilde{A}_0(0)|_{\alpha=2} = -\frac{1}{4}. \quad (2.56)$$

2. ABELIAN CHERN-SIMONS VORTICES AT FINITE CHEMICAL POTENTIAL

This is precisely what we see in figure 2.7 for the $\alpha = 2$ solution. However, we also find the unexpected feature that $\tilde{A}_0(0)$ for other values of α approaches $-1/4$ at large $|n|$. This suggests that solutions with generic α and large $|n|$ are not approximate solutions to the first order equation¹.

Positive flux solutions: We have explained how positive flux vortex solutions are qualitatively distinct from negative n solutions. In certain limits (large- α) they closely resemble Chern-Simons vortex solutions in vacuum. The majority of the flux resides in the ring region or edge of the solution as n is increased (see figure 2.8).

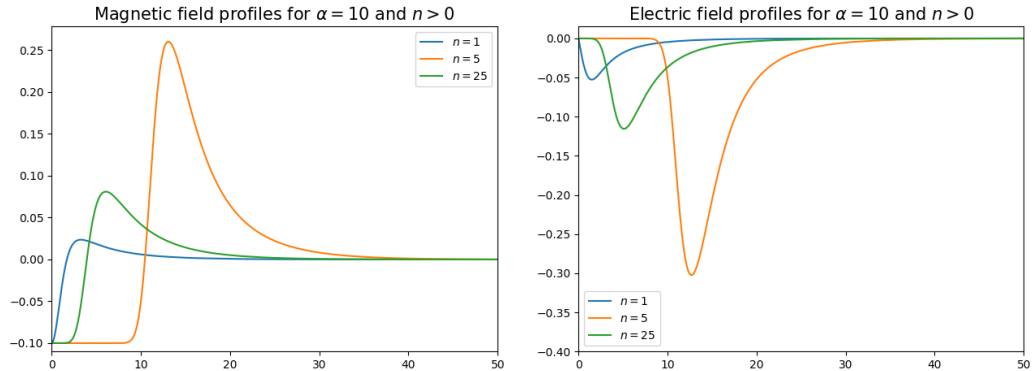


Figure 2.8: Magnetic and electric fields for positive flux vortices have support near the edge of the vortex and their peak values grow without bound as n is increased.

In figure 2.9 the dependence of the n -vortex energy on $|n|$, is displayed for the negative and positive flux solutions, and as expected the latter are more massive. It is surprising that $\mathcal{E}(n)/|n|$ appears to grow faster than $|n|$.

¹For generic α , eq. (2.40) along with the first order equation $\tilde{f}' = a\tilde{f}$, would imply $\tilde{A}_0(0) = -1/2\alpha$.

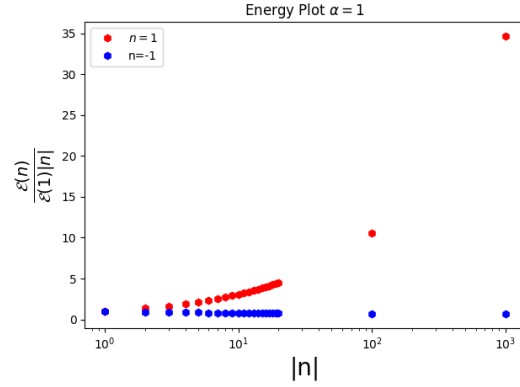


Figure 2.9: Positive flux vortices have higher energy than their negative flux counterparts.

2.5.2 Sextic potential ($s = 3$)

Finally we turn to numerical results for the higher power law potentials, in particular the $s = 3$ or sextic potential. We do not expect to see major qualitative differences overall. One special feature of the quartic potential ($s = 2$) is that when $\alpha = 2$, there is a precise cancellation of the scalar potential energy contribution to the energy functional. This is not the case for general power laws. Nevertheless there is an approximate cancellation when evaluated on the vortex background at the critical value of $\alpha = \frac{s}{s-1}$. The critical value for the sextic potential is $\alpha = \frac{3}{2}$. The profiles for the negative flux vortex with sextic and quartic potentials are shown on the same plot in figure 2.10. For the same values of the dimensionless parameter α there is very little difference between the two systems. The transition between the two phases is slightly steeper for the sextic potential. The ratios of the energies of the n -vortex to single vortex and the BPS value ($2\pi\nu^2 n$) are shown in figure 2.11.

2. ABELIAN CHERN-SIMONS VORTICES AT FINITE CHEMICAL POTENTIAL

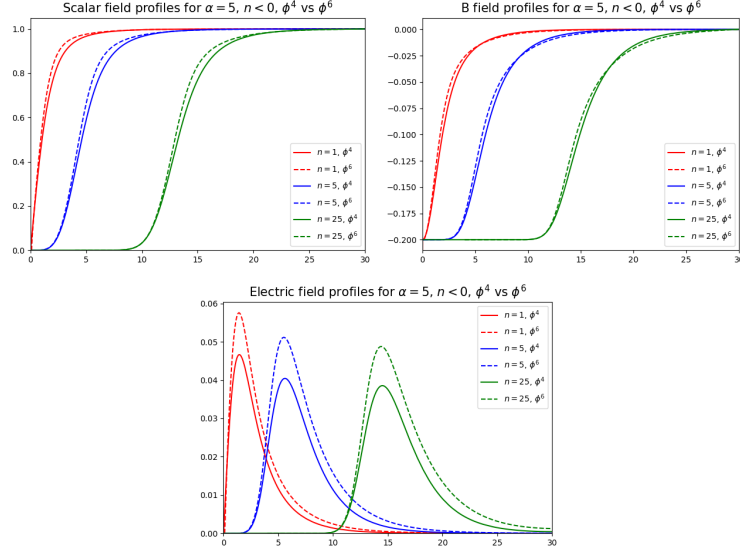


Figure 2.10: Vortex profiles with negative winding number for quartic(solid) and sextic(dashed) potentials.

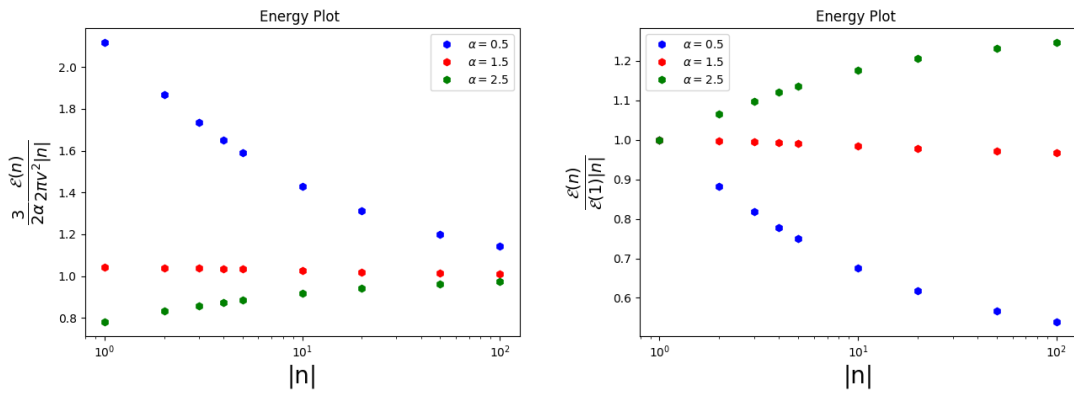


Figure 2.11: The scaling of the energy of the n -vortex with $|n|$ and α , with sextic potential.

The dependence of the energy on $|n|$ and α matches the prediction (2.51), and we find a transition line between type I and type II vortices at the critical coupling $\alpha_c = \frac{3}{2}$ which represents the marginally bound “BPS” case for the sextic potential. Again the value of $\tilde{A}_0(0)$ indicates that the profiles almost

satisfy the first order equation which would imply,

$$\tilde{A}_0(0) = -\frac{1}{2\alpha_c} = -\frac{1}{3}. \quad (2.57)$$

This is indeed what we observe in figure 2.12. All large n vortex profiles approach this value

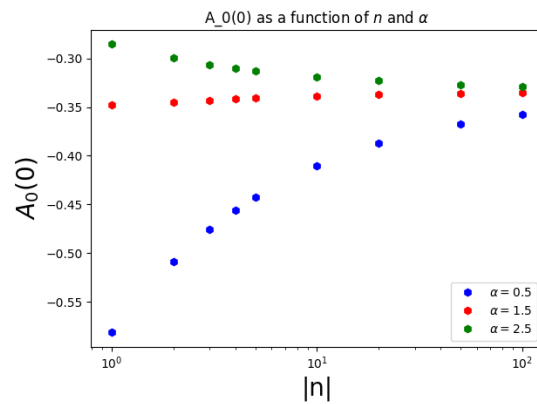


Figure 2.12: Value of \tilde{A}_0 at the origin for different values of α , as a function of $|n|$, with the sextic potential.

2.6 Discussion

We have studied Abelian Chern-Simons vortices in the presence of a chemical potential driving the theory into the Higgs phase. The numerical solutions reveal several features which are in line with the physical picture presented in an analytically solvable (nonrelativistic) supersymmetric model [61, 68]. The configurations with large (negative) flux show precise BPS-like scaling of energy/grand potential and appear (numerically) to closely solve first order equations. It would be interesting to make use of the large flux limit to understand the edge excitations of the vortex droplet. We expect that some of the lessons learnt from analyzing this system will be of use in $SU(N)$ and $U(N)$ Chern-Simons-scalar theories with a particle number chemical potential. In these theories the ground state putatively breaks rotational invariance due to condensation of vector fields [52], and depending on whether we are in the

2. ABELIAN CHERN-SIMONS VORTICES AT FINITE CHEMICAL POTENTIAL

$SU(N)$ or $U(N)$ theory, particle number is ungauged or gauged, and we will have superfluid or superconducting vortices.

Chapter 3

Roton-phonon excitations in Chern-Simons matter theory at finite density

3.1 Introduction

Relativistic field theories in three dimensions consisting of Chern-Simons gauge fields coupled to matter have been conjectured to enjoy a Bose-Fermi/level-rank duality symmetry [39]. Mounting evidence for the conjecture has appeared in various forms. These include detailed aspects of correlators [26, 39, 56, 69, 70] and S-matrices [71, 72] in large- N vector models coupled to Chern-Simons gauge fields in the 't Hooft limit when the theory becomes exactly solvable. Further, the large- N thermal partition functions have been shown to exhibit Bose-Fermi duality as the 't Hooft coupling is varied [38, 39, 57–59]. A crucial role in this is played by the nontrivial eigenvalue distributions of the holonomy matrix around the Euclidean thermal circle, and the duality manifests itself in various phases characterized by the large- N eigenvalue distributions. The finite N versions of the duality can be precisely formulated [7], and include an intricate web of abelian dualities [20, 21, 55] with particle-vortex duality as one of its strands.

In this work, motivated by the goal of understanding the manifestations of Bose-Fermi duality at finite density, we study the zero temperature ground

3. ROTON-PHONON EXCITATIONS IN CHERN-SIMONS MATTER THEORY AT FINITE DENSITY

states of a fundamental scalar coupled to Chern-Simons gauge fields in the presence of a chemical potential for particle number. In particular, we will be mainly interested in finite density ground states in the (semi-)classical limit which spontaneously break the global $U(1)_B$ particle number symmetry. This is a subtle issue in 2+1 dimensions, as any finite temperature will result in thermal fluctuations that, by the Coleman-Mermin-Wagner theorem [73, 74], can destroy long-range order. For this reason, in this thesis we limit ourselves to the system at zero temperature. At non-zero temperature and finite density in the absence of condensates, exact results at large- N for Chern-Simons theory with a fundamental fermion [60, 75] show nontrivial agreement at strong 't Hooft coupling¹ with the weakly interacting bosonic counterpart.

In our analysis of the Chern-Simons-scalar system we assume a classical limit i.e. the Chern-Simons level k is large (but finite), and any other scalar self-couplings taken to be suitably weak so that the semiclassical description applies. Our main findings are summarized below:

- We find that the theory with $SU(N)$ gauge group, Chern-Simons level k and non-zero chemical potential for particle number, exhibits a zero temperature ground state where the scalar field condenses and all gauge fields acquire noncommuting background expectation values. This ground state breaks the $SU(N)$ gauge symmetry completely and spontaneously breaks the global $U(1)_B$ particle number symmetry. While spatial rotations act nontrivially on the background gauge potentials, they can be undone by a $U(1)_C$ subgroup of global $SU(N)$ transformations. Thus gauge invariant operators acquire rotationally invariant expectation values. The scalar VEV itself is left invariant by a combination of the flavour $U(1)_B$ and global colour $U(1)_C$ rotations.
- For the $SU(2)$ theory, assuming $k \gg 1$, we obtain the spectrum of physical fluctuations and their dispersion relations in the Bose condensed ground state. The fluctuation spectrum exhibits a massless phonon mode with linear dispersion relation for the frequency $\omega \sim c_s |\mathbf{k}|$, for low spatial momenta \mathbf{k} , accompanied by a local maximum and a roton minimum at

¹The 't Hooft coupling λ is defined in the limit $N, k \rightarrow \infty$ (k is the Chern-Simons level) where $\lambda \equiv \frac{N}{k}$, ranging between 0 and 1.

some finite spatial momentum. Roton-maxon excitations are well known within the context of superfluidity in 4He [76, 77] and explain various physical characteristics such as heat capacity and the superfluid critical velocity. The roton minimum, for instance, lowers the superfluid critical velocity to below the speed of sound, as can be understood by applying the Landau criterion [76, 77]. In the context of this chapter, we understand the appearance of the roton minimum as a consequence of level crossing of states. In the strict limit $k \rightarrow \infty$ when the Chern-Simons fields decouple, the interacting scalar theory has a Bose condensate with two gapless excitations at zero momentum, one with quadratic and the other with a linear dispersion relation. At large but finite k , the former acquires a gap at zero momentum, and the putative intersection between the linear and quadratic dispersion curves is replaced by a roton-maxon pair in the diagonalized spectrum. The background VEVs for the gauge fields are directly responsible for these features. Roton-like excitations with very similar origin i.e. constant background gauge fields have been identified in Yang-Mills-Higgs systems at finite density in 3+1 dimensions [53].

We find that the roton minimum in the phonon dispersion relation persists in the free scalar theory coupled to Chern-Simons gauge fields (at large k). In this case the only dimensionful scale is provided by the chemical potential which can be rescaled to unity and the resulting spectra and dispersion relations acquire a universal form.

- For the general $SU(N)$ case an interesting picture emerges. The $N \times N$ matrices of VEVs for the Chern-Simons gauge fields provide finite dimensional versions of harmonic oscillator creation and annihilation operators. In particular, they can be viewed as the noncommuting coordinates of N particles in a disc of fixed radius. The same matrices have been used to describe the ground state of the quantum Hall droplet [50, 78]. Fluctuations about the finite density ground state may thus be viewed as fluctuations of this droplet (in configuration space), carrying spatial momentum and frequency.

The zero temperature finite density properties of the Chern-Simons-scalar sys-

3. ROTON-PHONON EXCITATIONS IN CHERN-SIMONS MATTER THEORY AT FINITE DENSITY

tem present a range of physical phenomena interesting in their own right. Importantly, they provide predictions for the fermionic dual. The $SU(N)_k$ theory with a fundamental scalar (and level k) is level-rank dual to the $U(k-N)_{-k,-N}$ theory¹ with a fundamental fermion [7]. In particular, the free scalar coupled to Chern-Simons fields is dual to the Chern-Simons plus critical fermion theory [79]. It is clearly of great interest to understand whether features of the spectrum of the weakly coupled scalar system can be understood from the conjectured fermionic dual at strong coupling.

This chapter is organized as follows. In section 3.2 we study the Bose condensed ground state of the $SU(2)$ system in the classical limit. In section 3.3 we find the spectrum of quadratic fluctuations after gauge fixing, and identify the phonon-roton branch for different regimes of parameters. Section 3.4 is devoted to the generalization of the classical vacuum structure to general $N > 2$. Finally we outline a number of questions for future study in section 3.5.

3.2 The $SU(2)_k$ theory

We consider Chern-Simons theory with $SU(2)$ gauge group and one scalar flavour transforming in the fundamental representation. Working with an anti-hermitean gauge potential A_μ ,

$$A_\mu = A_\mu^{(a)} t^a, \quad t^a \equiv \frac{i}{2} \sigma^a, \quad a = 1, 2, 3, \quad (3.1)$$

where $\{\sigma^a\}$ are the Pauli matrices and $\{A_\mu^{(a)}\}$ are real valued fields, the Chern-Simons action with (quantized) level k is then,

$$S_{CS} = \frac{k}{4\pi} \int d^3x \epsilon^{\mu\nu\rho} Tr \left(A_\mu \partial_\nu A_\rho + \frac{2}{3} A_\mu A_\nu A_\rho \right). \quad (3.2)$$

This is the action for both Euclidean (+++) and Lorentzian (-++) signatures. The Wick rotation from Lorentzian to Euclidean is implemented by the re-

¹The two subscripts denote the Chern-Simons levels of the $SU(k-N)$ and $U(1)$ factors of the gauge group respectively.

placement $t \rightarrow -i\tau$ and $A_0 \rightarrow iA_0$, which together leave S_{CS} invariant. In Lorentzian signature, the complete action involving Chern-Simons and matter fields has the general form,

$$S = S_{matter} + S_{CS}, \quad (3.3)$$

where, in Lorentzian signature $(-++)$, for a scalar Φ transforming in the fundamental representation of $SU(2)$,

$$S_{matter} = - \int d^3x \left((D_\mu \Phi)^\dagger (D^\mu \Phi) + V(\Phi^\dagger \Phi) \right), \quad (3.4)$$

$$D_\mu \equiv \partial_\mu + A_\mu.$$

The theory possesses a *global* $U(1)$ symmetry which we refer to as “baryon number” or $U(1)_B$,

$$U(1)_B : \quad \Phi \rightarrow e^{i\vartheta} \Phi, \quad (3.5)$$

generated by a phase rotation of Φ . The corresponding conserved current is

$$j_B^\mu = i \left[(D^\mu \Phi)^\dagger \Phi - \Phi^\dagger D^\mu \Phi \right]. \quad (3.6)$$

The chemical potential μ_B is a Lagrange multiplier for the $U(1)_B$ charge. In Lorentzian signature, it therefore appears in the Lagrangian as a time component for a background $U(1)_B$ gauge field:

$$D_\nu \rightarrow D_\nu + i\mu_B \delta_{\nu,0}. \quad (3.7)$$

3.2.1 Classical ground states with $\mu_B \neq 0$

The coupling of the Chern-Simons fields to the matter sector is controlled by $1/\sqrt{k}$ ¹. In the limit $k \rightarrow \infty$, the scalar field Φ with $\mu_B \neq 0$ has the potential:

$$V_{scalar}(\mu_B, k \rightarrow \infty) = V(\Phi^\dagger \Phi) - \mu_B^2 \Phi^\dagger \Phi. \quad (3.8)$$

¹This can be understood via the rescaling $A_\mu \rightarrow A_\mu/\sqrt{k}$, following which the Chern-Simons action is order 1 in the large k limit.

3. ROTON-PHONON EXCITATIONS IN CHERN-SIMONS MATTER THEORY AT FINITE DENSITY

As usual, the effective negative mass squared due to the chemical potential drives the system to form a Bose condensate for large enough μ_B . The tree level 3D scalar potential (at $\mu_B = 0$) can be taken to be of the form,

$$V(\Phi^\dagger \Phi) = m^2 \Phi^\dagger \Phi + g_4 (\Phi^\dagger \Phi)^2 + g_6 (\Phi^\dagger \Phi)^3, \quad (3.9)$$

where we have allowed for relevant and marginal operators in the scalar potential. Assuming that the ground state of the theory with $\mu_B \neq 0$ is static and translation invariant, we look for vacuum solutions with all terms involving derivatives being set to zero. Anticipating a scalar condensate at the classical level¹, we can always choose gauge rotations to take the VEV to be real and of the form,

$$\langle \Phi \rangle = \begin{pmatrix} 0 \\ v \end{pmatrix} \quad v \in \mathbb{R}. \quad (3.10)$$

We then collectively view all non-derivative terms as potential energy contributions:

$$\begin{aligned} V_{CS} + V_{scalar} &= -\frac{k}{4\pi} \epsilon^{\mu\nu\rho} A_\mu^{(1)} A_\nu^{(2)} A_\rho^{(3)} - \frac{v^2}{4} \left[\left(A_0^{(1)} \right)^2 + \left(A_0^{(2)} \right)^2 + \left(A_0^{(3)} - 2\mu_B \right)^2 \right] \\ &\quad + \frac{v^2}{4} \sum_{i=1,2} \left[\left(A_i^{(1)} \right)^2 + \left(A_i^{(2)} \right)^2 + \left(A_i^{(3)} \right)^2 \right] + m^2 v^2 + g_4 v^4 + g_6 v^6. \end{aligned} \quad (3.11)$$

One consistent extremum is given by $v = 0$, and all gauge fields also vanishing. This is the trivial solution. However, this solution cannot dominate the grand canonical ensemble for generic values of the chemical potential. In particular, the scalar field theory without Chern-Simons terms ($k^{-1} \rightarrow 0$), and at weak coupling ($g_4 \ll m, g_6 \ll 1$), develops a Bose condensate when $|\mu_B| > m$. This non-trivial phase with $v \neq 0$ must persist when the coupling to Chern-Simons gauge fields is turned on. In order to arrive at a static and translationally invariant ground state, we need to find the minima of the potential energy function (3.11). We adopt a notation which is appropriate for $SU(2)$ by introducing

¹The analysis will remain purely classical and at zero temperature at this stage. At finite temperature, we know that quantum thermal fluctuations in 2+1 dimensions preclude symmetry breaking of continuous global symmetries.

3.2 The $SU(2)_k$ theory

three-vectors in the internal “isospin” directions:

$$\mathbf{A}_\mu \equiv \left(\langle A_\mu^{(1)} \rangle, \langle A_\mu^{(2)} \rangle, \langle A_\mu^{(3)} \rangle \right)^T \quad \mathbf{e}^a \equiv \left(\delta^{a,1}, \delta^{a,2}, \delta^{a,3} \right)^T. \quad (3.12)$$

In terms of these, the vacuum equations determining the ground state are (here the ‘ \times ’ and ‘ \cdot ’ symbols denote cross- and dot-products in the internal space):

$$v^2 \mathbf{A}_y = \frac{k}{2\pi} \mathbf{A}_0 \times \mathbf{A}_x, \quad v^2 \mathbf{A}_x = \frac{k}{2\pi} \mathbf{A}_y \times \mathbf{A}_0, \quad (3.13)$$

$$-v^2 (\mathbf{A}_0 - 2\mu_B \mathbf{e}^3) = \frac{k}{2\pi} \mathbf{A}_x \times \mathbf{A}_y, \quad (3.14)$$

$$\frac{v}{2} \left[(\mathbf{A}_0 - 2\mu_B \mathbf{e}^3)^2 - (\mathbf{A}_x)^2 - (\mathbf{A}_y)^2 \right] = \frac{\partial V}{\partial v}. \quad (3.15)$$

The two equations in (3.13) together imply that $\mathbf{A}_0, \mathbf{A}_x$ and \mathbf{A}_y are mutually orthogonal in the internal isospin directions, and that

$$|\mathbf{A}_x| = |\mathbf{A}_y| \quad |\mathbf{A}_0| = \frac{2\pi v^2}{|k|}, \quad \text{sgn}[(\mathbf{A}_x \times \mathbf{A}_y) \cdot \mathbf{A}_0] = \text{sgn}(k). \quad (3.16)$$

Next, by taking a cross-product of eq.(3.14) with \mathbf{A}_0 , we deduce that $\mathbf{A}_0 = \langle A_0^{(3)} \rangle \mathbf{e}^3$:

$$(\mathbf{A}_x \times \mathbf{A}_y) \times \mathbf{A}_0 = 0 \implies \mathbf{A}_0 \times \mathbf{e}^3 = 0. \quad (3.17)$$

Finally, combining equations (3.14) and (3.15), we obtain conditions on the magnitudes of the background field expectation values:

$$|\mathbf{A}_x|^2 = |\mathbf{A}_y|^2 = \frac{2\pi v^2}{|k|} \left| \langle A_0^{(3)} \rangle - 2\mu_B \right| \quad (3.18)$$

$$\left(\langle A_0^{(3)} \rangle - 2\mu_B \right)^2 - \frac{4\pi v^2}{|k|} \left| \langle A_0^{(3)} \rangle - 2\mu_B \right| - \frac{2}{v} \frac{\partial V}{\partial v} = 0. \quad (3.19)$$

To proceed further, it is useful to work with the (isospin) basis elements

$$\mathbf{A}_0 = \eta \frac{2\pi v^2}{|k|} \mathbf{e}^3, \quad \mathbf{A}_x = a_1 \mathbf{e}^1 + a_2 \mathbf{e}^2, \quad \mathbf{A}_y = \eta \text{sgn}(k) (-a_2 \mathbf{e}^1 + a_1 \mathbf{e}^2),$$

3. ROTON-PHONON EXCITATIONS IN CHERN-SIMONS MATTER THEORY AT FINITE DENSITY

where $\eta = \pm 1$ and $a_{1,2} \in \mathbb{R}$. Using the equations of motion (3.13) and (3.14) we then find that

$$\eta = \text{sgn}(\mu_B), \quad (a_1)^2 + (a_2)^2 = \frac{4\pi v^2}{|k|} \left(|\mu_B| - \frac{v^2 \pi}{|k|} \right), \quad |\mu_B| > \frac{\pi v^2}{|k|}. \quad (3.20)$$

The classical configuration is endowed with a non-zero $U(1)_B$ charge density,

$$\langle j_B^0 \rangle = \text{sgn}(\mu_B) \frac{2\pi v^4}{|k|}, \quad (3.21)$$

with vanishing $U(1)_B$ currents. To calculate the scalar VEV we need the form of the tree level potential. For simplicity we set $g_6 = 0$. With a quartic potential there exists a unique solution¹ for the vacuum expectation value (3.19),

$$v^2 = \frac{|k|}{3\pi} \left(\frac{g_4 |k|}{\pi} + 2|\mu_B| - \sqrt{\left(\frac{g_4 |k|}{\pi} + 2|\mu_B| \right)^2 - 3(\mu_B^2 - m^2)} \right), \quad (3.22)$$

which also satisfies the condition (3.20). As expected, the VEV is real only when $\mu_B^2 > m^2$, and in the large k limit when the Chern-Simons gauge fields decouple, $v^2 \simeq (\mu_B^2 - m^2)/2g_4$. This is, of course, the scalar VEV in the pure scalar theory in the Bose condensed phase. In the massless theory, the scalar VEV is controlled by the dimensionless combination $|\pi\mu_B/g_4 k|$:

$$m = 0 : \quad v^2 = \frac{|\mu_B k|}{2\pi} f(\tilde{\mu}), \quad \tilde{\mu} \equiv \frac{\pi|\mu_B|}{g_4 |k|} \quad (3.23)$$

$$f(\tilde{\mu}) = \frac{2}{3} \left(\tilde{\mu}^{-1} + 2 - \sqrt{(\tilde{\mu}^{-1} + 2)^2 - 3} \right),$$

where $f(\tilde{\mu})$ is monotonically increasing with $f(0) = 0$ and $f(\infty) \simeq \frac{2}{3}$. A noteworthy point here is that the scalar VEV exists even when g_4 technically vanishes. More generally, one may view the semiclassical limit in which the condensate is well defined as $(g_4/\mu_B) \rightarrow 0$ and $k \rightarrow \infty$ such that $g_4 k / \mu_B$ is kept fixed.

¹The second root for v^2 yields $v^2 > |\mu_B k|/2\pi$ and violates the condition in eq. (3.20).

Free energy: For static configurations we can compute the free energy density by evaluating the potential energy function on the ground state. In terms of the VEV, the free energy is,

$$F = v^2 \left[g_4 v^2 + m^2 - \left(|\mu_B| - \frac{\pi v^2}{k} \right)^2 \right]. \quad (3.24)$$

It is easy to check that (assuming $|\mu_B| > m$) the function is negative definite. In the massless case, the free energy of the Bose condensed phase is determined by the function $f(\tilde{\mu})$:

$$F|_{m=0} = \frac{|\mu_B^3 k|}{4\pi} \frac{f(\tilde{\mu})}{\tilde{\mu}} \left[f(\tilde{\mu}) - \frac{\tilde{\mu}}{2} (f(\tilde{\mu}) - 2)^2 \right], \quad (3.25)$$

which is a negative definite, monotonically decreasing function of $\tilde{\mu}$. Therefore, in the semiclassical regime, the nontrivial vacuum dominates over the trivial one with vanishing VEVs for all fields. For instance, in the massless theory with $g_4 = 0$, the free energy in the Higgsed phase is

$$F|_{m=0, g_4=0} = -4 \frac{|\mu_B^3 k|}{27\pi}, \quad (3.26)$$

valid in the semiclassical limit $k \gg 1$. Quantum corrections are parametrically suppressed in this limit. In this case the theory enters the Higgsed phase for any non-zero chemical potential, while the theory with vanishing chemical potential is conformal. When the mass is non-zero and the chemical potential is dialed past the classical threshold value $\mu_B = m$, following a second order phase transition, the theory enters a Bose condensed Higgs phase. The symmetric phase is unstable beyond this point. This interpretation is supported by the plot (figure 3.1) of the free energy as a function of the VEV v (taking $g_4 = 0$ for simplicity). The effect of quantum corrections at large k will be to renormalize the mass in the symmetric phase and change the threshold value of the chemical potential at which the (second order) phase transition from the symmetric to the Higgsed phase occurs. This qualitative picture may change for finite k when quantum corrections are large.

3. ROTON-PHONON EXCITATIONS IN CHERN-SIMONS MATTER THEORY AT FINITE DENSITY

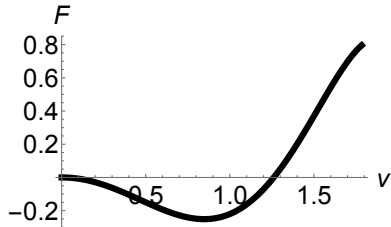


Figure 3.1: The effective potential (free energy density) as a function of the VEV ν for $\mu_B = 1$, $m = 0.5$ and $g_4 = 0$.

3.2.2 Colour-flavour locked symmetry

We have found a one-parameter family of gauge field solutions parametrised by the variables (a_1, a_2) , satisfying a constraint (3.20). Any given realization breaks the $SU(2)$ gauge symmetry completely due to the scalar VEV which also breaks $U(1)_B$. However, the scalar VEV is left invariant by the diagonal combination of $U(1)_B$ and a $U(1)$ subgroup of the *global* $SU(2)$ colour rotations:

$$U(1)_B : \langle \Phi \rangle \rightarrow e^{i\vartheta/2} \langle \Phi \rangle \quad U(1)_C : \Phi \rightarrow U(\vartheta)\Phi, \quad U(\vartheta) \equiv e^{i\vartheta\sigma_3/2} \quad (3.27)$$

While the gauge fields do not transform under $U(1)_B$, they do transform under the global $U(1)_C$. The transformation acts on the background gauge fields $\langle A_i \rangle = \langle A_i^{(a)} \rangle t^a$ exactly as a rotation (R) by a constant angle ϑ in the x - y plane:

$$U(1)_C : \begin{pmatrix} \langle A_x \rangle \\ \langle A_y \rangle \end{pmatrix} \rightarrow \begin{pmatrix} U(\vartheta)\langle A_x \rangle U^\dagger(\vartheta) \\ U(\vartheta)\langle A_y \rangle U^\dagger(\vartheta) \end{pmatrix} = \begin{pmatrix} \cos \vartheta & -\sin \vartheta \\ \sin \vartheta & \cos \vartheta \end{pmatrix} \begin{pmatrix} \langle A_x \rangle \\ \langle A_y \rangle \end{pmatrix}, \quad (3.28)$$

Therefore the vacuum gauge configuration is invariant under a global $U(1)_{B+C+R}$ symmetry which can be viewed as a linear combination of global colour, flavour (or baryon number) and $SO(2)$ rotations in the x - y plane.

The above observation has an important consequence. It implies that the ground state does *not* actually break rotational invariance¹, since the action

¹This will be corroborated by the spectrum of physical fluctuations which we extract subsequently.

of rotations can be undone by a gauge transformation. This is naturally reflected in the expectation values of all gauge invariant operators built from field strengths. In particular, the expectation values of single trace operators built from the chromoelectric and chromomagnetic field strengths are independent of the spatial direction or spatial component in question:

$$\langle \text{Tr}(F_{0i})^2 \rangle = -\frac{2\pi^3 v^6}{|k|^3} \left(\mu_B - \frac{v^2 \pi}{|k|} \right), \quad \langle \text{Tr}(F_{ij})^2 \rangle = -\frac{8\pi^2 v^4}{|k|^3} \left(\mu_B - \frac{v^2 \pi}{|k|} \right)^2. \quad (3.29)$$

3.3 Spectrum of fluctuations

We now turn to the spectrum of quadratic fluctuations about the classical vacuum configuration. In the quantum theory this is reliable at weak coupling i.e. $k \gg 1$ and $\mu_B \gg g_4$.

3.3.1 The $k \rightarrow \infty$ theory

It is useful to first recall the situation when the Chern-Simons fields are decoupled in the limit $k \rightarrow \infty$. In this limit we have a pure scalar field theory with a global $O(4) \supset SU(2) \times U(1)_B$ symmetry. A large enough chemical potential for $U(1)_B$ leads to Bose condensation via the scalar VEV,

$$k \rightarrow \infty: \quad v^2 = \frac{\mu_B^2 - m^2}{2g_4}, \quad (3.30)$$

and the weak coupling spectrum is readily obtained after diagonalizing the matrix of quadratic fluctuations. There are four physical excitations corresponding to the four real scalar degrees of freedom with the following dispersion relations for the frequency ω as a function of the spatial momentum \mathbf{p} , where we have set $m = 0$ for simplicity:

$$\omega_{I(\pm)}^2 = \mathbf{p}^2 + 3\mu_B^2 \pm \mu_B \sqrt{4\mathbf{p}^2 + 9\mu_B^2}, \quad (3.31)$$

$$\omega_{II(\pm)}^2 = \mathbf{p}^2 + 2\mu_B^2 \pm 2\mu_B \sqrt{\mathbf{p}^2 + \mu_B^2}.$$

3. ROTON-PHONON EXCITATIONS IN CHERN-SIMONS MATTER THEORY AT FINITE DENSITY

Two of these states are gapless¹. Of the two, only one has a linear dispersion relation at low momentum and corresponds to the phonon mode while the other has a quadratic dependence on the spatial momentum,

$$\omega_{I(-)} = \frac{|\mathbf{p}|}{\sqrt{3}} + \dots, \quad \omega_{II(-)} = \frac{\mathbf{p}^2}{2\mu_B} + \dots \quad (3.32)$$

The presence of the second gapless mode with quadratic dependence on momentum implies that the Bose condensed ground state cannot be viewed as a superfluid, due to vanishing critical velocity according to the Landau criterion [76, 77]. This picture undergoes a qualitative change for finite large k .

3.3.2 Finite, large k

For any finite value of k , the Chern-Simons gauge fields couple to the scalars. However, since the gauge fields are non-dynamical, the number of physical degrees of freedom remains unaltered and is given by the number of real scalars. To calculate the semiclassical spectrum we expand in fluctuations about the gauge and scalar VEVs,

$$A_\mu = \langle A_\mu \rangle + \mathcal{A}_\mu, \quad \Phi = \langle \Phi \rangle + \delta\Phi, \quad \delta\Phi \equiv \begin{pmatrix} \varphi_1 + i\varphi_2 \\ \varphi_3 + i\varphi_4 \end{pmatrix}, \quad (3.33)$$

where \mathcal{A}_μ and $\{\varphi_i\}$ ($i = 1, \dots, 4$) are respectively, the gauge field and matter fluctuations. Substituting these into the original action (3.2) and (3.4), and expanding to quadratic order in fluctuations,

$$\begin{aligned} \mathcal{L}^{(2)} = & \delta\Phi^\dagger \mathcal{D}_\mu \mathcal{D}^\mu \delta\Phi + \langle \Phi^\dagger \rangle \mathcal{A}_\mu \mathcal{D}^\mu \delta\Phi - \mathcal{D}_\mu \delta\Phi^\dagger \mathcal{A}_\mu \langle \Phi \rangle + \langle \Phi^\dagger \rangle \mathcal{A}_\mu \mathcal{A}^\mu \langle \Phi \rangle \\ & + \frac{k}{4\pi} \epsilon^{\mu\nu\lambda} \text{Tr}(\mathcal{A}_\mu \mathcal{D}_\nu \mathcal{A}_\lambda) - \frac{1}{2} \varphi_j \varphi_k \left\langle \frac{\partial^2 V}{\partial \varphi_j \partial \varphi_k} \right\rangle. \end{aligned} \quad (3.34)$$

¹The chemical potential picks out a $U(1)_B \simeq SO(2) \subset O(4)$ and breaks the symmetry to $SO(3) \simeq SU(2)$. The scalar condensate spontaneously breaks both the $SU(2)$ and the $U(1)_B$, and the number of Goldstone bosons is lesser than the number of broken generators, as expected when relativistic invariance is absent [80, 81].

3.3 Spectrum of fluctuations

Here \mathcal{D}_μ denotes the covariant derivative with respect to the background gauge field $\langle A_\mu \rangle$:

$$\mathcal{D}_\mu \delta\Phi \equiv \partial_\mu \delta\Phi + (\langle A_\mu \rangle + i\mu_B \delta_{\mu,0}) \delta\Phi, \quad \mathcal{D}_\mu \mathcal{A}_\nu \equiv \partial_\mu \mathcal{A}_\nu + [\langle A_\mu \rangle, \mathcal{A}_\nu]. \quad (3.35)$$

The main point to note here is that in the presence of the VEV for both scalars and gauge fields, all the fluctuations (matter and gauge) couple to each other at quadratic order. Due to the mixings, the physical degrees of freedom and their dispersion relations are not immediately obvious. In order to extract these, we first need to gauge-fix the action for the quadratic fluctuations. The gauge-*unfixed* action would yield a degenerate matrix with vanishing determinant. In the presence of background gauge fields and symmetry breaking scalar VEVs, it is natural to adopt an R_ξ gauge which is covariant with respect to the non-zero background gauge fields:

$$\mathcal{L}^{(2)} \rightarrow \mathcal{L}^{(2)} + \mathcal{L}_{gf}, \quad \mathcal{L}_{gf} = \frac{1}{2\xi} \text{Tr} \left(\mathcal{D}_\mu \mathcal{A}^\mu - \xi \langle \Phi \rangle \delta\Phi^\dagger + \xi \delta\Phi \langle \Phi^\dagger \rangle \right)^2. \quad (3.36)$$

The R_ξ gauge above removes the derivative couplings between the would-be Goldstone modes and the gauge field fluctuations \mathcal{A}_μ , and introduces a non-trivial mass matrix for them.

The determinant of the gauge-fixed fluctuation matrix then exhibits zeroes with both ξ -dependent and ξ -independent dispersion relations. The latter correspond to the physical states of the theory. In fact, these can be isolated by identifying the leading term in the large- ξ expansion of the determinant of fluctuations at fixed frequency and momentum.

3.3.2.1 Physical states

We have checked numerically that the physical states inferred from the procedure above are indeed ξ -independent. For the $SU(2)$ theory there are precisely four physical states corresponding to the two complex components of the scalar doublet, since the Chern-Simons gauge fields cannot contribute any additional physical, propagating degrees of freedom. The dispersion relations for these four physical states are given by the solutions to a quartic equation

3. ROTON-PHONON EXCITATIONS IN CHERN-SIMONS MATTER THEORY AT FINITE DENSITY

in (ω^2, \mathbf{p}^2) ,

$$\omega^8 + \mu_B^2 C_3 \omega^6 + \mu_B^4 C_2 \omega^4 + \mu_B^6 C_1 \omega^2 + \mu_B^8 C_0 = 0. \quad (3.37)$$

where the $\{C_i\}$ ($i = 0, \dots, 3$) are functions of dimensionless variables,

$$C_i = C_i \left(\frac{\mathbf{p}^2}{\mu_B^2}, \frac{g_4}{\mu_B}, \frac{m^2}{\mu_B^2}, k \right), \quad (3.38)$$

whose explicit forms are given in (A.2).

The phonon mode: We first recall that the $U(1)_B$ global symmetry is spontaneously broken and the corresponding Goldstone mode is the phonon. Since the remaining broken symmetries are local, the phonon should be the only massless state. This is confirmed by solving for the spectrum using (3.37) at $\mathbf{p} = 0$ which yields¹

$$\begin{aligned} \mathbf{p} = \mathbf{0} : \quad \omega_{I-} &= 0 & \omega_{I+} &= \sqrt{m^2 + 6g_4v^2 - \mu_B^2 + \left(2|\mu_B| - \frac{\pi v}{|k|}\right)^2}, \\ \omega_{II(-)} &= \frac{4\pi}{|k|} v^2 & \omega_{II(+)} &= 2|\mu_B|. \end{aligned} \quad (3.39)$$

As expected the gapless mode with a quadratic dispersion in the $k = \infty$ theory is lifted. It is then straightforward to find the velocity of the phonon mode. In the limit of small ω and $|\mathbf{p}|$ we identify the coefficients of the terms quadratic in ω and \mathbf{p} in the polynomial (3.37). The resulting speed of sound is then,

$$\begin{aligned} c_s &= \left. \frac{d\omega}{d|\mathbf{p}|} \right|_{|\mathbf{p}| \rightarrow 0} = (1-y)^{1/2} \left(\frac{-15y^2 + 12y + (m^2 + 6g_4v^2)\mu_B^{-2} - 1}{y^2 - 4y + (m^2 + 6g_4v^2)\mu_B^{-2} - 3} \right)^{1/2} \\ y &\equiv \frac{\pi v^2}{|k\mu_B|}. \end{aligned} \quad (3.40)$$

¹We follow the branches with the same nomenclature used for the $k = \infty$ theory. The subscripts $I(-)$ and $II(-)$ refer to the gapless states in that theory with linear and quadratic dispersion relations, respectively.

3.3 Spectrum of fluctuations

The scalar VEV is given in eq.(3.22). In the massless limit ($m = 0$), the expression is purely a function of the dimensionless combination $\tilde{\mu} = \pi\mu_B/|g_4 k|$ introduced earlier. In particular, the two distinct regimes of large k (with g_4 fixed) and small g_4 (with k fixed), which correspond to small and large $\tilde{\mu}$ respectively, are distinguished by two different limiting values for the speed of sound:

$$m = 0, \quad \tilde{\mu} \ll 1 : \quad c_s = \frac{1}{\sqrt{3}} \left(1 + \frac{5\tilde{\mu}}{12} - \frac{91\tilde{\mu}^2}{96} + \dots \right) \quad (3.41)$$

$$m = 0, \quad \tilde{\mu} \gg 1 : \quad c_s = \frac{1}{\sqrt{2}} \left(1 - \frac{1}{8\tilde{\mu}} + \frac{11}{128\tilde{\mu}^2} + \dots \right)$$

The limit of vanishing g_4 yields the free scalar field coupled to Chern-Simons gauge fields. In this limit the theory is conformal and therefore the speed of sound is as expected for a scale-invariant theory in $2+1$ dimensions. This is a consistency check of the nontrivial Bose-condensed ground state we have discussed, stabilized by gauge field expectation values. It is also a consistency check on the dispersion relations for the semiclassical quadratic fluctuations. For non-zero scalar masses the phonon velocity is a nontrivial function of both

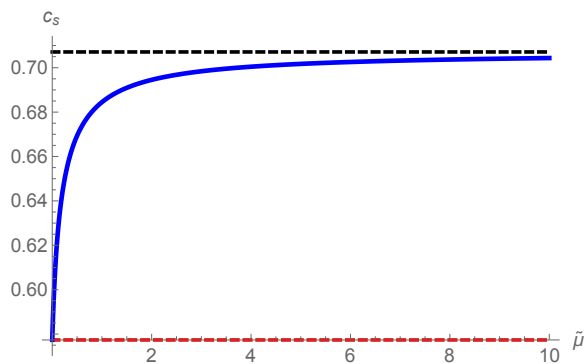


Figure 3.2: The solid blue curve shows the slope of the phonon dispersion relation at $\mathbf{p} = 0$ as a function of $\tilde{\mu} = \pi|\mu_B/g_4 k|$ for the massless theory. It interpolates between $c_s = 1/\sqrt{3}$ at small $\tilde{\mu}$ and the conformal value of $c_s = 1/\sqrt{2}$ when g_4 is taken to zero.

m and μ_B . For instance, at large values of k and all other parameters held fixed,

3. ROTON-PHONON EXCITATIONS IN CHERN-SIMONS MATTER THEORY AT FINITE DENSITY

we obtain

$$c_s^2 = \frac{\mu_B^2 - m^2}{3\mu_B^2 - m^2} + \frac{\pi(5\mu_B^2 + m^2)(m^2 - \mu_B^2)^2}{2|k\mu_B|g_4(m^2 - \mu_B^2)^2} + O(1/k^2). \quad (3.42)$$

The expression can be rewritten as a function of the two dimensionless parameters $\tilde{\mu} = \pi\mu_B/g_4|k|$ and $\tilde{m} \equiv \pi m/g_4|k|$.

Level crossing: The perturbative spectrum in the regime of small ω and \mathbf{p} displays an interesting feature. This is a nontrivial consequence of crossing of energy levels which occurs as we tune the Chern-Simons level from $k = \infty$ to finite (large) values. This unavoidable crossing is between the phonon ($\omega_{I(-)}$ branch) and the light state with energy $\omega_{II(-)}$ which happens to be gapless with quadratic dispersion relation at $k = \infty$, but acquires a small gap $\sim 4\pi v^2/k$ at large k . The crossing is accompanied by off-diagonal mixings between these two fluctuations. In the low energy, long wavelength limit $\omega, |\mathbf{p}| \ll \mu_B$ (where we are ignoring m for simplicity) it should suffice to focus attention on the two-level system comprising of the two lightest excitations. In this limit, the gapped modes only yield an overall multiplicative constant in the fluctuation determinant which takes the approximate form,

$$(\omega^2 - c_s^2 \mathbf{p}^2) \left(\omega^2 - \frac{\mathbf{p}^4}{4\mu^2} - \delta \right) - \varepsilon \mathbf{p}^4 = 0. \quad (3.43)$$

The mixing term $\varepsilon \sim k^{-1}$, whilst the gap generated for the branch $\omega_{II(-)}$ with quadratic dispersion scales as $\delta \sim k^{-2}$, both vanishing in the large k limit. The mixing must necessarily be momentum dependent so that the gapless phonon mode persists as a Goldstone boson for the broken $U(1)_B$. At low momentum the leading such contribution scales as \mathbf{p}^4 (using eq.(A.2)). The new solutions to (3.43) provide a qualitative description of the perturbed light spectrum at large, finite k . In particular, as shown in figure 3.3, the two branches do not cross and the phonon branch displays a “maxon” or a local maximum in its dispersion relation. For non-zero ε the two dispersion relations (viewed as functions of \mathbf{p}^2) have a branch-point in the complex plane. For small enough ε , the location of the maximum in $\omega_{I(-)}$ is close to the putative intersection point

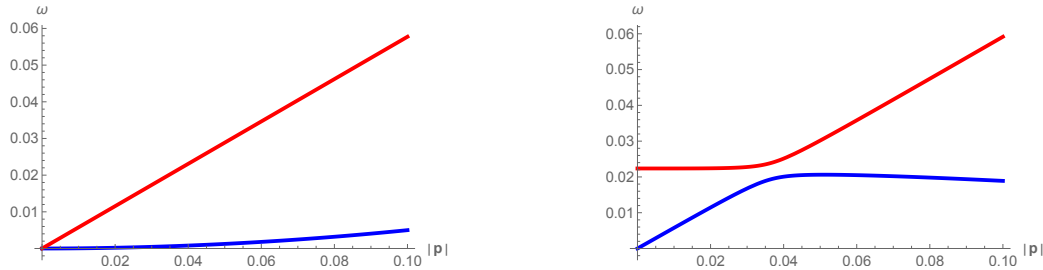


Figure 3.3: Left: The $k = \infty$ theory displays two gapless excitations with linear and quadratic dispersion relation. **Right:** At finite large k , the two modes potentially cross, and also mix. The diagonalized modes display a splitting and “repulsion” resulting in a local maximum in the phonon branch.

of the two curves. The presence of this local maximum implies the existence of a “roton” minimum since all dispersion curves must eventually increase linearly at large $|\mathbf{p}|$ consistent with UV relativistic invariance.

3.3.3 Roton minimum and complete spectrum

Our main observation is that for any (large) finite value of k , consistent with being in the semiclassical regime the phonon branch always displays a roton minimum. At large k and fixed g_4 , the position of the maximum can be estimated quite easily. It sits close to the potential intersection point of the dispersion curves for $\omega_{II(-)}$ and $\omega_{I(-)}$. In the large k regime, the former is flat, $\omega_{II(-)} \approx 4\pi v^2/|k|$, while the latter is linear, $\omega_{I(-)} \approx |\mathbf{p}|/\sqrt{3}$, and their putative intersection is at

$$k \gg 1, g_4 \text{fixed} : \quad (\omega_{max}, |\mathbf{p}|_{max}) \approx \left(\frac{4\pi v^2}{|k|}, \frac{4\pi v^2 \sqrt{3}}{|k|} \right). \quad (3.44)$$

On the other hand, the location of the roton minimum is more subtle. In the large k theory we expect the minimum to be located at parametrically small values close to the origin. In fact, it turns out that $\omega_{rot} \sim k^{-1}$ whilst $\mathbf{p}_{rot} \sim k^{-1/2}$. This can be checked by first performing the scaling

$$\omega = \frac{1}{k} \tilde{\omega} \quad \mathbf{p} = \frac{1}{\sqrt{k}} \rho, \quad (3.45)$$

3. ROTON-PHONON EXCITATIONS IN CHERN-SIMONS MATTER THEORY AT FINITE DENSITY

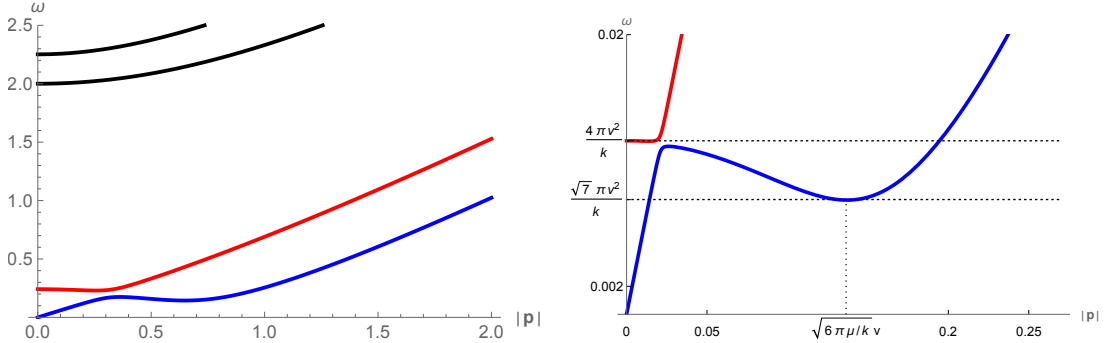


Figure 3.4: **Left:** The spectrum for $m = 0$ with $\tilde{\mu} = \pi\mu_B/g_4k = \pi/20$. **Right:** The two lightest states, including the phonon-roton branch (blue) with $\tilde{\mu} = \pi/500$. The dotted lines indicate the large- k limiting values of the roton maximum and minimum.

then substituting into the fluctuation determinant (A.2), and the expression for $\omega'(\mathbf{p})$ by differentiating (A.2). Subsequently, setting the determinant and $\omega'(\mathbf{p})$ to zero, and then taking the large k limit, we find (setting $m = 0$ for simplicity):

$$3\rho^4 - 24\pi\mu_B\rho^2v^2 + 4\mu_B^2(16\pi^2v^4 - \omega^2) = 0 \quad (3.46)$$

$$\rho^4 - 12\pi\mu_B\rho^2v^2 + 4\mu_B^2(16\pi^2v^4 - \omega^2) = 0.$$

The solutions to these yield the roton minimum at large k for the massless theory:

$$k \gg 1 : \quad (\omega_{rot}, |\mathbf{p}|_{rot}) = \left(\frac{\sqrt{7}\pi v^2}{k}, \sqrt{\frac{6\pi\mu}{k}} v \right), \quad (3.47)$$

where the VEV is given by (3.22) with $m = 0$. The results for the roton minimum and maximum agree perfectly with the numerical curves for the phonon-roton branch at large k , displayed in figure 3.4. The qualitative nature of the dispersion relations persists for all values of m , μ_B and g_4k . Figure 3.5 shows the relevant plots for one non-zero value of m .

Critical case with $g_4 = m = 0$: A nontrivial aspect of the Bose condensed ground state is that all generic features of the spectrum of fluctuations persist

3.3 Spectrum of fluctuations

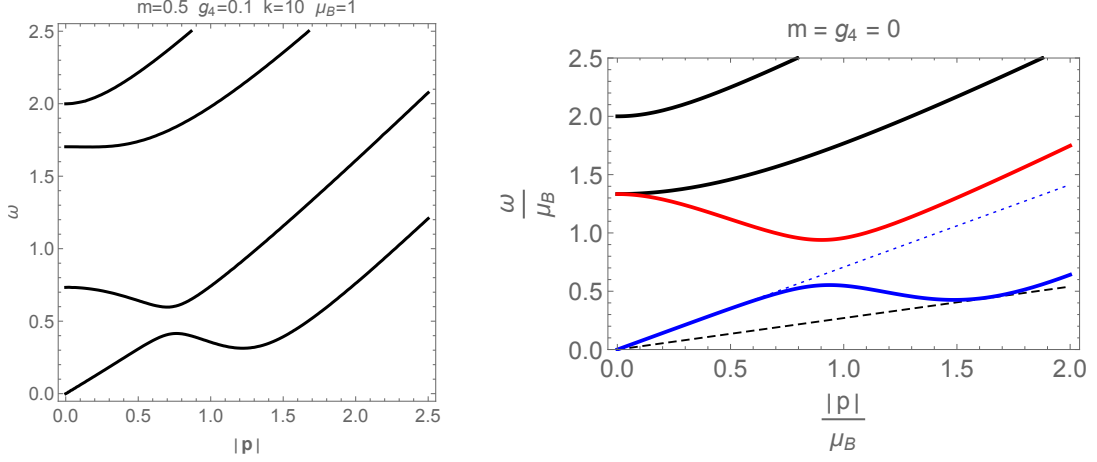


Figure 3.5: **Left:** The physical spectrum for the massive case. **Right:** In the scale invariant situation, the dispersion relations have a universal form, independent of k and μ . The dotted blue line with slope $1/\sqrt{2}$ matches the phonon velocity at low momentum.

even when $g_4 = m = 0$ (and $\mu_B \neq 0$) so that the classical theory is scale invariant. The determinant of physical fluctuations (A.2) simplifies greatly, and the relevant dispersion relations are obtained from its zeroes:

$$\tilde{p} \equiv \frac{|\mathbf{p}|}{\mu_B} \quad \tilde{\omega} \equiv \frac{\omega}{\mu_B}, \quad (3.48)$$

$$\tilde{p}^8 - \tilde{p}^6 \left(4\tilde{\omega}^2 + \frac{28}{9} \right) + \tilde{p}^4 \left(6\tilde{\omega}^4 - \frac{4}{3}\tilde{\omega}^2 + \frac{160}{81} \right) - \tilde{p}^2 \left(4\tilde{\omega}^6 - 12\tilde{\omega}^4 + \frac{992}{81}\tilde{\omega}^2 - \frac{512}{81} \right)$$

$$+ \tilde{\omega}^8 - \frac{68}{9}\tilde{\omega}^6 + \frac{1408}{81}\tilde{\omega}^4 - \frac{1024}{81}\tilde{\omega}^2 = 0.$$

At zero momentum the energies of the four physical states are:

$$\omega_{I(-)} = 0, \quad \omega_{I(+)} = \frac{4\mu_B}{3}, \quad \omega_{II(-)} = \frac{4\mu_B}{3}, \quad \omega_{II(+)} = 2\mu_B, \quad (3.49)$$

so that two of the massive states become degenerate, whilst the roton maximum and minimum are at

$$(\omega_{max}, |\mathbf{p}|_{max}) = (0.553\mu_B, 0.937\mu_B), \quad (\omega_{rot}, |\mathbf{p}|_{rot}) = (0.426\mu_B, 1.487\mu_B)$$

3. ROTON-PHONON EXCITATIONS IN CHERN-SIMONS MATTER THEORY AT FINITE DENSITY

We expect these results to be stable against quantum corrections for large enough k , since $\frac{1}{k}$ is the only small parameter in the system. It is interesting and somewhat unexpected (given that the roton minimum is often attributed to the presence of a new scale) that the roton persists in the theory where the chemical potential is the only dimensionful scale.

3.3.4 Landau critical velocity

According to Landau's criterion, for a nonrelativistic superfluid flowing with velocity v_s (with respect to a vessel or capillary), when the velocity exceeds a critical value [77] given by

$$v_{crit} = \min_{|\mathbf{p}|} \left(\frac{\omega(\mathbf{p})}{|\mathbf{p}|} \right) \implies \frac{\partial \omega}{\partial |\mathbf{p}|} = \frac{\omega}{|\mathbf{p}|}, \quad (3.50)$$

the fluid loses energy through dissipation and the superfluid phase can be wholly or partially destroyed e.g. by a condensate of rotons [82, 83]. In particular, [82] argues for the appearance, within superfluid 4He flows, of a one dimensional periodic structure at rest with respect to the walls so that the superfluidity criterion is not violated. The Landau criterion is derived by boosting the Bose condensate in the ground state along a particular direction (say the $+x$ -axis) with a velocity v_s , and considering excitations that could reduce or dissipate the energy of the moving condensate. In the frame where the condensate has velocity v_s , the energy of a backscattered nonrelativistic excitation with momentum \mathbf{p} , causing dissipation from the condensate, must satisfy

$$\omega(|\mathbf{p}|) - v_s |\mathbf{p}| < 0, \quad (3.51)$$

where the second term is the result of transformation under the Galilean boost. The critical value of the superfluid velocity is then given as $v_{crit} = \min(\omega/|\mathbf{p}|)$. The arguments can also be carried out in the appropriate relativistic context (e.g.[77, 83]). The critical velocity is inferred from the slope of the straight line passing through the origin and tangent to the dispersion curve for the phonon-roton branch (see dashed black line in figure 3.5).

The behaviour of the critical velocity as a function of $\mu_B/g_4 k$ in the massless

theory is shown in figure 3.6. At large k , the critical velocity vanishes as $1/\sqrt{k}$,

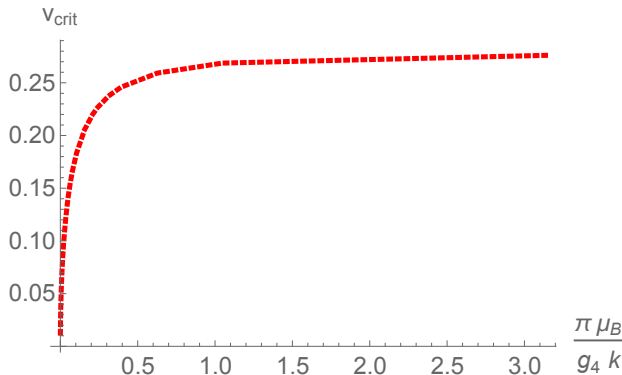


Figure 3.6: The Landau critical velocity as a function of the dimensionless parameter $\pi\mu_B/g_4k$ in the theory with $m = 0$.

and approaches a constant value, $v_{\text{crit}} \approx 0.27$, in the theory with $g_4 = 0$.

3.3.5 The $U(2)_k$ theory

It is interesting to note the qualitative difference between $SU(2)$ and $U(2)$ gauge groups. In the latter case the $U(1)_B$ symmetry is gauged and the chemical potential is synonymous with a fixed background expectation value for the temporal component of the abelian gauge field. The classical vacuum equations are satisfied by the same configuration as in the $SU(2)$ theory. The condensates of the scalar and gauge fields break both the $SU(2)$ and $U(1)_B$ local symmetries to a diagonal $U(1)$. Since all symmetries are local we expect only massive physical states. We obtain the physical fluctuations by employing Coulomb gauge for the abelian gauge field, and retaining the covariant R_ξ gauge-fixing for the $SU(2)$ part. The situation with $m = g_4 = 0$ suffices to demonstrate the existence of the gap. In this case, the dispersion relations of the four physical states can be obtained from the roots of the following poly-

3. ROTON-PHONON EXCITATIONS IN CHERN-SIMONS MATTER THEORY AT FINITE DENSITY

nomial in $(\tilde{\omega}, \tilde{p}) = (\omega/\mu_B, |\mathbf{p}|/\mu_B)$:

$$\tilde{p} \equiv \frac{|\mathbf{p}|}{\mu_B} \quad \tilde{\omega} \equiv \frac{\omega}{\mu_B}, \quad (3.52)$$

$$\begin{aligned} & \tilde{p}^8 - \tilde{p}^6 \left(4\tilde{\omega}^2 + \frac{224}{81} \right) + \tilde{p}^4 \left(6\tilde{\omega}^4 - \frac{64}{27}\tilde{\omega}^2 + \frac{512}{243} \right) - \tilde{p}^2 \left(4\tilde{\omega}^6 - \frac{352}{27}\tilde{\omega}^4 + \frac{3328}{243}\tilde{\omega}^2 - \frac{4096}{729} \right) \\ & + \tilde{\omega}^8 - \frac{640}{81}\tilde{\omega}^6 + \frac{4544}{243}\tilde{\omega}^4 - \frac{10240}{729}\tilde{\omega}^2 + \frac{16384}{59049}. \end{aligned}$$

Unlike the $SU(2)$ theory (3.48) we see that $\tilde{\omega} = \tilde{p} = 0$ is no longer a solution. All states are gapped at $\mathbf{p} = 0$, with the energies given by $\tilde{\omega}^2 = 16/9, 16/9, (22 \pm 5\sqrt{19})/81$. The dispersion relations for non-zero \mathbf{p} are shown in figure 3.7.

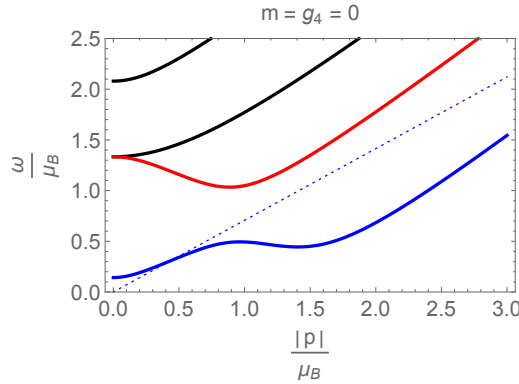


Figure 3.7: The semiclassical spectrum of the $U(2) \simeq SU(2) \times U(1)$ theory. All states are gapped. Nevertheless, the lightest state displays a roton-like minimum. The dotted blue line passing through the origin with slope $1/\sqrt{2}$ is shown to emphasize the absence of phonon-like linear dispersion.

3.4 The $SU(N > 2)$ case

We now generalize the above analysis for Chern-Simons scalar theory with $SU(N)$ gauge group. We use lower case subscripts and superscripts, $(p, q, r\dots)$ to label fundamental and antifundamental representation indices. The gauge covariant derivative is defined to include the chemical potential as a timelike

background gauge field:

$$(D_\mu)_p^q = \delta_p^q \partial_\mu + (A_\mu)_p^q + i\mu_B \delta_p^q \delta_\mu^0. \quad (3.53)$$

For general N , it is useful to define the quartic coupling so that a consistent large N limit can be taken if necessary. The potential contributions involving both gauge and scalar fields can be put together so that,

$$\begin{aligned} V_{CS} + V_{scalar} &= -\frac{k}{4\pi} \frac{2}{3} Tr(A_\mu A_\nu A_\rho) \epsilon^{\mu\nu\rho} - \Phi^\dagger (A^\mu + i\mu_B \eta^{\mu 0}) (A_\mu + i\mu_B \delta_\mu^0) \Phi \\ &\quad + m^2 \Phi^\dagger \Phi + \frac{g_4}{N} (\Phi^\dagger \Phi)^2. \end{aligned} \quad (3.54)$$

Assuming that the scalar obtains a vacuum expectation value, we can always use $SU(N)$ gauge rotations to place the VEV in the N -th component,

$$\langle \Phi_p \rangle = \sqrt{N} v \delta_{p,N}. \quad (3.55)$$

We have scaled out a factor of \sqrt{N} in anticipation of the expected scaling in the large- N limit of vector models. In particular, the action for the matter fields should be $\mathcal{O}(N)$ in the large- N limit. The choice of scalar VEV leaves a residual $SU(N-1)$ gauge symmetry, which is then completely broken by the gauge field backgrounds in the ground state. In order to obtain the correct matrix equations of motion, we vary the action (3.54) subject to a tracelessness condition for $SU(N)$ gauge fields, implemented by Lagrange multipliers $\Lambda^{0,1,2}$:

$$V_{CS} + V_{scalar} \rightarrow V_{CS} + V_{scalar} + \Lambda^\mu Tr(A_\mu). \quad (3.56)$$

3.4.1 Vacuum configuration

The complete vacuum equations extremizing the potential function are:

$$\begin{aligned} -\frac{k}{4\pi} [A_\mu, A_\nu] \epsilon^{\mu\nu\lambda} - \left\{ \Phi \Phi^\dagger, (A^\lambda + i\mu_B \eta^{\lambda 0} \mathbf{1}) \right\} + \Lambda^\lambda \mathbf{1} &= 0, \quad Tr A_\mu = 0, \\ -(A_\mu)_N^p (A^\mu)_p^N + 2i\mu_B (A_0)_N^N + (m^2 - \mu_B^2) + 2g_4 v^2 &= 0. \end{aligned} \quad (3.57)$$

3. ROTON-PHONON EXCITATIONS IN CHERN-SIMONS MATTER THEORY AT FINITE DENSITY

The matrix $\Phi\Phi^\dagger$ is a projector, and given that the scalar VEV can be rotated into the lowest component, it has only one non-zero element,

$$(\Phi\Phi^\dagger)_p^q = N \delta_{p,N} \delta^{q,N} v^2. \quad (3.58)$$

The Lagrange multipliers $\{\Lambda^\lambda\}$ are determined by taking the trace of each of the respective equations of motion so that,

$$\Lambda^\lambda = 2v^2 \left[\left(A^\lambda \right)_N^N + i\mu_B \eta^{\lambda 0} \right]. \quad (3.59)$$

Following the hint provided by the $SU(2)$ vacuum solution, we take A_0 to be diagonal (note that residual $SU(N-1)$ rotations can be used to diagonalize an $(N-1) \times (N-1)$ block of A_0). It then follows that the commutator $[A_x, A_y]$ must be diagonal $\sim \text{diag}(1, 1, \dots, 1 - N)$. This is reminiscent of the N -dimensional representation of the $SU(2)$ algebra, where the off-diagonal ladder operators commute to yield a diagonal matrix. Motivated by this similarity, we find a simple solution for the Chern-Simons equations of motion:

$$\langle A_x \rangle_1^q = i\alpha \delta^{q,2}, \quad \langle A_x \rangle_N^q = i\alpha \sqrt{N-1} \delta^{q,N-1} \quad (3.60)$$

$$\langle A_y \rangle_1^q = \alpha \delta^{q,2}, \quad \langle A_y \rangle_N^q = -\alpha \sqrt{N-1} \delta^{q,N-1}$$

$$\langle A_x \rangle_p^q = i\alpha \left(\sqrt{p} \delta^{q,p+1} + \sqrt{p-1} \delta^{q,p-1} \right), \quad p = 2, \dots, N-1$$

$$\langle A_y \rangle_p^q = \alpha \left(\sqrt{p} \delta^{q,p+1} - \sqrt{p-1} \delta^{q,p-1} \right), \quad p = 2, \dots, N-1$$

$$\langle A_0 \rangle_p^q = i\beta \left(\frac{1}{N} \delta_p^q - \delta_{p,N} \delta^{q,N} \right), \quad p, q = 1 \dots N,$$

where the constants α and β are determined by the VEV and chemical potential as,

$$\alpha = \frac{\beta}{\sqrt{N}} \sqrt{\frac{\mu_B}{\beta} - \frac{N-1}{N}}, \quad \beta = \frac{v^2}{\kappa}, \quad \kappa \equiv \frac{k}{2\pi N}. \quad (3.61)$$

The equation of motion for the scalar VEV (discarding the trivial extremum) is then given by,

$$-\frac{3}{\kappa^2} \left(1 - \frac{1}{N}\right)^2 v^4 + v^2 \left[2g_4 + \frac{4\mu_B}{\kappa} \left(1 - \frac{1}{N}\right) \right] - (\mu_B^2 - m^2) = 0. \quad (3.62)$$

Solving as a quadratic in v^2 , only one solution is physical¹ and matches smoothly onto the semiclassical ($\kappa \gg 1$) limit:

$$v^2 = \frac{N\kappa}{3(N-1)} \left[\frac{g_4 N \kappa}{(N-1)} + 2\mu_B - \sqrt{\left(\frac{g_4 N \kappa}{N-1} + 2\mu_B\right)^2 - 3(\mu_B^2 - m^2)} \right]. \quad (3.63)$$

This agrees precisely with the result (3.22) for $N = 2$ after we perform the rescalings, $v \rightarrow v/\sqrt{N}$ and $g_4 \rightarrow g_4 N$, required to match the conventions adopted in our analysis of the $SU(2)$ theory. It is also worth remarking that the $N \rightarrow \infty$ limit, keeping κ and g_4 fixed, can be readily taken and v remains finite in this limit.

For the free massless scalar coupled to Chern-Simons fields ($m = g_4 = 0$), we obtain

$$v^2 = \kappa \frac{N\mu_B}{3(N-1)}, \quad \alpha = \frac{\mu_B}{3} \sqrt{\frac{2}{N-1}}. \quad (3.64)$$

3.4.2 Interpretation as quantum Hall droplet state

The vacuum configuration breaks the $SU(N)$ gauge symmetry completely. The scalar field VEV also breaks the global $U(1)_B$ spontaneously and therefore the spectrum must yield a massless phonon mode. As seen previously in the $SU(2)$ theory, the classical background is left invariant by a diagonal combination of $U(1)_B$, global colour and spatial rotations. An $SO(2)$ rotation in the x - y plane by an angle ϑ , as in eq.(3.28), can be undone by a global gauge transformation

¹The second root yields $v^2 > \kappa\mu_B N/(N-1)$ which would render α imaginary. In addition, this solution does not have a smooth $k \rightarrow \infty$ limit.

3. ROTON-PHONON EXCITATIONS IN CHERN-SIMONS MATTER THEORY AT FINITE DENSITY

generated by the diagonal matrix J_3 :

$$U(1)_C : \langle A_j \rangle \rightarrow e^{i\vartheta J_3} \langle A_j \rangle e^{-i\vartheta J_3} \quad (3.65)$$

$$J_3 \equiv \text{diag}\left(-\frac{N-1}{2}, -\frac{N-3}{2}, -\frac{N-5}{2}, \dots, \frac{N-3}{2}, \frac{N-1}{2}\right).$$

J_3 is the N -dimensional representation of one of the three generators of the $SU(2)$ algebra. The phase rotation of the scalar VEV generated by J_3 can clearly be compensated by a $U(1)_B$ transformation.

An interesting feature of the vacuum solution is that the Hermitean matrices $i\langle A_x \rangle$ and $i\langle A_y \rangle$ provide a matrix realization of coordinates on the noncommutative plane:

$$[i\langle A_x \rangle, i\langle A_y \rangle] = 2i\alpha^2 \begin{bmatrix} & 1_{(N-1) \times (N-1)} & 0 \\ \hline & 0 & 1-N \end{bmatrix} \quad (3.66)$$

where the noncommutativity parameter is $2\alpha^2$ as defined in eq.(3.61), and scales as $\alpha^2 \sim 1/N$ for large N ¹. Furthermore, it appears that the coordinates are restricted to within a disc or droplet:

$$(i\langle A_x \rangle)^2 + (i\langle A_y \rangle)^2 = 2\alpha^2 \text{diag}(1, 3, 5, \dots, (2N-3), (N-1)). \quad (3.67)$$

The radius of the droplet is bounded in the large N limit since $\alpha^2 \sim 1/N$ with limiting value

$$R_{\text{droplet}}|_{N \rightarrow \infty} = 2\beta \sqrt{\frac{\mu_B}{\beta} - 1}. \quad (3.68)$$

The algebra of matrices is closely related to that of harmonic oscillator creation and annihilation operators, when written in terms of the ladder operators:

$$A^\pm = i(\langle A_x \rangle \pm i\langle A_y \rangle), \quad (3.69)$$

¹It is tempting to look for solutions to the vacuum equations which are reducible and consist of irreducible lower dimensional blocks each satisfying the finite dimensional algebra implied by the vacuum conditions. We have not succeeded in finding any solutions of this type.

which, for any finite N , satisfy $(A^+)^N = (A^-)^N = 0$. Precisely the same set of matrices were introduced to describe the fractional quantum Hall droplet in [50], building on the connection between Abelian noncommutative Chern-Simons theory on the plane and the quantum Hall fluid [78]. The matrix model has also been shown to describe the low energy dynamics of vortices in 2+1 dimensional Yang-Mills-Higgs theory with a Chern-Simons term [61, 68]. In this picture, the matrices $i\langle A_x \rangle$ and $i\langle A_y \rangle$ parametrize the (noncommuting) coordinates of N particles in the droplet. As eq.(3.67) indicates, the particles are placed in concentric circles of radius $\sim \sqrt{2n-1}$ for $n = 0, 1, 2, \dots, N-1$. In the present context, the two matrices appear to deconstruct two dimensions (at large N) on top of the 2+1 spacetime dimensions in which the field theory is originally formulated.

Given the finite density “droplet” ground state for general N , we need to calculate the spectrum of fluctuations around it. This will be addressed in detail in future work [84]. However, we can already make a few remarks. The spectrum must exhibit a massless state corresponding to the phonon arising from the spontaneous breaking of $U(1)_B$. In the droplet picture, physical excitations live only on the boundary of the quantum Hall droplet and are associated to area preserving deformations of the droplet boundary, subject to a Gauss’ law constraint following from the Chern-Simons equations of motion [50]. These have a zero mode corresponding to rotations of the circular droplet ground state, which could naturally be identified with the phonon. In the language of the $N \times N$ matrices comprising the gauge field fluctuations, in an appropriate gauge (more precisely, unitary gauge), the excitations are encoded in the entries of the N -th row and column of gauge field fluctuations of A_x and A_y , all other fluctuations corresponding to pure gauge or “bulk” degrees of freedom of the droplet. It would be extremely interesting to flesh out this picture in detail and explore the implications of this interpretation for the spectrum of the theory for generic N , and in particular its large- N limit.

3.5 Summary and future directions

There are several immediate questions of interest that follow on from the results above. The Bose condensed vacuum should have semiclassical vortex

3. ROTON-PHONON EXCITATIONS IN CHERN-SIMONS MATTER THEORY AT FINITE DENSITY

solutions, and it would be interesting to understand their explicit construction given the non-Abelian nature of the vacuum configuration. The ground state has a $U(1)$ colour-flavour locked global symmetry. A vortex solution that breaks this global symmetry will have an internal zero mode corresponding to a $U(1)$ moduli space of solutions. Such vortices in a (non-Abelian) Higgs phase with noncommuting VEVs, carrying internal zero modes have been encountered previously in different contexts [67, 85, 86]. The physical properties of such vortices and their role in the Bose-Fermi duality would be extremely interesting to explore.

The origin of roton-like minima is often attributed to long range interactions. The interpretation of the background VEVs as noncommuting “coordinates” for a quantum Hall droplet could thus provide a natural route to establish the existence of roton-like excitations¹ for general $N > 2$. In general, the computation of the spectrum of excitations and their dispersion relations about the Bose condensed ground state should be facilitated by the connection to the droplet picture of [50]. The goal would be to eventually understand the putative matching between the spectra of the bosonic theory at weak ’t Hooft coupling ($\lambda_B \ll 1$) and that of the dual critical fermion theory (coupled to Chern-Simons) at strong ’t Hooft coupling ($\lambda_F \rightarrow 1$). Perhaps the most puzzling aspect of this is the interpretation of the Higgsed ground state. When $\lambda_F = 0$, and a $U(1)_B$ chemical potential is switched on in the critical theory, we do not expect fermion bilinears to condense (see e.g. [88]). As λ_F is increased from zero it is conceivable that the effective potential for charged fermion bilinears carrying $U(1)_B$ favours a condensate either for any non-zero λ_F or at some critical value. It would be extremely interesting to understand the behaviour of the large- N effective potential for fermion bilinears for non-zero λ_F and μ_B .

A related question has recently been explored in [89] where Bose-Fermi duality at finite temperature and in the presence of scalar condensate has been established in the large- N ’t Hooft limit. We will need to understand the modification of the zero temperature finite density state, and in particular the background gauge fields VEVs, by any non-zero temperature since the Euclidean

¹See e.g. [87] for a discussion of the relation between noncommutative field theory and roton excitations in bosonic and fermionic systems.

3.5 Summary and future directions

finite temperature theory is effectively two dimensional at long distances and thus fluctuations in the phase of the scalar VEV are unsuppressed. It will be interesting to understand the fate of the phonon-roton mode at finite temperature and non-zero 't Hooft coupling in the Chern-Simons-scalar theory.

3. ROTON-PHONON EXCITATIONS IN CHERN-SIMONS MATTER THEORY AT FINITE DENSITY

Chapter 4

Vortices in $U(2)$ and $SU(2)$ Chern-Simons scalar theories.

Non-abelian vortices have been studied in [90–93]. These are notably different to their abelian counterparts since the scalars appearing in those models, are in the adjoint representation. This allows for the VEV to remain invariant under the center of the gauge group. If $z \in Z(G)$, where $Z(G)$ is the center of G , then by definition z commutes with all elements in the algebra. Thus if an adjoint scalar Φ has a non-zero VEV, then under a gauge transformation generated by z , we have $\Phi \rightarrow z\Phi z^\dagger = \Phi zz^\dagger = \Phi$. In the above cases, the gauge group is $SU(N)$ with center \mathbb{Z}_N . In contrast to these studies, we will be interested in fundamental scalars so this argument does not apply directly to our subject matter. However, due to the appearance of a non-zero chemical potential, we have found out that non-zero VEVs in the gauge sector come to play a role. Since the gauge fields are in the adjoint representation, this allows for the same type of argument for topological stability to reappear in a theory with fundamental matter. In the context of Yang-Mills theory, this type of vortex has been explored by [54].

Similarly to the situation that we encountered in Chapter 2, in the non-abelian case, we also observe a non-trivial ground state. This means that we can expect that there will be a circularly symmetric classical solution that interpolates between this ground state at infinity and the zero fields configuration at the centre. And just as we elaborated in the previous paragraph, we ex-

4. VORTICES IN U(2) AND SU(2) CHERN-SIMONS SCALAR THEORIES.

pect to have two different types of topological vortices, depending on whether we are interested in the U(2) or SU(2) system.

4.1 U(2) theory

The action for the $U(2)$ theory can be written down as follows.

$$S_{\text{CS}}^{\text{SU}(2)} = \frac{k}{4\pi} \int d^3x \epsilon^{\mu\nu\rho} \text{Tr} \left[A_\mu \partial_\nu A_\rho + \frac{2}{3} A_\mu A_\nu A_\rho \right], \quad (4.1)$$

$$S_{\text{CS}}^{\text{U}(1)} = \frac{k'}{4\pi} \int d^3x \epsilon^{\mu\nu\rho} B_\mu \partial_\nu B_\rho, \quad (4.2)$$

$$S_{\text{matter}} = - \int d^3x \left[(D_\mu \Phi)^\dagger (D^\mu \Phi) + V(\Phi^\dagger \Phi) \right], \quad (4.3)$$

$$S = S_{\text{CS}}^{\text{SU}(2)} + S_{\text{CS}}^{\text{U}(1)} + S_{\text{matter}}, \quad (4.4)$$

$$D_\mu = \partial_\mu + A_\mu + B_\mu. \quad (4.5)$$

This leads to the classical equations of motion for the gauge sector.

$$\frac{k}{2\pi} F_{\mu\nu} = \epsilon_{\mu\nu\lambda} J^\lambda \quad (4.6)$$

$$\frac{k'}{2\pi} f_{\mu\nu} = \epsilon_{\mu\nu\lambda} \frac{1}{2} \text{Tr} [\hat{J}^\lambda], \quad (4.7)$$

where

$$F_{\mu\nu} = \partial_\mu A_\nu - \partial_\nu A_\mu + [A_\mu, A_\nu], \quad f_{\mu\nu} = \partial_\mu B_\nu - \partial_\nu B_\mu, \quad (4.8)$$

$$\hat{J}^\lambda = \sqrt{-g} g^{\lambda\nu} (\Phi (D_\nu \Phi)^\dagger - D_\nu \Phi \Phi^\dagger - 2i \mu_B \delta_\nu^0 \Phi \Phi^\dagger), \quad (4.9)$$

$$J^\lambda = \hat{J}^\lambda - \frac{1}{2} \text{Tr} [\hat{J}^\lambda] \mathbb{I} \quad \Rightarrow \quad \text{Tr} [J^\lambda] = 0. \quad (4.10)$$

4.1 U(2) theory

More explicitly the equations become

$$\frac{k}{2\pi}(\partial_r A_\theta - \partial_\theta A_r + [A_r, A_\theta]) = r\{(A_0 + B_0 + i\mu_B), \Phi\Phi^\dagger\} - \frac{1}{2}Tr[\hat{J}^0] \quad (4.11)$$

$$\frac{k}{2\pi}(\partial_0 A_r - \partial_r A_0 + [A_0, A_r]) = -\frac{1}{r}(\partial_\theta\Phi\Phi^\dagger - \Phi\partial_\theta\Phi^\dagger + \{(A_\theta + B_\theta), \Phi\Phi^\dagger\}) - \frac{1}{2}Tr[\hat{J}^\theta] \quad (4.12)$$

$$\frac{k}{2\pi}(\partial_\theta A_0 - \partial_0 A_\theta + [A_\theta, A_0]) = -r(\partial_r\Phi\Phi^\dagger\Phi\partial_r\Phi^\dagger + \{(A_r + B_r), \Phi\Phi^\dagger\}) - \frac{1}{2}Tr[\hat{J}^r]. \quad (4.13)$$

$$\frac{k'}{2\pi}(\partial_r B_\theta - \partial_\theta B_r) = \frac{1}{2}Tr[\hat{J}^0] \quad (4.14)$$

$$\frac{k'}{2\pi}(\partial_0 B_r - \partial_r B_0) = \frac{1}{2}Tr[\hat{J}^\theta] \quad (4.15)$$

$$\frac{k'}{2\pi}(\partial_\theta B_0 - \partial_0 B_\theta) = \frac{1}{2}Tr[\hat{J}^r] \quad (4.16)$$

$$(4.17)$$

The scalar equations are

$$(D_\mu + i\mu\delta_\mu^0)\left[\sqrt{-g}(D^\mu + i\mu g^{\mu 0})\right]\Phi = -\sqrt{-g}\frac{\delta V}{\delta\Phi^\dagger}. \quad (4.18)$$

Inserting the ansatz

$$A_\mu = i(a_\mu^3\sigma_3 + a_\mu^+\sigma_+ + a_\mu^-\sigma_-), \quad (4.19)$$

$$B_\mu = i(a_\mu\mathbb{I}), \quad (4.20)$$

$$\Phi = e^{in\theta} \begin{pmatrix} 0 \\ \varphi(r) \end{pmatrix}, \quad n \in \mathbb{Z}, \quad \varphi(r) \xrightarrow{r \rightarrow \infty} v, \quad (4.21)$$

where

$$\sigma_3 = \begin{bmatrix} 1 & 0 \\ 0 & -1 \end{bmatrix}, \quad \mathbb{I} = \begin{bmatrix} 1 & 0 \\ 0 & 1 \end{bmatrix} \quad (4.22)$$

$$\sigma_+ = \begin{bmatrix} 0 & 1 \\ 0 & 0 \end{bmatrix}, \quad \sigma_- = \begin{bmatrix} 0 & 0 \\ 1 & 0 \end{bmatrix} \quad (4.23)$$

4. VORTICES IN U(2) AND SU(2) CHERN-SIMONS SCALAR THEORIES.

$$\Phi\Phi^\dagger = \varphi(r)^2 \begin{pmatrix} 0 & 0 \\ 0 & 1 \end{pmatrix} = \varphi(r)^2 \sigma_- \sigma_+. \quad (4.24)$$

And using the following relations in order to simplify the equations of motion.

$$[\sigma_+, \sigma_-] = \sigma_3, \quad [\sigma_3, \sigma_+] = 2\sigma_+, \quad [\sigma_3, \sigma_-] = -2\sigma_-. \quad (4.25)$$

The gauge equations of motion become

$$\frac{k}{2\pi} \left(\partial_r a_\theta^3 - \partial_\theta a_r^{(3)} + i(a_r^+ a_\theta^- - a_r^- a_\theta^+) \right) = -r \left(a_0 + \mu - a_0^{(3)} \right) \varphi^2 \quad (4.26)$$

$$\frac{k}{2\pi} \left(\partial_r a_\theta^+ - \partial_\theta a_r^+ + 2i(a_r^{(3)} a_\theta^+ - a_r^+ a_\theta^{(3)}) \right) = r a_0^+ \varphi^2 \quad (4.27)$$

$$\frac{k'}{2\pi} (\partial_r a_\theta - \partial_\theta a_r) = r \left(a_0 + \mu - a_0^{(3)} \right) \varphi^2 + r J_0 \quad (4.28)$$

$$\frac{k}{2\pi} \left(\partial_0 a_r^{(3)} - \partial_r a_0^{(3)} + i(a_0^+ a_r^- - a_0^- a_r^+) \right) = \frac{1}{r} \left(a_\theta + n - a_\theta^{(3)} \right) \varphi^2 \quad (4.29)$$

$$\frac{k}{2\pi} \left(\partial_0 a_r^+ - \partial_r a_0^+ + 2i(a_0^{(3)} a_r^+ - a_0^+ a_r^{(3)}) \right) = -\frac{1}{r} a_\theta^+ \varphi^2 \quad (4.30)$$

$$\frac{k'}{2\pi} (\partial_0 a_r - \partial_r a_0) = -\frac{1}{r} \left(a_\theta + n - a_\theta^{(3)} \right) \varphi^2 \quad (4.31)$$

$$\frac{k}{2\pi} \left(\partial_\theta a_0^{(3)} - \partial_0 a_\theta^{(3)} + i(a_\theta^+ a_0^- - a_\theta^- a_0^+) \right) = r \left(a_r - a_r^{(3)} \right) \varphi^2 \quad (4.32)$$

$$\frac{k}{2\pi} \left(\partial_\theta a_0^+ - \partial_0 a_\theta^+ + 2i(a_\theta^{(3)} a_0^+ - a_\theta^+ a_0^{(3)}) \right) = -r a_r^+ \varphi^2 \quad (4.33)$$

$$\frac{k'}{2\pi} (\partial_\theta a_0 - \partial_0 a_\theta) = r \left(a_r^{(3)} - a_r \right) \varphi^2, \quad (4.34)$$

where J_0 is determined by requiring that the system is neutral when evaluated at the VEV. This implies that

$$J_0 = -\frac{\pi v^2}{k} \left(\frac{\mu k}{\pi} - v^2 \right). \quad (4.35)$$

For static solutions, we may take

$$a_\mu^{(3)} = f_\mu(r), \quad a_\mu^+ = g_\mu(r) e^{-i\theta}, \quad a_\mu^- = g_\mu^*(r) e^{i\theta}, \quad a_\mu = a_\mu(r). \quad (4.36)$$

4.1 U(2) theory

With this ansatz, we have

$$\frac{k}{2\pi} \left(f'_\theta(r) + i(g_r g_\theta^* - g_r^* g_\theta) \right) = -r(a_0 + \mu - f_0) \phi^2 \quad (4.37)$$

$$\frac{k}{2\pi} \left(g'_\theta(r) - ig_r + 2i(f_r g_\theta - g_r f_\theta) \right) = rg_0 \phi^2 \quad (4.38)$$

$$\frac{k'}{2\pi} a'_\theta = r(a_0 + \mu - f_0) \phi^2 - rJ_0 \quad (4.39)$$

$$\frac{k}{2\pi} (f'_0 + i(g_0 g_r^* - g_0^* g_r)) = \frac{1}{r} (a_\theta + n - f_\theta) \phi^2 \quad (4.40)$$

$$\frac{k}{2\pi} (g'_0 - 2i(f_0 g_r - g_0 f_r)) = \frac{1}{r} g_\theta \phi^2 \quad (4.41)$$

$$\frac{k'}{2\pi} a'_0 = \frac{1}{r} (a_\theta + n - f_\theta) \phi^2 \quad (4.42)$$

$$\frac{ik}{2\pi} (g_\theta g_0^* - g_\theta^* g_0) = r(a_r - f_r) \phi^2 \quad (4.43)$$

$$\frac{ik}{2\pi} (g_0 - 2(f_\theta g_0 - g_\theta f_0)) = rg_r \phi^2 \quad (4.44)$$

$$r(f_r - a_r) \phi^2 = 0. \quad (4.45)$$

From these equations we can see that we can further restrict the ansatz so that

$$f_r = a_r = 0 \quad (4.46)$$

$$g_0(r) = \tilde{g}_0(r) e^{i\alpha}, \quad g_\theta(r) = \tilde{g}_\theta(r) e^{i\alpha}, \quad g_r(r) = \tilde{g}_r(r) e^{i(\alpha + \frac{\pi}{2})}, \quad (4.47)$$

where all of $\tilde{g}_\mu \in \mathbb{R}$. Note the $\frac{\pi}{2}$ shift of the phase of the g_r component relative to the rest of the functions. This is analogous to how the vacuum components of A_θ and A_r relate to one another. The phase factor $e^{i\alpha}$ has to do with the remaining global colour-flavour locked $U(1)$ symmetry in the system. The sys-

4. VORTICES IN U(2) AND SU(2) CHERN-SIMONS SCALAR THEORIES.

tem of equations then simplifies to

$$\frac{k}{2\pi} (f'_\theta - 2\tilde{g}_r \tilde{g}_\theta) = -r(a_0 + \mu - f_0)\phi^2 \quad (4.48)$$

$$\frac{k}{2\pi} (\tilde{g}'_\theta + \tilde{g}_r - 2\tilde{g}_r f_\theta) = r\tilde{g}_0 \phi^2 \quad (4.49)$$

$$\frac{k'}{2\pi} a'_\theta = r(a_0 + \mu - f_0)\phi^2 - rJ_0 \quad (4.50)$$

$$\frac{k}{2\pi} (f'_0 + 2\tilde{g}_0 \tilde{g}_r) = \frac{1}{r}(a_\theta + n - f_\theta)\phi^2 \quad (4.51)$$

$$\frac{k}{2\pi} (\tilde{g}'_0 + 2f_0 \tilde{g}_r) = \frac{1}{r}\tilde{g}_\theta \phi^2 \quad (4.52)$$

$$\frac{k'}{2\pi} a'_0 = \frac{1}{r}(a_\theta + n - f_\theta)\phi^2 \quad (4.53)$$

$$\frac{k}{2\pi} (\tilde{g}_0 - 2(f_\theta \tilde{g}_0 - \tilde{g}_\theta f_0)) = r\tilde{g}_r \phi^2. \quad (4.54)$$

Inserting the ansatz 4.19, 4.20, 4.21, 4.36 into the scalar equation of motion 4.18 we arrive at

$$\begin{aligned} \frac{1}{r} \frac{d}{dr} (r\varphi) + \varphi \left((f_0 - a_0 - \mu)^2 + |g_0|^2 - (a_r - f_r)^2 - |g_r|^2 \right) \\ + \varphi \left(-\frac{1}{r^2} (f_\theta - a_\theta - n)^2 + |g_\theta|^2 \right) = -\frac{\delta V}{\delta \Phi^\dagger}. \end{aligned} \quad (4.55)$$

We would like a solution that asymptotes to ground state that we explored in Chapter 3 ((3.20),(3.22)). This implies the following boundary conditions

$$\varphi \xrightarrow{r \rightarrow \infty} v, \quad \varphi \xrightarrow{r \rightarrow 0} 0, \quad (4.56)$$

$$\tilde{g}_\theta \xrightarrow{r \rightarrow \infty} r \frac{\pi v}{k} \sqrt{\frac{\mu k}{\pi} - v^2}, \quad \tilde{g}_\theta \xrightarrow{r \rightarrow \infty} 0, \quad (4.57)$$

$$\tilde{g}_0 \xrightarrow{r \rightarrow \infty} 0, \quad f_0 \xrightarrow{r \rightarrow \infty} \frac{\pi v^2}{k}, \quad (4.58)$$

$$a_0 \xrightarrow{r \rightarrow \infty} 0, \quad a_\theta \xrightarrow{r \rightarrow \infty} 0, \quad (4.59)$$

$$\tilde{g}_r \xrightarrow{r \rightarrow \infty} \frac{\pi v}{k} \sqrt{\frac{\mu k}{\pi} - v^2}. \quad (4.60)$$

4.2 SU(2) theory

The $SU(2)$ equations of motion are determined by requiring that the trace of the $U(2)$ equations of motion vanishes. This leads to the simplified system

$$\frac{k}{2\pi} \left(\partial_r a_\theta^3 - \partial_\theta a_r^{(3)} + i(a_r^+ a_\theta^- - a_r^- a_\theta^+) \right) = -r(\mu - a^{(3)})\phi^2 \quad (4.61)$$

$$\frac{k}{2\pi} \left(\partial_r a_\theta^+ - \partial_\theta a_r^+ + 2i(a_r^{(3)} a_\theta^+ - a_r^+ a_\theta^{(3)}) \right) = r a_0^+ \phi^2 \quad (4.62)$$

$$\frac{k}{2\pi} \left(\partial_0 a_r^{(3)} - \partial_r a_0^{(3)} + i(a_0^+ a_r^- - a_0^- a_r^+) \right) = \frac{1}{r}(n - a_\theta^{(3)})\phi^2 \quad (4.63)$$

$$\frac{k}{2\pi} \left(\partial_0 a_r^+ - \partial_r a_0^+ + 2i(a_0^{(3)} a_r^+ - a_0^+ a_r^{(3)}) \right) = -\frac{1}{r} a_\theta^+ \phi^2 \quad (4.64)$$

$$\frac{k}{2\pi} \left(\partial_\theta a_0^{(3)} - \partial_0 a_\theta^{(3)} + i(a_\theta^+ a_0^- - a_\theta^- a_0^+) \right) = -r a_r^{(3)} \phi^2 \quad (4.65)$$

$$\frac{k}{2\pi} \left(\partial_\theta a_0^+ - \partial_0 a_\theta^+ + 2i(a_\theta^{(3)} a_0^+ - a_\theta^+ a_0^{(3)}) \right) = -r a_r^+ \phi^2. \quad (4.66)$$

$$\frac{k}{2\pi} (f'_\theta - 2\tilde{g}_r \tilde{g}_\theta) = -r(\mu - f_0)\phi^2 \quad (4.67)$$

$$\frac{k}{2\pi} (\tilde{g}'_\theta + \tilde{g}_r - 2\tilde{g}_r f_\theta) = r \tilde{g}_0 \phi^2 \quad (4.68)$$

$$\frac{k}{2\pi} (f'_0 + 2\tilde{g}_0 \tilde{g}_r) = \frac{1}{r}(n - f_\theta)\phi^2 \quad (4.69)$$

$$\frac{k}{2\pi} (\tilde{g}'_0 + 2f_0 \tilde{g}_r) = \frac{1}{r} \tilde{g}_\theta \phi^2 \quad (4.70)$$

$$\frac{k}{2\pi} (\tilde{g}_0 - 2(f_\theta \tilde{g}_0 - \tilde{g}_\theta f_0)) = r \tilde{g}_r \phi^2. \quad (4.71)$$

4. VORTICES IN U(2) AND SU(2) CHERN-SIMONS SCALAR THEORIES.

Conclusions

- Vortex creation driven by chemical potential only. No SB potential.
- Symmetry broken phase in the $SU(2)$ theory that persists in the conformal phase of quartic coupling going to zero. The ground state exists both in WF fixed point and in the free scalar CS theory.
- Non-commutative gauge theory arising from a ground state that seems to only appear in the finite chemical potential limit.
- Non-abelian Topological Chern-Simons vortices that also seem to only exist in the finite chemical potential regime.
- The Non-commutative description seems to be a gateway into understanding and solving the large N $SU(N)$ theory exactly. In addition, this non-commutativity gives us a hint into how the fermionic description might arise in this sort of system.

4. VORTICES IN U(2) AND SU(2) CHERN-SIMONS SCALAR THEORIES.

Appendix A

Determinant of fluctuation matrix for $SU(2)$

The determinant for the physical fluctuations is given in terms of frequency ω and momentum \mathbf{p} as,

$$\omega^8 + \mu_B^2 C_3 \omega^6 + \mu_B^4 C_2 \omega^4 + \mu_B^6 C_1 \omega^2 + \mu_B^8 C_0 = 0. \quad (\text{A.1})$$

A. DETERMINANT OF FLUCTUATION MATRIX FOR $SU(2)$

Assuming $k > 0, \mu_B > 0$ the coefficients $\{C_i\}$ are (for general choice of signs, it is understood that k and μ_B will be replaced by their absolute values below):

$$\begin{aligned}
C_0 = & \left(\frac{\mathbf{p}^2}{\mu_B^2}\right)^4 + \left(\frac{\mathbf{p}^2}{\mu_B^2}\right)^3 \left(\frac{m^2}{\mu_B^2} - 1 + \frac{6g_4v^2}{\mu_B^2} + \frac{17\pi^2v^4}{k^2\mu_B^2} - \frac{12\pi v^2}{k\mu_B}\right) + \left(\frac{\mathbf{p}^2}{\mu_B^2}\right)^2 \times \\
& \times \left(\frac{16\pi^2m^2v^4}{k^2\mu_B^4} - \frac{12\pi m^2v^2}{k\mu_B^3} + \frac{96\pi^2g_4v^6}{k^2\mu_B^4} - \frac{72\pi g_4v^4}{k\mu_B^3} + \frac{16\pi^4v^8}{k^4\mu_B^4} - \frac{12\pi^3v^6}{k^3\mu_B^3} - \frac{16\pi^2v^4}{k^2\mu_B^2} \right. \\
& \left. + \frac{12\pi v^2}{k\mu_B}\right) + \left(\frac{\mathbf{p}^2}{\mu_B^2}\right) \left(-\frac{384\pi^3g_4v^8}{k^3\mu_B^5} + \frac{384\pi^2g_4v^6}{k^2\mu_B^4} + \frac{960\pi^5v^{10}}{k^5\mu_B^5} - \frac{1728\pi^4v^8}{k^4\mu_B^4} \right. \\
& \left. - \frac{64\pi^3m^2v^6}{k^3\mu_B^5} + \frac{832\pi^3v^6}{k^3\mu_B^3} + \frac{64\pi^2m^2v^4}{k^2\mu_B^4} - \frac{64\pi^2v^4}{k^2\mu_B^2}\right) \tag{A.2} \\
C_1 = & -4\left(\frac{\mathbf{p}^2}{\mu_B^2}\right)^3 + \left(\frac{\mathbf{p}^2}{\mu_B^2}\right)^2 \left(-5 - \frac{3m^2}{\mu_B^2} - \frac{18g_4v^2}{\mu_B^2} - \frac{51\pi^2v^4}{k^2\mu_B^2} + \frac{28\pi v^2}{k\mu_B}\right) + \\
& + \left(\frac{\mathbf{p}^2}{\mu_B^2}\right) \left(4 - 4\frac{m^2}{\mu_B^2} - 24\frac{g_4v^2}{\mu_B^2} - \frac{192\pi^2g_4v^6}{k^2\mu_B^4} + \frac{72\pi g_4v^4}{k\mu_B^3} - \frac{32\pi^4v^8}{k^4\mu_B^4} \right. \\
& \left. + \frac{76\pi^3v^6}{k^3\mu_B^3} - \frac{32\pi^2m^2v^4}{k^2\mu_B^4} - \frac{84\pi^2v^4}{k^2\mu_B^2} + \frac{12\pi m^2v^2}{k\mu_B^3} - \frac{28\pi v^2}{k\mu_B}\right) - \frac{384\pi^2g_4v^6}{k^2\mu_B^4} \\
& - \frac{64\pi^4v^8}{k^4\mu_B^4} + \frac{256\pi^3v^6}{k^3\mu_B^3} - \frac{64\pi^2m^2v^4}{k^2\mu_B^4} - \frac{192\pi^2v^4}{k^2\mu_B^2} \\
C_2 = & 6\left(\frac{\mathbf{p}^2}{\mu_B^2}\right)^2 + \left(\frac{\mathbf{p}^2}{\mu_B^2}\right) \left(\frac{18g_4v^2}{\mu_B^2} + \frac{51\pi^2v^4}{k^2\mu_B^2} - \frac{20\pi v^2}{k\mu_B} + \frac{3m^2}{\mu_B^2} + 13\right) + \frac{96\pi^2g_4v^6}{k^2\mu_B^4} \\
& + \frac{24g_4v^2}{\mu_B^2} + \frac{16\pi^4v^8}{k^4\mu_B^4} - \frac{64\pi^3v^6}{k^3\mu_B^3} + \frac{16\pi^2m^2v^4}{k^2\mu_B^4} + \frac{116\pi^2v^4}{k^2\mu_B^2} - \frac{16\pi v^2}{k\mu_B} + \frac{4m^2}{\mu_B^2} + 12 \\
C_3 = & -4\left(\frac{\mathbf{p}^2}{\mu_B^2}\right) - \frac{6g_Bv^2}{\mu_B^2} - \frac{17\pi^2v^4}{k^2\mu_B^2} + \frac{4\pi v^2}{k\mu_B} - \frac{m^2}{\mu_B^2} - 7
\end{aligned}$$

References

- [1] A. Polyakov, “Quark confinement and topology of gauge theories,” *Nuclear Physics B* **120** no. 3, (Mar., 1977) 429–458.
[https://doi.org/10.1016/0550-3213\(77\)90086-4](https://doi.org/10.1016/0550-3213(77)90086-4). 1
- [2] S. Carlip, “Conformal field theory, (2+1)-dimensional gravity, and the btz black hole,” [arXiv:gr-qc/0503022](https://arxiv.org/abs/gr-qc/0503022). 6
- [3] A. Zee, “Quantum hall fluids,” [arXiv:cond-mat/9501022](https://arxiv.org/abs/cond-mat/9501022). 6
- [4] D. Tong, “Lectures on the quantum hall effect,” 2016. 6, 41
- [5] G. Moore and N. Seiberg, “Taming the conformal zoo,” *Physics Letters B* **220** no. 3, (Apr., 1989) 422–430.
[https://doi.org/10.1016/0370-2693\(89\)90897-6](https://doi.org/10.1016/0370-2693(89)90897-6). 6
- [6] E. Witten, “Quantum field theory and the jones polynomial,” *Communications in Mathematical Physics* **121** no. 3, (Sept., 1989) 351–399. <https://doi.org/10.1007/bf01217730>. 6
- [7] O. Aharony, “Baryons, monopoles and dualities in chern-simons-matter theories,” [arXiv:1512.00161](https://arxiv.org/abs/1512.00161). 6, 35, 42, 45, 67, 70
- [8] G. V. Dunne, “Aspects of chern-simons theory,” 1999. 7, 41
- [9] M. Nakahara, *Geometry, Topology and Physics*. Institute of Physics Publishing, 2003. 9
- [10] S. M. Girvin and A. H. MacDonald, “Off-diagonal long-range order, oblique confinement, and the fractional quantum hall effect,” *Physical*

REFERENCES

- Review Letters* **58** no. 12, (Mar., 1987) 1252–1255.
<https://doi.org/10.1103/physrevlett.58.1252>.
- [11] N. Read, “Order parameter and ginzburg-landau theory for the fractional quantum hall effect,” *Physical Review Letters* **62** no. 1, (Jan., 1989) 86–89. <https://doi.org/10.1103/physrevlett.62.86>.
- [12] S. C. Zhang, T. H. Hansson, and S. Kivelson, “Effective-field-theory model for the fractional quantum hall effect,” *Phys. Rev. Lett.* **62** (Jan, 1989) 82–85.
<https://link.aps.org/doi/10.1103/PhysRevLett.62.82.41>
- [13] H. Nielsen and P. Olesen, “Vortex-line models for dual strings,” *Nuclear Physics B* **61** (Sept., 1973) 45–61.
[https://doi.org/10.1016/0550-3213\(73\)90350-7](https://doi.org/10.1016/0550-3213(73)90350-7). 26
- [14] S. K. Paul and A. Khare, “Charged vortices in an abelian higgs model with chern-simons term,” *Physics Letters B* **174** no. 4, (July, 1986) 420–422. [https://doi.org/10.1016/0370-2693\(86\)91028-2](https://doi.org/10.1016/0370-2693(86)91028-2). 26, 41
- [15] J. Hong, Y. Kim, and P. Y. Pac, “Multivortex solutions of the abelian chern-simons-higgs theory,” *Physical Review Letters* **64** no. 19, (May, 1990) 2230–2233. <https://doi.org/10.1103/physrevlett.64.2230>. 26
- [16] R. Jackiw and E. J. Weinberg, “Self-dual chern-simons vortices,” *Physical Review Letters* **64** no. 19, (May, 1990) 2234–2237.
<https://doi.org/10.1103/physrevlett.64.2234>. 26
- [17] R. Jackiw, K. Lee, and E. J. Weinberg, “Self-dual chern-simons solitons,” *Physical Review D* **42** no. 10, (Nov., 1990) 3488–3499.
<https://doi.org/10.1103/physrevd.42.3488>. 26, 41
- [18] E. B. Bogomolny, “Stability of Classical Solutions,” *Sov. J. Nucl. Phys.* **24** (1976) 449. [Yad. Fiz.24,861(1976)]. 31
- [19] M. K. Prasad and C. M. Sommerfield, “Exact classical solution for the 't hooft monopole and the julia-zee dyon,” *Physical Review Letters* **35**

REFERENCES

- no. 12, (Sept., 1975) 760–762.
<https://doi.org/10.1103/physrevlett.35.760>. 31
- [20] A. Karch and D. Tong, “Particle-vortex duality from 3d bosonization,” arXiv:1606.01893. 33, 42, 67
- [21] J. Murugan and H. Nastase, “Particle-vortex duality in topological insulators and superconductors,” arXiv:1606.01912. 42, 67
- [22] A. Abrikosov, “The magnetic properties of superconducting alloys,” *Journal of Physics and Chemistry of Solids* 2 no. 3, (Jan., 1957) 199–208.
[https://doi.org/10.1016/0022-3697\(57\)90083-5](https://doi.org/10.1016/0022-3697(57)90083-5). 26
- [23] D. Tong, “Tasi lectures on solitons,” 2005.
- [24] R. Feynman, *The Character of Physical Law*. MIT Press, 1965. 34
- [25] I. R. Klebanov and A. M. Polyakov, “Ads dual of the critical $\mathrm{o}(n)$ vector model,” arXiv:hep-th/0210114. 34
- [26] O. Aharony, G. Gur-Ari, and R. Yacoby, “ $d=3$ bosonic vector models coupled to chern-simons gauge theories,” arXiv:1110.4382. 34, 42, 67
- [27] C. P. Burgess and F. Quevedo, “Bosonization as duality,” arXiv:hep-th/9401105. 34
- [28] D. Barci, C. Fosco, and L. Oxman, “On bosonization in 3 dimensions,” *Physics Letters B* 375 no. 1-4, (May, 1996) 267–272.
[https://doi.org/10.1016/0370-2693\(96\)00224-9](https://doi.org/10.1016/0370-2693(96)00224-9). 34
- [29] S. Naculich, H. Riggs, and H. Schnitzer, “Group-level duality in WZW models and chern-simons theory,” *Physics Letters B* 246 no. 3-4, (Aug., 1990) 417–422. [https://doi.org/10.1016/0370-2693\(90\)90623-e](https://doi.org/10.1016/0370-2693(90)90623-e). 34
- [30] M. Camperi, F. Levstein, and G. Zemba, “The large n limit of chern-simons gauge theory,” *Physics Letters B* 247 no. 4, (Sept., 1990) 549–554. [https://doi.org/10.1016/0370-2693\(90\)91899-m](https://doi.org/10.1016/0370-2693(90)91899-m).

REFERENCES

- [31] E. J. Mlawer, S. G. Naculich, H. A. Riggs, and H. J. Schnitzer, “Group-level duality of WZW fusion coefficients and chern-simons link observables,” *Nuclear Physics B* **352** no. 3, (Apr., 1991) 863–896.
[https://doi.org/10.1016/0550-3213\(91\)90110-j](https://doi.org/10.1016/0550-3213(91)90110-j).
- [32] T. Nakanishi and A. Tsuchiya, “Level-rank duality of WZW models in conformal field theory,” *Communications in Mathematical Physics* **144** no. 2, (Feb., 1992) 351–372. <https://doi.org/10.1007/bf02101097>.
- [33] S. G. Naculich and H. J. Schnitzer, “Level-rank duality of the $u(n)$ wzw model, chern-simons theory, and 2d qym theory,” [arXiv:hep-th/0703089](https://arxiv.org/abs/hep-th/0703089). 34
- [34] A. Giveon and D. Kutasov, “Seiberg duality in chern-simons theory,” [arXiv:0808.0360](https://arxiv.org/abs/0808.0360). 35
- [35] F. Benini, C. Closset, and S. Cremonesi, “Comments on 3d seiberg-like dualities,” [arXiv:1108.5373](https://arxiv.org/abs/1108.5373).
- [36] O. Aharony, S. S. Razamat, N. Seiberg, and B. Willett, “3d dualities from 4d dualities,” [arXiv:1305.3924](https://arxiv.org/abs/1305.3924).
- [37] O. Aharony and D. Fleischer, “Ir dualities in general 3d supersymmetric $su(n)$ qcd theories,” [arXiv:1411.5475](https://arxiv.org/abs/1411.5475). 35
- [38] O. Aharony, S. Giombi, G. Gur-Ari, J. Maldacena, and R. Yacoby, “The thermal free energy in large n chern-simons-matter theories,” [arXiv:1211.4843](https://arxiv.org/abs/1211.4843). 35, 42, 67
- [39] S. Giombi, S. Minwalla, S. Prakash, S. P. Trivedi, S. R. Wadia, and X. Yin, “Chern-simons theory with vector fermion matter,” [arXiv:1110.4386](https://arxiv.org/abs/1110.4386). 35, 42, 67
- [40] S. Jain, S. Minwalla, and S. Yokoyama, “Chern simons duality with a fundamental boson and fermion,” [arXiv:1305.7235](https://arxiv.org/abs/1305.7235). 35
- [41] G. Gur-Ari and R. Yacoby, “Three dimensional bosonization from supersymmetry,” 2015. 35

REFERENCES

- [42] C. P. Burgess, C. A. Ltken, and F. Quevedo, “Bosonization in higher dimensions,” arXiv:hep-th/9407078.
- [43] E. Fradkin and F. A. Schaposnik, “The fermion-boson mapping in three dimensional quantum field theory,” arXiv:hep-th/9407182.
- [44] A. P. Polychronakos, “Noncommutative fluids,” arXiv:0706.1095. 36
- [45] R. J. Szabo, “Quantum field theory on noncommutative spaces,” arXiv:hep-th/0109162.
- [46] M. R. Douglas and N. A. Nekrasov, “Noncommutative field theory,” arXiv:hep-th/0106048. 36
- [47] R. Jackiw, S.-Y. Pi, and A. Polychronakos, “Noncommuting gauge fields as a lagrange fluid,” *Annals of Physics* **301** no. 2, (Nov., 2002) 157–173.
<https://doi.org/10.1006/aphy.2002.6290>. 36
- [48] H. S. Snyder, “Quantized space-time,” *Physical Review* **71** no. 1, (Jan., 1947) 38–41. <https://doi.org/10.1103/physrev.71.38>. 36
- [49] H. S. Snyder, “The electromagnetic field in quantized space-time,” *Physical Review* **72** no. 1, (July, 1947) 68–71.
<https://doi.org/10.1103/physrev.72.68>. 36
- [50] A. P. Polychronakos, “Quantum hall states as matrix chern-simons theory,” arXiv:hep-th/0103013. 39, 69, 93, 94
- [51] P. A. Horvathy and P. Zhang, “Vortices in (abelian) chern-simons gauge theory,” arXiv:0811.2094. 41, 56, 57
- [52] S. P. Kumar, D. Roychowdhury, and S. Stratiev, “Roton-phonon excitations in Chern-Simons matter theory at finite density,” *JHEP* **12** (2018) 116, arXiv:1806.06976 [hep-th]. 42, 65
- [53] V. Gusynin, V. Miransky, and I. Shovkovy, “Spontaneous rotational symmetry breaking and roton like excitations in gauged σ -model at finite density,” *Physics Letters B* **581** no. 1-2, (Feb., 2004) 82–92.
<https://doi.org/10.1016/j.physletb.2003.11.042>. 42, 69

REFERENCES

- [54] E. V. Gorbar, J. Jia, and V. A. Miransky, “Vortices in gauge models at finite density with vector condensates,” arXiv:hep-ph/0512203. 42, 97
- [55] N. Seiberg, T. Senthil, C. Wang, and E. Witten, “A Duality Web in 2+1 Dimensions and Condensed Matter Physics,” *Annals Phys.* **374** (2016) 395–433, arXiv:1606.01989 [hep-th]. 42, 67
- [56] O. Aharony, G. Gur-Ari, and R. Yacoby, “Correlation Functions of Large N Chern-Simons-Matter Theories and Bosonization in Three Dimensions,” *JHEP* **12** (2012) 028, arXiv:1207.4593 [hep-th]. 2, 42, 67
- [57] S. Jain, S. Minwalla, T. Sharma, T. Takimi, S. R. Wadia, and S. Yokoyama, “Phases of large N vector Chern-Simons theories on $S^2 \times S^1$,” *JHEP* **09** (2013) 009, arXiv:1301.6169 [hep-th]. 67
- [58] S. Jain, S. Minwalla, and S. Yokoyama, “Chern Simons duality with a fundamental boson and fermion,” *JHEP* **11** (2013) 037, arXiv:1305.7235 [hep-th].
- [59] T. Takimi, “Duality and higher temperature phases of large N Chern-Simons matter theories on $S^2 \times S^1$,” *JHEP* **07** (2013) 177, arXiv:1304.3725 [hep-th]. 67
- [60] M. Geracie, M. Goykhman, and D. T. Son, “Dense Chern-Simons Matter with Fermions at Large N,” *JHEP* **04** (2016) 103, arXiv:1511.04772 [hep-th]. 42, 68
- [61] D. Tong and C. Turner, “Quantum Hall effect in supersymmetric Chern-Simons theories,” *Phys. Rev.* **B92** no. 23, (2015) 235125, arXiv:1508.00580 [hep-th]. 43, 65, 93
- [62] S. Bolognesi, “Large N, Z(N) strings and bag models,” *Nucl. Phys.* **B730** (2005) 150–163, arXiv:hep-th/0507286 [hep-th]. 43
- [63] S. Bolognesi, “Multi-monopoles and magnetic bags,” *Nucl. Phys.* **B752** (2006) 93–123, arXiv:hep-th/0512133 [hep-th].

REFERENCES

- [64] S. Bolognesi and S. B. Gudnason, “A Note on Chern-Simons solitons: A Type III vortex from the wall vortex,” *Nucl. Phys.* **B805** (2008) 104–123, arXiv:0711.3803 [hep-th]. 43, 51, 57
- [65] J. I. Kapusta, “Bose-einstein condensation, spontaneous symmetry breaking, and gauge theories,” *Physical Review D* **24** no. 2, (July, 1981) 426–439. <https://doi.org/10.1103/physrevd.24.426>. 44
- [66] R. A. Rosen, “Phase Transitions of Charged Scalars at Finite Temperature and Chemical Potential,” *JHEP* **12** (2010) 024, arXiv:1009.0752 [hep-th]. 44
- [67] R. Auzzi and S. P. Kumar, “Non-abelian vortices at weak and strong coupling in mass deformed abjm theory,” arXiv:0906.2366. 54, 94
- [68] D. Tong, “A Quantum Hall fluid of vortices,” *JHEP* **02** (2004) 046, arXiv:hep-th/0306266 [hep-th]. 65, 93
- [69] J. Maldacena and A. Zhiboedov, “Constraining Conformal Field Theories with A Higher Spin Symmetry,” *J. Phys.* **A46** (2013) 214011, arXiv:1112.1016 [hep-th]. 67
- [70] J. Maldacena and A. Zhiboedov, “Constraining conformal field theories with a slightly broken higher spin symmetry,” *Class. Quant. Grav.* **30** (2013) 104003, arXiv:1204.3882 [hep-th]. 67
- [71] S. Jain, M. Mandlik, S. Minwalla, T. Takimi, S. R. Wadia, and S. Yokoyama, “Unitarity, Crossing Symmetry and Duality of the S-matrix in large N Chern-Simons theories with fundamental matter,” *JHEP* **04** (2015) 129, arXiv:1404.6373 [hep-th]. 67
- [72] Y. Dandekar, M. Mandlik, and S. Minwalla, “Poles in the S-Matrix of Relativistic Chern-Simons Matter theories from Quantum Mechanics,” *JHEP* **04** (2015) 102, arXiv:1407.1322 [hep-th]. 67
- [73] S. R. Coleman, “There are no Goldstone bosons in two-dimensions,” *Commun. Math. Phys.* **31** (1973) 259–264. 68

REFERENCES

- [74] N. D. Mermin and H. Wagner, “Absence of ferromagnetism or antiferromagnetism in one-dimensional or two-dimensional isotropic Heisenberg models,” *Phys. Rev. Lett.* **17** (1966) 1133–1136. 68
- [75] G. Gur-Ari, S. A. Hartnoll, and R. Mahajan, “Transport in Chern-Simons-Matter Theories,” *JHEP* **07** (2016) 090, arXiv:1605.01122 [hep-th]. 68
- [76] L. D. Landau, “The theory of superfluidity of helium II,” *J. Phys.(USSR)* **5** (1941) 71–100. 69, 78
- [77] A. Schmitt, “Introduction to Superfluidity,” *Lect. Notes Phys.* **888** (2015) pp.1–155, arXiv:1404.1284 [hep-ph]. 69, 78, 86
- [78] L. Susskind, “The Quantum Hall fluid and noncommutative Chern-Simons theory,” arXiv:hep-th/0101029 [hep-th]. 69, 93
- [79] S. Minwalla and S. Yokoyama, “Chern Simons Bosonization along RG Flows,” *JHEP* **02** (2016) 103, arXiv:1507.04546 [hep-th]. 70
- [80] H. B. Nielsen and S. Chadha, “On How to Count Goldstone Bosons,” *Nucl. Phys.* **B105** (1976) 445–453. 78
- [81] H. Watanabe and H. Murayama, “Unified Description of Nambu-Goldstone Bosons without Lorentz Invariance,” *Phys. Rev. Lett.* **108** (2012) 251602, arXiv:1203.0609 [hep-th]. 78
- [82] L. P. Pitaevskii, “Layered structure of 4He with supercritical motion,” *JETP* **39(9)** (1984) 511–514. 86
- [83] D. N. Voskresenskii, “Condensate with finite momentum in a moving medium,” *JETP* **77(6)** (1993) 917–932. 86
- [84] S. P. Kumar and S. Stratiev, “Work in progress,”. 93
- [85] V. Markov, A. Marshakov, and A. Yung, “Non-Abelian vortices in $N = 1^*$ gauge theory,” *Nucl. Phys.* **B709** (2005) 267–295, arXiv:hep-th/0408235 [hep-th]. 94

REFERENCES

- [86] R. Auzzi and S. P. Kumar, “Non-Abelian k-Vortex Dynamics in N=1* theory and its Gravity Dual,” *JHEP* **12** (2008) 077, arXiv:0810.3201 [hep-th]. 94
- [87] P. Castorina, G. Riccobene, and D. Zappala, “Non-commutative dynamics and roton-like spectra in bosonic and fermionic condensates,” *Phys. Lett.* **A337** (2005) 463–468, arXiv:hep-th/0405093 [hep-th]. 94
- [88] S. Hands, “Four fermion models at nonzero density,” *Nucl. Phys.* **A642** (1998) 228–238, arXiv:hep-lat/9806022 [hep-lat]. 94
- [89] S. Choudhury, A. Dey, I. Halder, S. Jain, L. Janagal, S. Minwalla, and N. Prabhakar, “Bose-Fermi Chern-Simons Dualities in the Higgsed Phase,” *JHEP* **11** (2018) 177, arXiv:1804.08635 [hep-th]. 94
- [90] H. J. de Vega and F. A. Schaposnik, “Vortices and electrically charged vortices in non-abelian gauge theories,” *Physical Review D* **34** no. 10, (Nov., 1986) 3206–3213.
<https://doi.org/10.1103/physrevd.34.3206>. 97
- [91] C. N. Kumar and A. Khare, “Charged vortex of finite energy in nonabelian gauge theories with chern-simons term,” *Physics Letters B* **178** no. 4, (Oct., 1986) 395–399.
[https://doi.org/10.1016/0370-2693\(86\)91400-0](https://doi.org/10.1016/0370-2693(86)91400-0).
- [92] J. L. Blazquez-Salcedo, L. M. Gonzalez-Romero, F. Navarro-Lerida, and D. H. Tchrakian, “Non-abelian chern-simons-higgs vortices with a quartic potential,” arXiv:1306.5146.
- [93] F. Navarro-Lérida and D. H. Tchrakian, “Non-abelian yang-mills-higgs vortices,” *Physical Review D* **81** no. 12, (June, 2010) .
<https://doi.org/10.1103/physrevd.81.127702>. 97
- [94] T. Vachaspati and A. Achucarro, “Semi-local cosmic strings,”.